AFFINITY MEMBRANES WITH FUNCTIONALIZED POLYMER BRUSHES FOR RAPID, HIGH CAPACITY PURIFICATION OF TAGGED PROTEINS

By

Nishotha Anuraj

A THESIS

Submitted to
Michigan State University
in partial fulfillment of the requirements
for the degree of

MASTERS OF SCIENCE

Chemistry

2011

ABSTRACT

AFFINITY MEMBRANES WITH FUNCTIONALIZED POLYMER BRUSHES FOR RAPID, HIGH CAPACITY PURIFICATION OF TAGGED PROTEINS

By

Nishotha Anuraj

Porous membranes are useful for protein purification because convective mass transport rapidly brings proteins to binding sites, which should minimize diffusion-based limitations and also decrease non-specific adsorption and increase protein purity. Unfortunately membranes have low binding capacities compared to columns, but modifying membrane pores with polymer brushes can greatly enhance protein binding. This thesis describes an aqueous method to grow polymer brushes from macroinitiators adsorbed in membranes pores. Compared to growth of brushes from silane initiators, this method leads to 4-fold increases in membrane permeability and an order of magnitude decrease in the time required for brush polymerization. The aqueous method is applicable to a wide range of polymeric membrane including nylon, polyethersulfone and polyvinylidine fluoride. Poly(2-(methacryloyloxy)ethyl succinate brushes grown from macroinitiators in nylon membranes bind as much as 120 mg lysozyme/cm³ of membrane, and when functionalized with nitrilotriacetate-Ni²⁺ complexes these brushes bind 85 mg/cm³ of polyhistidine-tagged (His-tagged) proteins. More importantly, these membranes isolate Histagged proteins directly from complex cell extracts. This thesis also investigate the effect of reduction of the areal density of the polymer brushes on protein binding and purification of maltose binding protein using maltose attached to polymer brushes.

I dedicate this dissertation to my parents, Pushparanee Neelalojanan and Vinayagamoorthy Neelalojanan, my husband, Anuraj Sivarajah my sibling, Neshanthanan Neelalojanan and my children Preyan Anuraj and Poornimah Anuraj, for their love and support.

ACKNOWLEDGMENTS

This thesis would not have been possible without the guidance, help and support of some wonderful people. I owe my deepest gratitude to my advisor, Dr. Merlin Bruening; who was inspiring and ever so supportive. He guided me to become a researcher and not a follower, installing confidence in myself and allowing me to work independently and explore various avenues on my own. His help didn't just stop with developing scientific skills but also extended in developing my presentation and scribal skills. There are no words to express my gratitude and I am proud to be a student of a great scientist.

I am indebted to my second mentor, Dr. Gregory Baker, for the vast wisdom he willingly shared which helped my research work immensely and his invaluable assistance with writing the manuscript.

I would like to illustrate my deepest gratitude to my committee members, Dr. James Geiger and Dr. Dana Spence for their encouraging comments and great suggestions. I also thank Dr. Geiger and his research students Remie Touma and Zahra Nossoni for assisting and helping me in obtaining the cell extracts for protein studies.

My humble thanks to Dr. Parul Jain, who was an excellent mentor, a guide and a great friend. I am extremely grateful to the current and past Bruening research group members and my friends in the department of chemistry for all the help provided and most of all making this an enjoyable experience.

I acknowledge Dr. Kathy Severin for the guidance on transmission FTIR and UV/vis, Dr. Ruth Smith for training on ATR-IR, Dr. Dan Holmes for the help with NMR and Dr. Baokang Bi for training on SEM.

I will always be in debt to my undergraduate research supervisor and my favorite teacher Dr. Ramani Wijesekara, who sow the seeds to pursue this path with mammoth encouragement and abundant guidance. Also am grateful to my high school chemistry teacher Mrs. Rajathurai for crafting a deep passion and interest in the subject.

I thank my lovely parents without whom I would have not been who I am now. I am fortunate to have such parents and an awesome brother who has been a constant source of love, concern, support and strength. Importantly I thank my loving husband, for his understanding and constant encouragement. He took care of my children along with his work and commitments for me to attend school. Without him, I could not have done what I was able to do. I thank my little son and my new born daughter for bearing with such a busy mother and still loving her for what she is. I owe my success to my family.

TABLE OF CONTENTS

LIST OF F	IGURES	ix
LIST OF S	CHEMES	xii
LIST OF A	BBREVIATIONS	xiii
Chapter 1.	Introduction and background	1
1.1 Intr	oduction	1
	kground	
	Protein purification	
1.2.2.	<u> </u>	
	2.1. Immobilized metal ion affinity chromatography	
	for His-tagged protein purification	4
1.2.	2.2. Carbohydrate matrices for MBP-tagged	
	protein purification	6
1.2.3.	Stationary phases for isolation of protein	
1.2.4.	Membrane adsorbers	
1.2.5.	Polymer brushes	10
1.2.	5.1. Surface initiated ATRP	
1.2.	5.2. Functionalization of polymer brushes for	
	protein binding	13
1.2.	5.3. Protein purification with polymer brush	
	modified membranes	15
1.3. Out	line of the thesis	17
1.4. Ref	erences	19
Chapter 2.		
-	remarkable permeabilites and protein capture rates	25
2.1. Intr	oduction	25
	perimental	
	Materials	
2.2.2.	Initiator attachment	28
2.2.3.	Polymer brush synthesis	29
2.2.4.	Synthesis of multilayer polyelectrolyte films derivatized with NTA	30
2.2.5.	Protein binding	31
2.2.6.	Quantification of protein binding	
2.2.7.	Protein separation from cell extract and determination of protein purity	
2.2.8.	Determination of hydraulic permeability	
2.2.9.	Determination of the amount of Cu ²⁺ in the membrane	34

2.3. Resi	ults and discussion	34
2.3.1.	Synthesis and characterization of polymer brushes in nylon membrane	34
2.3.2.	Membrane permeability	40
2.3.3.	Lysozyme binding	
2.3.4.	Protein binding capacity as a function of flow rate	
2.3.5.	Scaling up poly(MES)-modified membranes	48
2.3.6.	HisU binding to poly(MES)-NTA-Ni ²⁺ -modified membranes	50
2.3.7.	Con A binding to a monolayer of NTA-Cu ²⁺ and other poly(MES)-NTA-	
	Cu ²⁺ brushes	52
2.3.8.	Purification of His-tagged MIPS and HisU from cell extracts and protein mixtures	
2.3.9.	Polymer growth and protein binding in other polymeric membranes	
	clusions	
	erences	
Chapter 3.	Protein binding to polymer brushes with a reduced areal chain density	65
3.1. Intro	oduction	65
	erimental	
3.2.1.	Materials	
3.2.2.	Preparation of initiator-modified Au substrates	69
3.2.3.	Polymerization of MES and HEMA on Au substrates	69
3.2.4.	Polymer brush derivatization and protein immobilization	70
3.2.5.	Quantification of protein binding	71
3.3. Resi	ults and Discussion	72
3.3.1.	Polymerization of MES and HEMA on Au wafers with controlled initiator	
	density	
3.3.2.	Protein binding as a function of chain areal density	76
3.4. Con	clusions	79
3.5. Refe	erences	81
Chapter 4.	Attempts to synthesize affinity membranes that isolate maltose binding protein-fusion proteins	84
	oduction	
	erimental	
4.2.1.	Materials	
	Formation of azide-modified poly(GMA) brushes on Au	
4.2.3.	Synthesis of propargyl maltose	
4.2.3.	Click chemistry to react propargyl maltose with azide groups on Au	
4.2.4.	Protein immobilization	
4.2.5.	Characterization of Au surface modification and protein binding	
	ults and Discussion	
	clusions	
4.3. Kere	erences	90

Chapter	5. Conclusions and future work	98
5.1. (Conclusions and future work	98
5.2. I	References	103
Appendi	x. Poly(MES) brushes grown from macroinitiators on Au-coated Si	106
A.1. I	Experimental	106
A.1.	1. Polymerization of MES on Au-coated wafers A.1.1. Polymerization of MES	
	on Au-coated wafers	106
A.1.	2. Derivatization of poly(MES) and protein binding	. 107
A.1.	3. Characterization of polymer brush growth, derivatization and protein binding	108
	4. Quantification of protein binding	
	Results and Discussion	
A.2.	1. Polymer brush growth and characterization	109
	2. Protein binding to poly(MES) and its derivatives on Au surfaces	
	3. Effect of multilayers of initiator on polymerization and protein binding	
	References	

LIST OF FIGURES

Figure 1.1.	Expression and purification of a recombinant, tagged protein2
Figure 1.2.	Binding of His-tagged protein to a NTA-Ni ²⁺ -derivatized poly(MES) brush inside a membrane pore
Figure 1.3.	Transport through packed columns with nanoporous beads and membrane pores
Figure 1.4.	Polymer brushes with multiple protein binding sites
Figure 2.1.	Schematic showing macroinitiator immobilization within membrane pores, polymerization of MES from an initiator-modified membrane, derivatization of poly(MES) with NTA-Ni ²⁺ complexes and protein binding to such polymer brushes.
Figure 2.2.	Apparatus for measuring hydraulic permeability of the membrane33
Figure 2.3.	ATR-FTIR spectra of a hydroxylated nylon membrane before and after modifications
Figure 2.4.	Binding capacities and elution efficiencies for 5 cycles of lysozyme adsorption and elution on a single hydroxylated nylon membrane modified with poly(MES)
Figure 2.5.	SEM images of a bare nylon membrane with nominal 1.2 µm pores, a similar membrane modified with poly(MES), and a membrane coated with poly(MES)-NTA-Cu ²⁺ polymer brushes
Figure 2.6.	Cu ²⁺ binding capacities of poly(MES)-NTA-modified nylon membranes as a function of polymerization time. Poly(MES) was grown from adsorbed macroinitiator
Figure 2.7.	Evolution of the lysozyme binding capacity and hydraulic permeability of nylon membranes with the time allowed for growth of poly(MES) brushes42
Figure 2.8.	Breakthrough curves for lysozyme binding on hydroxylated nylon membranes containing poly(MES) grown for 2 min, 5 min, 10 min, 15 min, 1 hr45
Figure 2.9.	Breakthrough curves for lysozyme binding to hydroxylated nylon membranes containing poly(MES) grown from adsorbed macroinitiator which was < 1 month old and about 6 months old

Figure 2.10.	Breakthrough curves for the passage of 0.3 mg/mL lysozyme through a poly(MES)-modified nylon membrane at flow rates of 1 mL/min and 30 mL/min
Figure 2.11.	Apparatus used to measure the binding capacity of a stack of polymer brush modified membranes
Figure 2.12.	Breakthrough curves for adsorption of lysozyme, HisU and Con A in nylor membranes modified with poly(MES)
Figure 2.13.	Formation of a monolayer of NTA-Cu ²⁺ from a polyelectrolyte multilayer adsorbed within a membrane pore
Figure 2.14.	Breakthrough curves for binding of Con A to a monolayer of NTA-Cu ²⁺ , a macroinitiator-based poly(MES)-NTA-Cu ²⁺ -modified membrane and a trichlorosilane initiator-based poly(MES)-NTA-Cu ²⁺ -modified membrane53
Figure 2.15.	SDS-PAGE analysis (silver staining) of an extract from E. <i>Coli</i> containing over expressed His-tagged MIPS and His-tagged MIPS purified from the cell extract using a poly(MES)-NTA-Ni ²⁺ -modified membrane; a mixture of BSA ovalbumin, Con A, myoglobin and HisU, the same solution after passing through the membrane and the eluent from the membrane
Figure 2.16	Extract from E. <i>Coli</i> containing spiked HisU, flow through from the membrane, elution from membrane and HisU standard solution
Figure 2.17.	ATR-FTIR spectra of PES, PVDF and non hydroxylated nylon membrane before and after growth of poly(MES) brushes
Figure 3.1.	Enhanced protein binding to reduced density polymer brushes compared to regular polymer brushes
Figure 3.2.	Thickness and normalized film thickness (measured thickness divided by the percentage of initiator in the monolayer) of poly(MES) brushes grown from complete and diluted initiator monolayer on Au -coated wafers
Figure 3.3.	Evolution of ellipsometric film thickness with time for polymerization of MES using Me ₆ (TREN) and HMTETA as the catalyst ligands
Figure 3.4.	Evolution of ellipsometric film thickness with time for polymerization of HEMA
Figure 3.5.	Lysozyme, and BSA binding capacities of 15 nm-thick poly(MES) (lysozyme) or

	poly(MES-NTA-Cu ²⁺) (BSA) brushes grown from monolayers containing 1%, 5% and 100 % initiator	
Figure 3.6.	Amount of lysozyme, and BSA bound to 50 nm poly(MES) and 50 nm poly(HEMA)-SA brushes grown from monolayers containing 5% and 100% initiator densities.	
Figure 4.1.	Expression and purification of MBP-tagged fusion protein85	
Figure 4.2.	Binding of MBP-tagged protein to polymer brushes attached to a gold coate silicon substrate8	
Figure 4.3.	Reflectance-FTIR spectra of poly(GMA) brushes on Au-coated wafers and the same brushes after, reaction with sodium azide, immobilization of maltose during exposure to in a propargyl maltose solution, and immersion in a solution of cellular extract with MBP-tagged protein	
Figure 5.1.	Synthesis of reduced-density polymer-brushes using monomers with long side chain and subsequent side chain hydrolysis	
Figure 5.2.	Proposed structure of a cleavable monomer (poly(ethyleneglycol)-bis-acrylate)	
Figure A.1.	Evolution of ellipsometric thickness with time for surface-initiated polymerization of MES on Au-coated Si	
Figure A.2.	Reflectance FTIR spectra of a poly(MES) brush grown from a macroinitiator adsorbed on MPA-modified Au	
Figure A.3.	Comparison of protein binding on polymer brushes grown from disulfide initiator and a macroinitiator as a function of poly(MES) film thickness	
Figure A.4.	Reflectance FTIR spectra of macroinitiator/ $(PSS/macroinitiator)_n$ films deposited on MPA-coated gold substrates (n = 0-4)	
Figure A.5.	Reflectance FTIR spectra of poly(MES) films grown from macroinitiator $/(PSS/macroinitiator)_n$ films deposited on Au-MPA substrate (n = 0-4)114	
Figure A.6.	Ellipsometric thicknesses of macroinitiator/(PSS/macro initiator) _n films and of poly(MES) brushes grown on these films. The figure also shows the amounts of lysozyme and BSA binding to the poly(MES) grown from the macro initiator/(PSS/macro initiator)n films. In the case of BSA, the film was derivatized with NTA-Cu ²⁺ prior to protein binding	

LIST OF SCHEMES

Scheme 1.1.	ATRP polymerization mechanism12
Scheme 1.2.	Synthesis of a protein binding polymer brush
Scheme 3.1	Synthesis of reduced density polymer-brushes from monolayers containing initiator and diluent molecules
Scheme 4.1.	Polymerization of poly(GMA) brushes from initiators on a Au-coated wafer, derivatization of the brushes with azide groups, and attachment of maltose to the brushes through "click" chemistry

LIST OF ABBREVIATIONS

Aminobutyl NTA N_{α} , N_{α} -bis(carboxymethyl)-L-lysine hydrate

ATR Attenuated total reflectance

ATRP Atom-transfer radical polymerization

Bpy 2,2'-Bipyridyl

BSA Bovine serum albumin

Con A Concanavalin A

DMAP 4-Dimethylaminopyridine

DMF Dimethylformamide

EDC 1-[3-(Dimethylamino)propyl]-3-ethylcarbodiimide hydrochloride

EDTA Ethylenediamine tetraacetic acid

FESEM Field-emission scanning electron microscopy

FTIR Fourier transform infrared

GMA glycidyl methacrylate

GST glutathione-S-transferase

HEMA 2-Hydroxyethyl methacrylate

His-tag Polyhistidine tag

His-tagged ubiquitin

HMTETA 1,1,4,7,10,10-Hexamethyltriethylenetetramine

IMAC Immobilized metal-affinity chromatography

MBP Maltose binding protein

MES 2-(Methacryloyloxy)ethyl succinate

Me₆TREN Tris[2-(dimethylamino)ethyl]amine

MIPS *myo--*inositol-1-phosphate synthase

MPA 3-Mercaptopropionic acid

MUD 11-Mercapto-1-undecanol

NHS N-Hydroxysuccinimide

NTA Nitrilotriacetate

PAA poly(acrylic acid)

PAH poly(allylamine hydrochloride)

PDADMAC poly(diallyldimethylammonium chloride

PES Polyethersulfone

PSS Poly(styrene sulfonate)

PVDF Polyvinylidine fluoride

SA Succinic anhydride

SDS-PAGE Sodium dodecyl sulfate-polyacrylamide gel electrophoresis

THF Tetrahydrofuran

TLC Thin layer chromatography

UV/Vis Ultra violet/visible

Chapter 1. Introduction and Background

1.1. Introduction

This thesis describes the growth of polymer brushes within porous substrates to create high-capacity membrane adsorbers for purification of tagged recombinant proteins. Specifically, adsorption of a macroinitiator in the membrane both simplifies growth of polymer brushes and increases the permeability of the resulting membranes 4-fold relative to polymerization from silane-based initiators. Moreover, the new membranes capture as much as 85 mg of polyhistidine-tagged (His-tagged) protein per cm³ of membrane and provide highly pure protein directly from cell extracts. Preliminary studies also examine the possibility of capturing maltose binding protein (MBP).

My research builds on previous methods to modify membranes with polymer brushes that bind tagged proteins. To put the work in perspective, this chapter first explains the importance of protein purification and compares different purification strategies. Subsequent sections describe prior work in the development and application of polymer brush-modified membranes for protein purification. Lastly, this chapter presents an outline of the thesis.

1.2. Background

1.2.1. Protein purification

Proteins are among the fundamental building blocks of cells, ^{1,2} and the ever-expanding research into protein structure, function, and interactions often requires convenient methods for

protein isolation. ^{3,4} An increasing demand for biopharmaceutical proteins such as monoclonal antibodies, plasma proteins and growth factors also requires efficient purification processes. ⁵ Protein isolation is vital to eliminate impurities that interfere with functionality, remove toxins

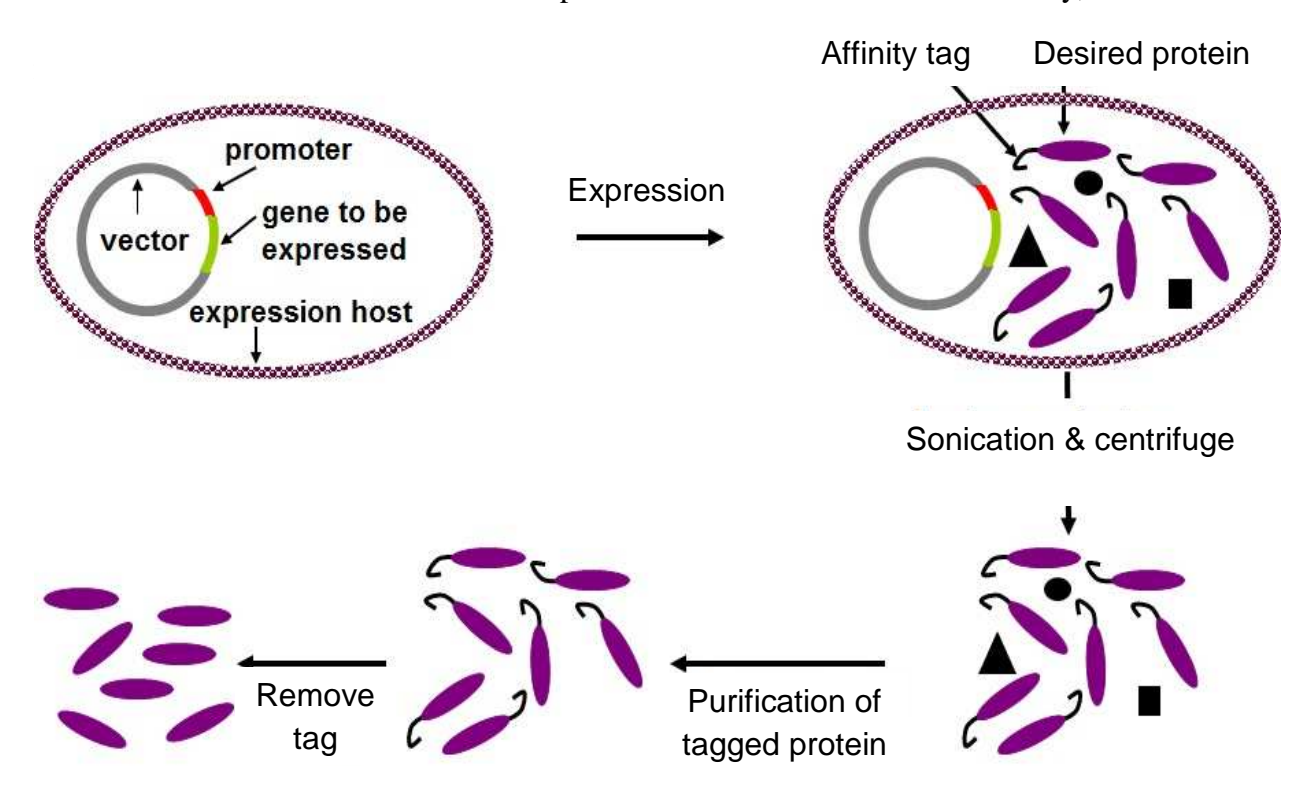


Figure 1.1. Expression and purification of a recombinant, tagged protein. Reproduced with thanks from Jinhua Dai. "For interpretation of the references to color in this and all other figures, the reader is referred to the electronic version of this thesis".

Although advances in cell culture technology have increased the titer of many recombinant proteins, downstream processing of crude cell culture media remains a bottle neck in obtaining pure proteins. Because an organism contains thousands of proteins and their amounts may vary over several orders of magnitude, isolation of a target protein is often challenging. To overcome this challenge, scientists frequently append affinity tags to recombinant proteins. Figure 1.1 illustrates the general scheme of recombinant protein

production and separation, where specific binding of the tagged protein to surfaces is an extremely powerful initial step in protein purification. ^{9,10} When performed in a column, this technique is often termed affinity chromatography, even though the separation often occurs in a batch mode.

1.2.2. Affinity chromatography

Several chromatographic techniques are available for protein separations. 11-13 Reversephase chromatography is reasonably selective and separates proteins in large part based on their relative hydrophobicities. However this method requires organic-solvent mobile phases that eliminate functionality. 11 Ion-exchange proteins and permanently denature some chromatography fractionates proteins based on their charge density, 11,14-16 whereas sizeexclusion chromatography (gel filtration) separates larger proteins from small ones, and is useful for concentrating protein samples. 11 Nevertheless, because of its high specificity, affinity chromatography is the most powerful method to isolate a single target protein from complex biological fluids. These separations rely on specific interactions such as those between antigens and antibodies or between receptors and ligands. 9,17,18 Additionally, affinity chromatography occurs with high yields and often mild elution conditions. 19,20

Affinity based purification of recombinant proteins typically exploits specific interactions between a binding tag appended to the protein of interest and a complementary ligand immobilized on a solid support. Some examples of affinity interactions include His-tags

binding to metal-ion complexes, ^{21,22} MBP interacting with carbohydrate matrices, ²³ glutathione-S- transferase binding to glutathione ²⁴ and streptavidin binding to biotin. ²⁵ This research focuses on His-tags and MBP, so the following sections describe purification with these particular tags.

1.2.2.1. Immobilized metal ion affinity chromatography for His-tagged protein purification

Immobilized metal-ion affinity chromatography (IMAC) is a robust, highly versatile method of protein purification based on the affinity of specific amino acids for transition metal ions bound to a solid support. Porath et al introduced IMAC in the mid-1970s. ^{19,26-28} In this technique, metal ions such as Ni²⁺, Co²⁺ or Cu²⁺ bind to chelators (e.g. iminodiacetic acid or nitrilotriacetic acid (NTA)) that are immobilized on a support. A wide range of solid supports are available for immobilization of metal chelates, and polymeric materials with hydroxyl groups are particularly common. ²⁷

In typical protein purification, interaction of different chelated metal ions with proteins occurs through histidine, tryptophan, or cysteine residues, depending on the metal-ion complex. Por metal-ion complexes that specifically bind imidazole, the number and relative position of accessible histidine residues determine the extent of protein binding. Thus, in expression of recombinant proteins in bacterial cells, a short DNA sequence is appended to the gene of interest to add a short stretch of histidine residues (typically 6) to either the N-terminal or C-terminal of the recombinant protein. This "His-tag" binds strongly to Ni²⁺, Co²⁺ or Cu²⁺ complexes. Because most proteins contain one or more native histidine residues, the metal-ion

complex selected for capturing His-tagged proteins should not interact too strongly to imidazole or many different proteins will bind to the support. For this reason, chelated Ni^{2+} and Co^{2+} , rather than Cu^{2+} complexes, are usually employed in purifying His-tagged proteins. 27,30,31

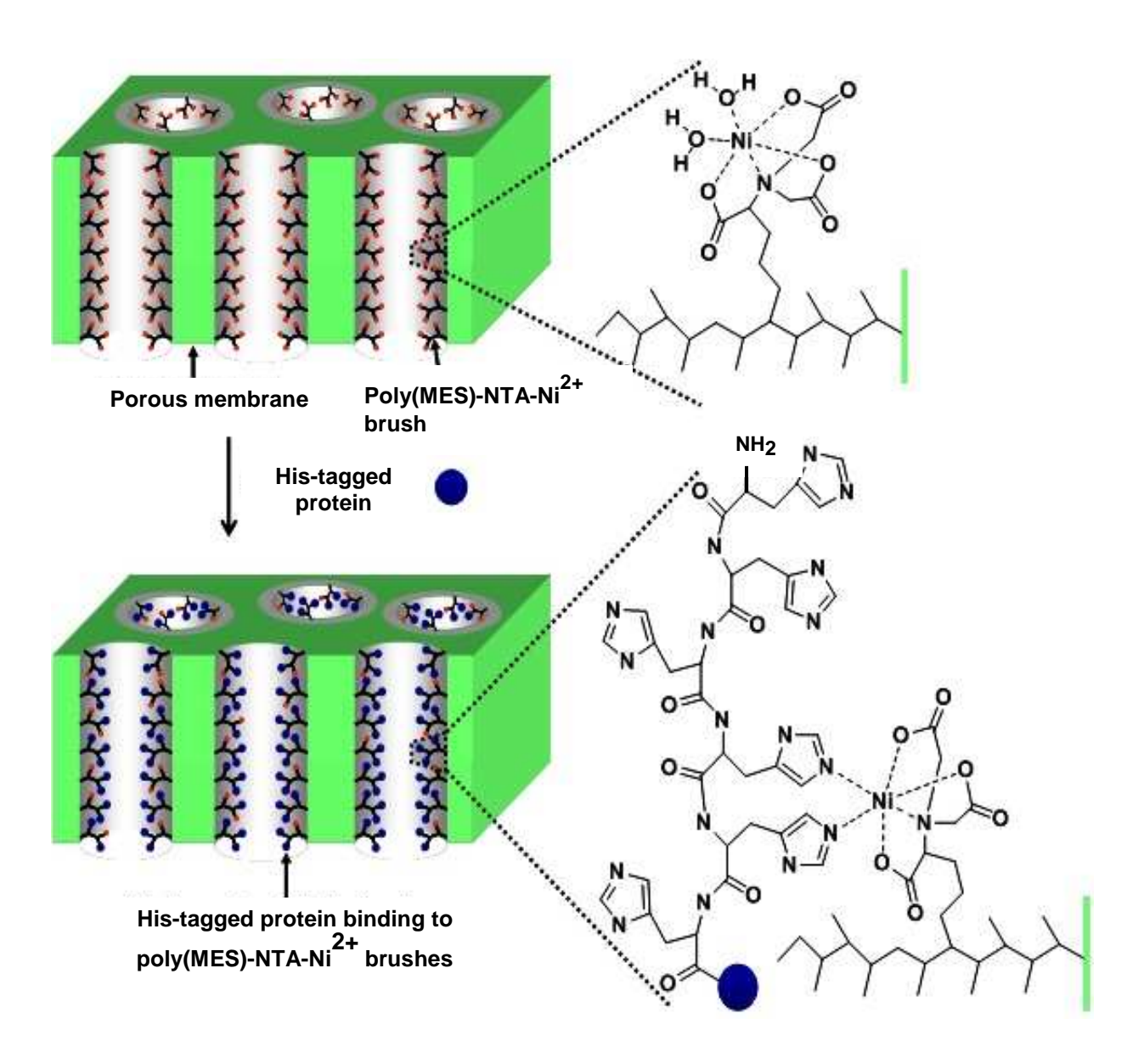


Figure 1.2. Binding of His-tagged protein to a NTA-Ni²⁺-derivatized poly(MES) brush inside a membrane pore. "Reprinted with permission from Jain, P.; Vyas, M. K.; Geiger, J. H.; Baker, G. L.; Bruening, M. L. *Biomacromolecules* **2010**, *11*, 1019-1026. Copyright 2010 American Chemical Society".

Figure 1.2 shows a typical affinity interaction between immobilized NTA-Ni²⁺ and a His-tagged protein. Elution of specifically bound His-tagged proteins can occur with displacements agents (usually free imidazole) that bind to the metal binding site or by altering conditions such as pH and ionic strength. ^{19,27}

IMAC has many assets including low cost, specificity, simplicity and mild elution conditions. Additionally the binding site can be regenerated many times without loss of performance, and the selectivity can be controlled by choosing different metal ions and altering physical properties such as pH, ionic strength and temperature. However, non-specific binding of proteins due to naturally occurring surface histidine or cysteine clusters presents a significant challenge in purification. Addition of low concentrations of a competing agent, such as imidazole, to the loading medium helps to overcome this challenge but often decreases protein binding capacity. ^{32,33}

1.2.2.2. Carbohydrate matrices for MBP-tagged protein purification

Although IMAC is the most common method for recombinant protein purification, other affinity-based methods address specific issues faced during recombinant protein production and purification. When a target protein or peptide is not stable within the cell, it is sometimes expressed as part of a fusion protein.³⁴ The fusion partner should express at high levels within the cell, and frequently it also facilitates the purification of the target protein. In *Escherichia coli* MBP frequently serves as a fusion partner because it expresses in high levels, facilitates the separation of the fusion proteins in a single chromatographic step, elutes under mild elution conditions and enhances the folding and solubility of the target protein.³⁵⁻³⁷

In 1978 Ferenci and Klotz reported that cross-linked amylose can successfully purify MBP proteins, ³⁶ and subsequent studies showed that a number of carbohydrate-based materials selectively capture MBP-fusion proteins. Examples include amylose-agarose composites, ³⁸ maltoheptaose-agarose resins, ³⁹ and dextrin sepharose media. ⁴⁰ A mixture of cellulose and starch ³⁴ and microporous cellulose membranes modified with amylose ²³ also provide MBP-fusion protein purification systems.

1.2.3. Stationary phases for isolation of proteins

For several decades, packed-bead columns have served as the primary mode of protein purification for both preparative and analytical needs. In a typical column-based chromatographic separation, the solution containing the target molecule is loaded on a chromatographic matrix, and the flow of mobile phase separates the components so the target appears in a band eluting from the column. In contrast, with an affinity-based column the target selectively binds to the ligand while the other components pass through the column. Washing with buffers removes any remaining impurities, and the bound target finally elutes in a pure form after displacement from the resin due to a competing binding agent, denaturation, or other mechanism.

The major drawback of packed-bead columns is that slow intra-bead diffusion of solutes results in long separation time and low throughput. This diffusion limitation also leads to large elution volumes and necessitates a post-separation concentration of the analyte. Additionally, compact stationary phases give rise to large pressure drops across the packed bed and difficulties

in packing columns for large scale purification. ^{6,10,12,17,42} The development of mono-disperse, non-porous chromatographic media has helped to overcome the diffusion limitations of packed-bed systems, but these media are generally expensive, exhibit a low binding capacity due to their low surface area and still cause high pressure drops. ^{43,44}

1.2.4. Membrane adsorbers

Numerous reviews and reports demonstrate and discuss the advantages of membrane adsorbers over column-based protein purification. 5,6,10,12,17,42,45-47 For affinity-based separations, micro-porous membranes overcome the main limitation of conventional bead-based columns, slow diffusion into bead pores. Convective transport in the membrane pores rapidly bring proteins to ligands grafted on the pore surface. In contrast, in columns packed with nanoporous beads, convective flow passes around the beads so diffusion in nanochannels must transport proteins to binding sites within the bead. The only diffusional limitation that exists in a porous membrane is transport of the target from the core of the flowing liquid to the pore surface. For micron-size pores, however, this limitation is minimal (Figure 1.3). Moreover since membranes are thinner than packed beds, the pressure drop across the membrane is significantly less than that across a packed column. This makes the membrane system particularly attractive for large scale protein purification. 6,12,42

Although membrane adsorbers provide rapid protein purification compared to column-based methods, membranes suffer from low binding capacities relative to porous beads due to their low internal surface area. Muller originally proposed overcoming this limitation by modifying membrane pores with polymer brushes that present multiple protein binding sites. ¹⁵

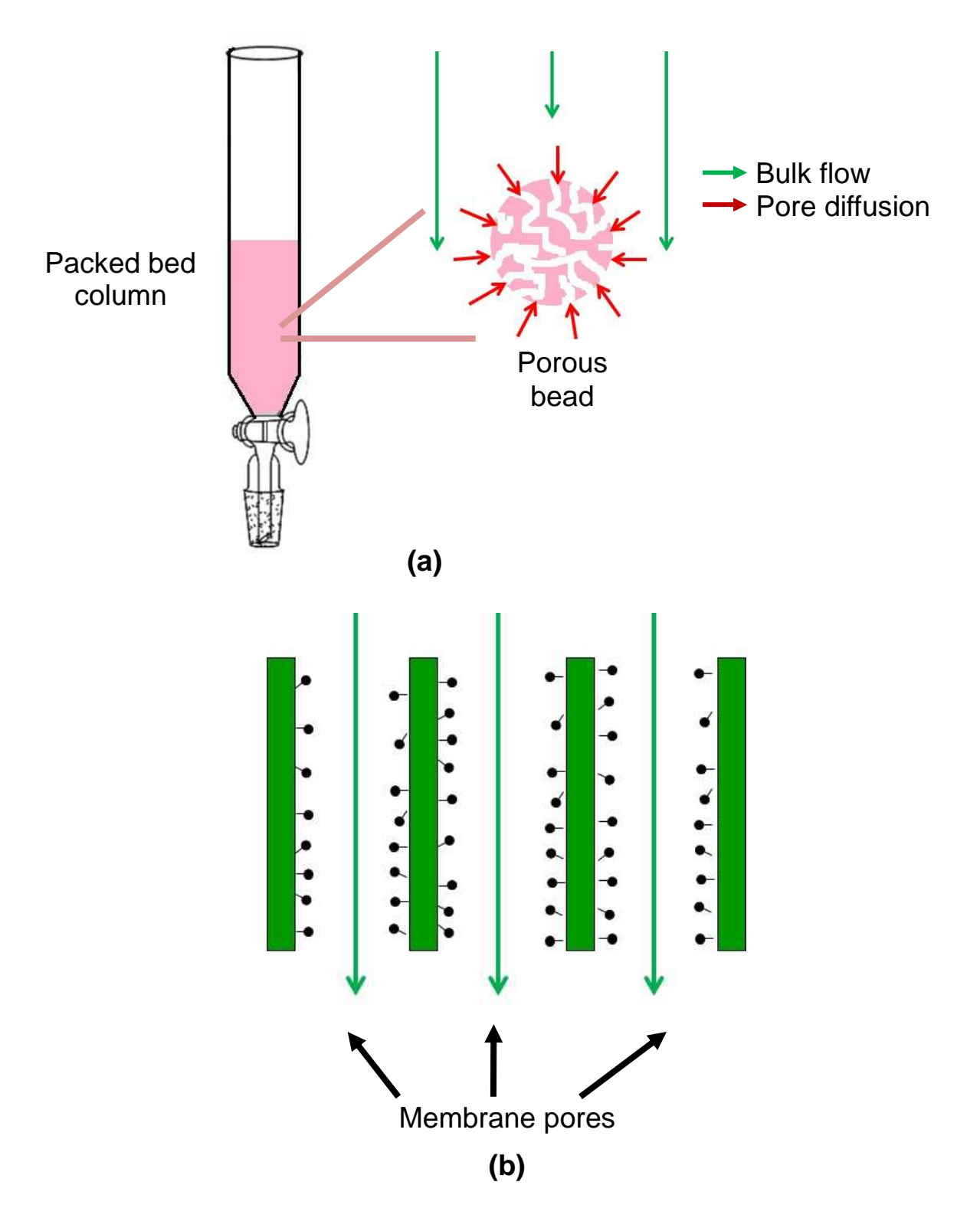


Figure 1.3. Transport through packed columns with nanoporous beads (a) and membrane pores (b).

Functionalization of the brushes with a variety of ligands yields membranes with a number of different specificities. ⁴⁸⁻⁵³ This thesis explores ways to enhance the permeabilities and protein-binding capacities of membrane adsorbers modified with polymer brushes. Thus, the next section discusses the details of polymer brush synthesis and modification.

1.2.5. Polymer brushes

Polymer brushes are assemblies of polymer chains with one end tethered to a substrate.⁵⁴ The high grafting density of the attached polymer chains causes them to stretch away from the surface,⁵⁵ and derivatization of the side chains of such brushes can immobilize protein binding ligands (Figure 1.4).

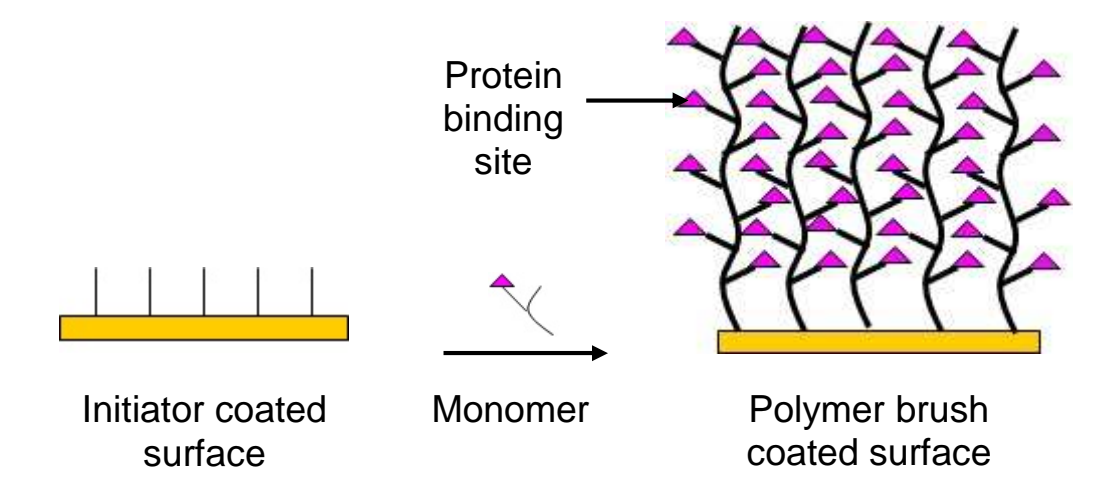


Figure 1.4. Polymer brushes with multiple protein binding sites.

When exposed to a favorable solvent the brushes swell and extend to better expose the binding sites for rapid protein immobilization. ⁵⁶ Attachment of polymer brushes to surfaces can rely on

physically adsorbing block copolymers⁵⁷ or covalent bonding of polymer end groups to a complementary group on the substrate. The latter mode is now more common because it provides more stable brushes. Covalent tethering can occur with either a grafting-to method, ⁵⁸ where end functionalized polymer chains binds to substrates through chemical bonding, or a grafting-from procedure, ⁵⁹ where polymer chains grow directly from initiators attached covalently to the surface (Figure 1.4). The two tethering methods form brushes with very different grafting densities. In the grafting-to method, steric hindrance from initially grafted chains limits the accessibility of the reactive surface to give relatively low grafting densities. In contrast, in the grafting-from method small monomers readily reach the reactive, growing surface to provide higher grafting densities. Additionally, variation of the initiator density on the surface affords control over the areal density of polymer chains in brushes grown from a substrate. ⁶⁰

Several types of polymerization can effect polymer growth from surfaces including cationic, ⁶¹ anionic, ⁶² radical, ⁶³ ring opening metathesis ⁶⁴ and photochemical polymerization. ⁶⁵ Controlled radical-based polymerization including atomic transfer radical polymerization (ATRP), ^{66,67} reversible addition fragmentation transfer ⁶⁸ and nitroxide-mediated polymerizations ⁶⁹ are most frequently used for brush formation as they offer control over thickness and architecture of the polymer brush. My work focused on growth of brushes by ATRP, ⁶⁶ which I describe in more detail in the next section.

1.2.5.1. Surface-initiated ATRP

ATRP is perhaps the most powerful and simple technique for the synthesis of polymer brushes with low polydispersity. When performed with initiators anchored to a substrate, ATRP is particularly powerful because radicals only form on the surface unless chain transfer occurs. This confines growth to the surface and minimizes polymerization in solution that could lead to physisorption of polymers not covalently linked to the substrate. ATRP is attractive for the growth of polymer brushes within membrane pores due to its mild reaction conditions such as room temperature in an aqueous medium. The use of readily available polymerization systems (catalyst, monomer) and a tolerance to many impurities also make ATRP appealing for membrane modification.

Scheme 1.1 ATRP polymerization mechanism.

ATRP achieves control over polymerization by maintaining a low concentration of radicals through transfer of a halogen atom between growing chains and a metal ion complex. In the activation step, the halogen atom (generally Cl or Br) transfers from the growing chain to the catalyst, typically a Cu(I) species, to form a radical on the surface (Scheme 1.1). The reverse reaction results in a reduced metal ion and a dormant chain. The equilibrium between the dormant and the active state lies significantly towards the dormant state so a low fraction of chains are active at a given time. This low concentration of active radicals leads to minimal chain

termination and a relatively constant rate of chain growth. The fast initiation and the rapid conversion between the active and radical-capped dormant stage also yield low polydispersity for chain molecular weights. The polymerization rate depends on the type and the amount of the transition metal catalyst, ligand, solvent and initiator. ATRP is particularly important for polymer brush formation within membrane pores, where controlled growth of the polymer chains allows optimization of protein binding capacity without plugging the pores and preventing fluid flow. ⁶⁷

1.2.5.2. Functionalization of polymer brushes for protein binding

Although ATRP can employ monomers with a wide variety of functional groups, post-polymerization derivatization of polymer brushes is still attractive for introducing protein-binding groups in the film. Derivatization requires the presence of versatile "handles" on the polymer brush, the most common of which are hydroxyl, carboxylic acid and epoxide groups.

Poly(2-hydroxyethyl methacrylate) (poly(HEMA)) is one of the polymer brushes most widely used to functionalize surfaces. Reaction of the hydroxyl groups of poly(HEMA) with succininc anhydride in the presence of a base leads to side chains containing terminal carboxylic acids that can bind protein through ion-exchange or be further derivatized to include IMAC ligands such as NTA. Activation of the hydroxyl groups of poly(HEMA) with p-nitrophenol chloroformate yields carbonate intermediates that readily react with amine groups to immobilize proteins and peptides. Poly(glycidyl methacrylate) brushes contain epoxide groups and are very attractive because they allow derivatization without activation. Unfortunately, however, the ring-opening reactions frequently require many hours.

Scheme 1.2. Synthesis of a protein binding polymer brush.

Poly(acrylic acid), poly(methacrylic acid) and poly(2-(methacryloyloxy)ethyl succinate) (poly(MES)) are also very attractive for immobilization of proteins because they contain native carboxylic acid groups. These carboxylic acids can be directly activated and reacted with amine groups of protein 73 or with aminobutyl NTA, which serves as an IMAC chelator (Scheme 1.2).

1.2.5.3. Protein purification with polymer brush-modified membranes

Several groups successfully modified a range of porous membranes with polymer brushes and achieved high protein-binding capacities and selectivity toward the protein of interest. The substrates in these studies include alumina and silica, and a variety of polymer membranes such as polyvinylidene difluoride (PVDF), 75 nylon, 51 polyethersulfone (PES), 76 polyethylene 77 and regenerated cellulose. 78 For example, He and coworkers prepared anion-exchange, hydrophilized polypropylene membranes containing poly((2-methacryloyloxy)ethyl) trimethylammonium chloride brushes and captured bovine serum albumin and trypsin inhibitor with binding capacities of 80 mg/cm³ and 120 mg/cm³ of membrane respectively.⁷⁹ Bhut and coworkers grafted poly(2-dimethylaminoethyl methacrylate) brushes in regenerated cellulose to form anion-exchange membranes with lysozyme binding capacities of 130 mg/cm³ and then purified anthrax protective antigen protein from E-coli cell extracts in these materials. ^{16,52} In poly(ethylene terephthalate) track-etched membranes, Yang and coworkers grew poly(HEMA) and subsequently grafted poly(2-lactobionamidoethyl methacrylate) from the poly(HEMA) to form a well-defined, comblike glycopolymer layer. These membranes showed a binding capacity of 23.6 mg/cm³ for lectins specifically binding to galactose.⁵³

Metal-ion affinity interactions have been exploited to create selective membrane adsorbers. Shi and coworkers purified hemoglobin from a hemolysate and achieved a binding capacity of 17.5 mg of hemoglobin per g of membrane using immobilized Cu²⁺ ions in a chitosan-modified anodisc alumina membrane. 80 Modification of alumina membranes with poly(HEMA) and subsequent derivatization of these brushes with NTA-Cu²⁺ or NTA-Ni²⁺ complexes gives affinity membranes with an equilibrium binding capacity of 130 mg of protein/cm³ of membrane. ⁵⁰ Ramstedt and co-workers bound His-tagged proteins selectively and reversibly to poly(oligoethylene glycol methacrylate) and poly(HEMA) brushes that were functionalized with $NTA-Ni^{2+}$ moieties. 81 Jain and coworkers showed that nylon membrane modified with poly(MES) brushes and functionalized with NTA-Ni²⁺ complexes selectively bind His-tagged cellular retinaldehyde binding protein directly from cellular extracts with purity levels comparable to those of commercial affinity columns. These membranes also have a remarkably high binding capacity of 85 mg/cm³ of membrane for His-tagged proteins. ⁵¹ These applications of polymer brush modified membranes clearly show the advantage of modifying membrane pores with polymer brushes.

This thesis presents a rapid, simplified procedure for growth and functionalization of polymer brushes in polymeric membranes. This method yields membranes that exhibit high-capacity protein binding along with highly specific protein separation. Remarkably these

modified polymer membranes have 1/4 the hydraulic resistance of similar membranes modified with polymer brushes, ⁵¹ and protein capture occurs in only 35 ms of residence time. Additionally the polymer brush synthesis requires only 5 min of polymerization of the monomer to yield binding capacities similar to or higher than previously reported values. ⁵¹ Moreover this is a completely aqueous method for the synthesis of polymer brushes so it is applicable to modification of many polymeric membranes such as nylon, PES and PVDF.

1.3. Outline of the thesis

Chapter 2 of this thesis describes a simple, rapid, and completely aqueous procedure for growth and functionalization of polymer brushes in nylon, PES, and PVDF membranes. The approach combines adsorption of a macroinitiator, polymerization of MES (a water-soluble, acid-containing monomer) from the initiator, and subsequent aqueous derivatization. This is the first application of macroinitiator adsorption to create protein-adsorbing membranes. The brushes grown from these initiators behave very differently from brushes grown from silane-based initiators immobilized in membranes. Compared to membranes modified with a trichlorosilane initiator, the macroinitiator-modified membranes require much shorter polymerization times (5 min versus 1 h) to achieve similar protein-binding capacities. A low hydraulic resistance and rapid protein capture make these new membranes very attractive for rapid purification of His-tagged protein directly from cell extracts.

The work described in chapter 3 aims to reduce the areal density of polymer-brushes and increase the capacity and kinetics of protein binding to polymer-brushes. To obtain reduced density polymer brushes, I examined two different strategies. In the first method, functionalizing

the surface with a mixture of initiator and an inert diluent reduces the density of the active immobilized initiators on the substrate. However, 15 nm-thick polymer films grown from 1% or 100% initiator in the monolayer show similar protein binding capacities. Thicker (50 nm) films also show similar protein binding with polymer films grown from monolayers with 5% and 100% initiator. In a second method, the selection of monomer and derivatization steps leads to variations in chain density. Specifically, poly(MES) was synthesized by polymerization of HEMA and subsequent reaction of this polymer brush with succinic anhydride (SA), or by direct polymerization of MES. The two methods yield the same polymer formula, but the spacing of the chains should be much greater with direct polymerization of MES because the monomer is much larger. Our results show that ~50 nm-thick poly(MES) brushes bind about 180 nm of lysozyme, while ~50nm-thick, poly(HEMA) brushes reacted with succinic anhydride bind only 80 nm of lysozyme. This suggests that less dense brushes bind more protein.

In chapter 4, I attempt to immobilize maltose on polymer-brush modified porous membranes for capture of MBP fusion proteins. In principle, this should yield a high protein-binding capacity due to the multiple binding sites present on polymer brushes. Infrared spectroscopy confirmed successful attachment of maltose to polymer brushes on gold surfaces, but unfortunately the immobilized maltose failed to bind MBP, perhaps because of the improper orientation of the binding sites of maltose.

The last chapter summarizes the conclusions of this thesis and presents some proposals for future work.

REFERENCES

1.4. References

- (1) Westermeier, R.; Naven, T.; Hopker, H.-R. *Proteomics in Practice: A Guide to Successful Experimental Design*; 2nd ed. ed.; Wiley-VCH, 2008.
- (2) Jensen, O. N. *Nature Reviews Molecular Cell Biology* **2006**, 7, 391-403.
- (3) Blackstock, W. P.; Weir, M. P. *Trends in Biotechnology* **1999**, *17*, 121-127.
- (4) Bonetta, L. *Nature* **2006**, *439*, 1017-1021.
- (5) Ghosh, R. Advanced Membrane Technology and Applications; John Wiley & sons, Inc., 2008.
- (6) Saxena, A.; Tripathi, B. P.; Kumar, M.; Shahi, V. K. Advances in Colloid and Interface Science 2009, 145, 1-22.
- (7) Wurm, F. *Nature Biotechnology* **2004**, 22 1393-1398.
- (8) Pavlou, A. K.; Reichert, J. M. *Nature Biotechnology* **2004**, 22, 1513-1519.
- (9) Clarke, W.; Hage, D. S. Separation and Purification Reviews 2003, 32, 19-60.
- (10) Kawai, T.; Saito, K.; Lee, W. Journal of Chromatography B 2003, 790, 131-142.
- (11) Zubay, G. *Biochemistry* 2nd Edition ed.; Macmillan Publishing Co., New York, NY, USA., 1988
- (12) Ghosh, R. *Journal of Chromatography A* **2002**, 952, 13-27.
- (13) Boschetti, E. *Journal of Chromatography A* **1994**, *658*, 207-236.
- (14) Liu, G.; Dotzauer, D. M.; Bruening, M. L. *Journal of Membrane Science* **2010**, *354*, 198-205.
- (15) Müller, W. Journal of Chromatography A **1990**, 510, 133-140.
- (16) Bhut, B. V.; Husson, S. M. Journal of Membrane Science **2009**, 337, 215-223.
- (17) Brandt, S.; Goffe, R. A.; Kessler, S. B.; O'Connor, J. L.; Zale, S. E. *Nature Biotechnology* **1988**, *6*, 779 782.
- (18) Shi, W.; Zhang, F.; Zhang, G. Journal of Chromatography A 2005, 1081, 156-162.
- (19) Arnau, J.; Lauritzen, C.; Petersen, G. E.; Pedersen, J. *Protein Expression and Purification* **2006**, *48*, 1-13.

- (20) Lichty, J. J.; Malecki, J. L.; Agnew, H. D.; Michelson-Horowitz, D. J.; Tan, S. *Protein Expression and Purification* **2005**, *41*, 98-105.
- (21) Hochuli, E.; Dobeli, H.; Schacher, A. Journal of Chromatography 1987, 411, 177-184.
- (22) Stiborova, H.; Kostal, J.; Mulchandani, A.; Chen, W. *Biotechnology and Bioengineering* **2003**, 82, 605-611.
- (23) Cattoli, F.; Sarti, G. C. Biotechnology Progress 2002, 18, 94-100.
- (24) Smith, D. B.; Johnson, K. S. Gene **1988**, 67, 31-40.
- (25) Skerra, A.; Schmidt, T. G. M. Biomolecular Engineering 1999, 16, 79-86.
- (26) Porath, J.; Carlsson, I. O.; Belfrage, G. *Nature* **1975**, 258, 598.
- (27) Porath, J. Trends in Analytical Chemistry 1988, 7, 254-259.
- (28) Graslund, S.; Nordlund, P.; Weigelt, J. Nature Methods 2008, 5, 135-146.
- (29) Porath, J. Protein Expression and Purification 1992, 3, 263-281.
- (30) Hochuli, E.; Bannwarth, W.; Döbeli, H.; Gentz, R.; Stüber, D. *Biotechnology* **1988** 6, 1321–1325
- (31) Hengen, P. Trends in Biochemical Sciences 1995, 20, 285–286.
- (32) Derewenda, Z. S. *Methods* **2004**, *34*, 354-363.
- (33) Westra, D. F.; Welling, G. W.; Koedijk, D. G. A. M.; Scheffer, A. J.; The, T. H.; Welling-Wester, S. *Journal of Chromatography B* **2001**, 760, 129-136.
- (34) Srinivasan, U.; Bell, J. A. *Journal of Biotechnology* **1998**, *62*, 163-167.
- (35) Guan, C. D.; Li, P.; Riggs, P. D.; Inouye, H. Gene **1988**, 67, 21-30.
- (36) Ferenci, T.; Klotz, U. Febs Letters **1978**, 94, 213-217.
- (37) Malhotra, A.; Richard, R. B. a. M. P. D. In *Methods in Enzymology*; Academic Press, 2009; Vol. Volume 463, pp 239-258.
- (38) http://www.neb.com/nebecomm/products/productE8021.asp (Binding Capacity 6 8 mg MBP-fusion protein / ml bed volume) (accessed March 21, 2011)

- (39) http://www.sigmaaldrich.com/etc/medialib/docs/Sigma/Datasheet/4/m9676dat. Par.0001.File.tmp/m9676dat.pdf (Maltoheptaose agarose resin binds a minimum of 6 mg of maltose binding protein per ml of packed resin) (accessed March 21, 2011)
- (40) http://www.gelifesciences.com/aptrix/upp00919.nsf/Content/78BDD97E3689F1 FFC1257628001D4242/\$file/28913633AB.pdf (Dextrin Sepharose chromatographic medium dynamic binding capacity 7-16 mg/ml medium) (accessed on March 21, 2011)
- (41) Skoog, D. A.; West, D. M.; Holler, F. J.; Crouch, S. R. Fundermetals of Analytical Chemistry; 8th edition ed.; Brooks/Cole, 2004.
- (42) Thommes, J.; Kula, M.-R. *Biotechnology Progress* **1995**, *11*, 357-367.
- (43) Kalghatgi, K.; Horvath, C. Journal of Chromatography A 1987, 398, 335-339.
- (44) Hashimoto, T. *Journal of Chromatography A* **1991**, *544*, 257-265.
- (45) Charcosset, C. Journal of Chemical Technology and Biotechnology **1998**, 71, 95-110.
- (46) Klein, E. *Journal of Membrane Science* **2000**, *179*, 1-27.
- (47) Roper, D. K.; Lightfoot, E. N. Journal of Chromatography A 1995, 702, 3-26.
- (48) Dai, J. H.; Bao, Z. Y.; Sun, L.; Hong, S. U.; Baker, G. L.; Bruening, M. L. *Langmuir* **2006**, 22, 4274-4281.
- (49) Sun, L.; Dai, J. H.; Baker, G. L.; Bruening, M. L. Chemistry of Materials **2006**, *18*, 4033-4039.
- (50) Jain, P.; Sun, L.; Dai, J. H.; Baker, G. L.; Bruening, M. L. *Biomacromolecules* **2007**, *8*, 3102-3107.
- (51) Jain, P.; Vyas, M. K.; Geiger, J. H.; Baker, G. L.; Bruening, M. L. *Biomacromolecules* **2010**, *11*, 1019-1026.
- (52) Bhut, B. V.; Christensen, K. A.; Husson, S. M. *Journal of Chromatography A* **2010**, *1217*, 4946-4957.
- (53) Yang, Q.; Ulbricht, M. *Macromolecules* **2011**, *ASAP*.
- (54) Milner, S. T. Science **1991**, 251, 905-914.
- (55) Bhat, R. R.; Tomlinson, M. R.; Wu, T.; Genzer, J. Advances in Polymer Science 2006, 198, 51-124.

- (56) Huang, W.; kim, J. B.; Bruening, M. L.; Baker, G. L. *Macromolecules* **2002**, *35*, 1175-1179.
- (57) Kent, M. S. Macromolecular Rapid Communications **2000**, 21, 243-270.
- (58) Jordan, R.; Graf, K.; Reigler, H.; Unger, K. K. *Chemical Communications* **1996**, *1996*, 1025-1026.
- (59) Huang, W. X.; Skanth, G.; Baker, G. L.; Bruening, M. L. *Langmuir* **2001** *17*, 1731–1736.
- (60) Jones, D. M.; Brown, A. A.; Huck, W. T. S. *Langmuir* **2002**, *18* 1265-1269.
- (61) Zhao, B.; Brittain, W. J. *Macromolecules* **2000**, *33*, 342-348.
- (62) Choi, I. S.; Langer, R. *Macromolecules* **2001**, *33*, 5361-5363.
- (63) Huang, X. Y.; Wirth, M. J. Analytical Chemistry **1997**, 69, 4577-4580.
- (64) Moon, J. H.; Swager, T. M. *Macromolecules* **2002**, *35*, 6086-6089.
- (65) Yang, H.; Ulbricht, M. Macromolecular Materials and Engineering 2008, 293, 419-427.
- (66) Wang, J.-S.; Matyjaszewski, K. *Journal of the American Chemical Society* **1995**, *117*, 5614-5615.
- (67) Matyjaszewski, K.; Xia, J. H. Chemical Reviews 2001, 101, 2921-2990.
- (68) Boyer, C.; Bulmus, V.; Liu, J. Q.; Davis, T. P.; Stenzel, M. H.; Barner-Kowollik, C. *Journal of the American Chemical Society* **2007**, *129*, 7145–7154.
- (69) Husemann, M.; Morrison, M.; Benoit, D.; Frommer, K. J.; Mate, C. M. *Journal of the American Chemical Society* **2000** *122*, 1844–1845.
- (70) Barbey, R.; Lavanant, L.; Paripovic, D.; Schuwer, N.; Sugnaux, C.; Tugulu, S.; Klok, H.-A. *Chemical Reviews* **2009**, *109*, 5437-5527.
- (71) Tugulu, S.; Silacci, P.; Stergiopulos, N.; Klok, H.-A. *Biomaterials* **2007**, 28, 2536-2546.
- (72) Ko, S.; Jang, J. *Biomacromolecules* **2007**, 8.
- (73) Cullen, S. P.; Liu, X.; Mandel, I. C.; Himpsel, F. J.; Gopalan, P. *Langmuir* **2008**, *24*, 913-920.
- (74) Kawakita, H.; H., M.; Nomura, K.; Uezu, K.; Akiba, I.; Tsuneda, S. *Journal of Porous Materials* **2007**, *14*, 387-391.

- (75) Singh, N.; Husson, S. M.; Zdyrko, B.; Luzinov, I. *Journal of Membrane Science* **2005**, 262, 81-90
- (76) Jain, P.; Dai, J.; Grajales, S.; Saha, S.; Baker, G. L.; Bruening, M. L. *Langmuir* **2007**, *23*, 11360-11365.
- (77) Kaubota, N.; Kounosu, M.; Saito, K.; Sugita, K.; Watanabe, K.; Sugo, T. *Biotechnology Progress* **1997**, *13*, 89-95.
- (78) Singh, N.; Chen, Z.; Tomer, N.; Wickramasinghe, S. R.; Soice, N.; Husson, S. M. *Journal of Membrane Science* **2008**, *311*, 225-234.
- (79) He, D.; Ulbricht, M. *Journal of Membrane Science* **2008**, *315*, 155-163.
- (80) Shi, W.; Shen, Y. Q.; Ge, D. T.; Xue, M. Q.; Cao, H. H.; Huang, S. Q.; Wang, J. X.; Zhang, F. B. *Journal of Membrane Science* **2008**, *325*, 801-808.
- (81) Gautrot, J. E.; Huck, W. T. S.; Welch, M.; Ramstedt, M. Applied Materials and Interfaces 2010, 2, 193-202.
- (82) Bao, Z. Y.; Bruening, M. L.; Baker, G. L. *Macromolecules* **2006**, *39*, 5251-5258.
- (83) Jain, P.; Dai, J. H.; Baker, G. L.; Bruening, M. L. *Macromolecules* **2008**, *41*, 8413-8417.

Chapter 2. An All-aqueous Route to Polymer

Brush-modified Membranes with

Remarkable Permeabilites and Protein

Capture Rates.

2.1. Introduction

Although rapid advances in biotechnology have greatly increased the synthesis and applications of recombinant proteins, isolation of these proteins remains a bottleneck in their production. Specific adsorption of proteins to ligands immobilized in packed columns is probably the most powerful step in protein purification. Nevertheless, high pressure drops, challenges in packing large columns and slow mass transfer may limit the utility of column-based separations. Membrane adsorbers provide an alternative for rapid protein isolation because flow through functionalized membrane pores rapidly transports the protein of interest to immobilized ligands. Moreover, scale-up of membrane separations by increasing surface area is relatively simple and causes little or no increase in pressure drop.

Despite the possibility of fast separations, however, membranes suffer from a modest binding capacity due to their low internal surface area relative to nanoporous beads. ¹⁶ In attempts to increase capacity, a number of groups grafted functionalized polymer chains to the

pores of the membrane. The chains contain multiple binding sites, and membranes modified with polymer brushes show high binding capacities and selective protein binding. ^{5,11,17-26} For example, Yang and Ulbricht grafted poly(2-hydroxyethyl methacrylate) (poly(HEMA)) in poly(ethylene terephthalate) track etched membranes and then grew poly(2-lactobionamidoethyl methacrylate) from poly(HEMA) to form a well-defined comb-like glycopolymer layer. Such membranes capture as much as 24 mg/cm³ of lectins that specifically bind to galactose. ¹⁹ Bhut and Husson grafted poly(2-dimethylaminoethyl methacrylate) brushes in regenerated cellulose to form anion-exchange membranes with lysozyme binding capacities of 130 mg/cm³. These membranes successfully captured anthrax protective antigen protein from E-*coli* cell extracts. ²⁷

The most common method for specific protein isolation exploits interactions between polyhistidine-tagged (His-tagged) protein and metal-ion complexes. Several recent studies demonstrate specific binding of His-tagged proteins to metal-ion complexes in polymer brushes.

11,18,20-22,28 We showed that growth of poly(2-(methacryloyloxy)ethyl succinate (poly(MES)) brushes in nylon membranes and functionalization of the brushes with nitrilotriacetate (NTA)-Ni²⁺ complexes leads to membranes that isolate His-tagged cellular retinaldehyde binding protein directly from cell extracts.

Nevertheless, modification of polymeric membranes is challenging because the membranes often dissolve or swell in organic solvents.

This chapter describes a simple, rapid, and completely aqueous procedure for growth and functionalization of polymer brushes in nylon, polyethersulfone (PES), and polyvinylidine

fluoride (PVDF) membranes. The approach combines adsorption of a macroinitiator, polymerization of MES (a water-soluble, acid-containing monomer) from the initiator, and subsequent aqueous derivatization. Although we demonstrated these different steps previously, ^{21,29} this is the first application of macroinitiator adsorption to create protein-adsorbing membranes. Most importantly, the brushes grown from these initiators behave very differently from brushes grown from silane-based initiators immobilized in membranes, presumably because of a lower density of grafted polymer chains. Compared to grafting using a trichlorosilane initiator, the macroinitiator-modified membranes require much shorter polymerization times (5 min versus 1 h) to achieve similar protein-binding capacities. Moreover, when using the macroinitiators, modified polymer membranes have 4-fold less hydraulic resistance than membranes prepared with the trichlorosilane initiator. Thus, these new systems are attractive for rapid purification of His-tagged protein directly from cell extracts. Remarkably, lysozyme capture in these membranes can occur during a ~35 ms residence time.

2.2. Experimental Section

2.2.1. Materials

Hydroxylated nylon (LoProdyne® LP, Pall, 1.2 μm pore size, 110 μm thick), nylon (GE, non-hydroxylated, 1.2 μm pore size, average thickness 95 μm), polyethersulfone, (GE, 1.2 μm pore size, average thickness 130 μm), hydrophilic PVDF (Millipore, 0.45 μm pore size, 115 μm thick), and regenerated cellulose membranes (Whatman, RC 60 – 1 μm pore size) were cut into 25 mm-diameter discs prior to use. Coomassie protein assay reagent (Thermo Scientific), Histidine₆-tagged Ubiquitin (HisU) (human recombinant, Enzo Life Sciences), Concanavalin A from *Canavalia ensiformis* (Jack bean) Type IV (Con-A, Sigma Aldrich), tris[2-

(dimethylamino)ethyl]amine (Me₆(TREN), ATRP Solutions), and other chemicals from Sigma-Aldrich were used as received unless noted otherwise. Trichlorosilane initiator (11-(2-bromo-2-methyl)propionyloxy)-undecyltrichlorosilane), and the macroinitiator [(poly(2-(trimethylammonium iodide)ethyl methacrylate-co-2-(2-bromoisobutyryloxy)ethyl acrylate)] were synthesized according to literature procedures. Buffers were prepared using analytical grade chemicals and deionized (Milli-Q, 18.2 M Ω cm) water.

2.2.2. Initiator attachment

Membranes discs were cleaned for 10 min with UV/ozone, and placed in a homemade teflon cell that exposed an external membrane surface area of 3.14 cm². (In a few cases we used larger membranes and holders that exposed 11.4 cm² external surface area.) The macroinitiator solution (2 mg/mL in water) was then passed through the membrane for 10 min at ~1 mL/min using a peristaltic pump, and the membrane was rinsed with 20 mL of water at the same flow rate before drying in a stream of N₂. For membranes other than hydroxylated nylon, prior to adsorption of the macroinitiator a poly(sodium 4-styrene sulfonate) (PSS, Mw ~ 70 000) layer was deposited by passing 10 mL of 0.02 M aqueous PSS (containing 0.5 M NaCl) through the membrane at 1 mL/min. Water (10 mL) was pumped through the membrane after deposition of PSS, followed by the macroinitiator and a subsequent 10 mL water rinse. Trichlorosilane initiator attachment occurred by circulating a 1 mM initiator solution in 20 mL of anhydrous THF through the clean nylon membrane for 2 h at a flow rate of 3 mL/min, followed by subsequent rinsing with 20 mL THF and 20 mL of ethanol. The membrane was dried under a steam of N₂ prior to polymerization.

2.2.3. Polymer brush synthesis

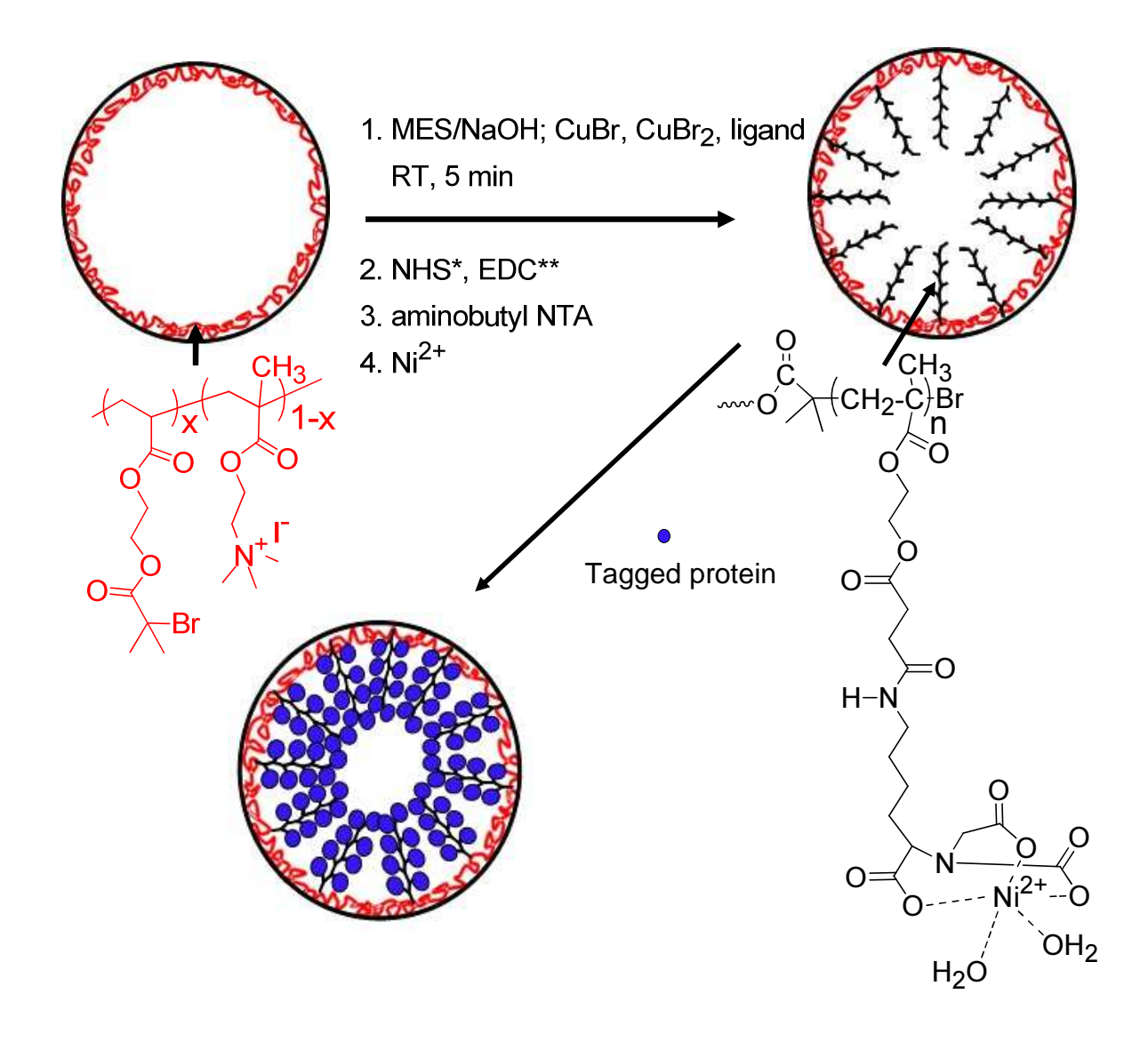


Figure 2.1. Schematic showing macroinitiator immobilization within membrane pores, polymerization of MES from an initiator-modified membrane, derivatization of poly(MES) with NTA-Ni²⁺ complexes and protein binding to such polymer brushes.

Using our prior procedure, ^{21,32} poly(MES) brushes were grown from membranes coated with initiators. A 10-mL mixture of neat MES monomer and 1 M aqueous NaOH (1:1, v/v) was degassed with three freeze-pump-thaw cycles. A 1 mL solution of anhydrous dimethyl formamide (DMF) containing CuBr (2 mM), CuBr₂ (1 mM), and Me₆(TREN) (6 mM) was

similarly degassed, and in a N_2 -filled glove bag, this solution of catalyst was mixed with the monomer/NaOH solution. Polymerization of MES within the pores of the membranes (Figure 2.1) occurred in a N_2 -filled glove bag by circulating the polymerization/catalyst solution through the initiator-modified membrane at a flow rate of 1 mL/min. *Unless mentioned otherwise, the polymerization time for membranes was 5 min.* Immediately after polymerization, 20 mL of ethanol followed by deionized water (20 mL) were passed through the membrane at ~2 mL/min. In the case of polymeric membranes other than hydroxylated nylon, the catalyst salts and ligand were added directly to the monomer-solvent mixture during the degassing process to avoid the presence of DMF, which may dissolve membranes like PES. Functionalization of the poly(MES) side chains with NTA-metal ion complexes occurred as reported previously (Figure 2.1). 21,32

Attenuated total reflectance Fourier transform infrared (ATR-FTIR) spectroscopy (Perkin Elmer Spectrum One Instrument, air background) as well as field-emission scanning electron microscopy (FESEM, Hitachi S-4700II) verified film growth on polymer membranes.

2.2.4. Synthesis of multilayer polyelectrolyte films derivatized with NTA

This procedure was adopted from a previous report. The membrane was cleaned with UV/ozone for 10 min, and 10 mL of 0.02 M aqueous PSS solution ($M_W \sim 70~000$, containing 0.5 M NaCl) was passed through the membrane at 1 mL/min. PSS deposition was followed by passage of 0.02 M poly(allylamine hydrochloride) (PAH, $M_W \sim 56~000$, containing 0.5 M NaCl, pH adjusted to 4.0) and subsequently 0.02 M poly(acrylic acid) (PAA, $M_W \sim 90~000$, containing

0.5 M NaCl, pH adjusted to 4.0). Water (10 mL) was passed through the membrane after deposition of each polyelectrolyte layer. Polymer concentrations are given with respect to repeating unit, and pH values were adjusted with NaOH or HCl. Membranes containing PSS/PAH/PAA films were then dried under a stream of N₂, and a solution containing NHS/EDC (0.1 M of each in water) was circulated through the membranes for 30 min followed by rinsing with water and ethanol, 20 mL each. An aqueous solution of NTA (0.1 M, pH 10.2) was then flowed through the NHS-modified membranes for 30 min, and the membrane was subsequently rinsed with 20 mL of water. Finally, the NTA-Cu²⁺ complex was formed by circulating aqueous 0.1 M CuSO₄ through the membrane for 2 h followed by rinsing with water and ethanol (20 mL each). The membrane was dried under a stream of N₂ and used for protein binding studies.

2.2.5. Protein binding

A solution of lysozyme (0.30 or 1.0 mg/mL) in 20 mM phosphate buffer (pH 7.4) was pumped through the poly(MES)-modified membrane using a peristaltic pump (flow rate of 1 or 30 mL/min), and the permeate was collected for analysis at specific time intervals. Subsequently, the membrane was rinsed with 20 mL of washing buffer I (20 mM phosphate buffer with 0.1 % Tween 20, pH 7.4) followed by 20 mL of phosphate buffer. The protein was then eluted using 5-10 mL of 20 mM phosphate buffer (pH 7.4) containing 1 M KSCN.

Similar procedures with different buffers and eluents were used for Con A and HisU binding studies. In case of HisU, the washing buffer (washing buffer II, 20 mM phosphate buffer containing 0.1% Tween-20 surfactant and 0.15 M NaCl) and elution buffer (0.5 M NaCl and 0.5 M imidazole in 20 mM phosphate buffer) were maintained at pH 7.4. For Con A, a

solution of 0.30 or 0.10 mg protein/mL was made in 20 mM phosphate buffer of pH 6 to avoid protein aggregation. The washing buffer II and elution buffer (20 mM phosphate buffer containing 50 mM EDTA) were also maintained at pH 6. For Con A binding, the membrane could be reloaded with Cu²⁺ by passing a 0.1 M CuSO₄ solution through the membrane and rinsing prior to reuse. The concentrations of protein in loading, rinsing, and eluate solutions were determine using a Bradford assay as described below. In each case, 3 membranes were individually tested, and the average binding capacity is reported. (For HisU only 2 measurements were performed due to the high cost of the protein.) Error bars and reported uncertainties are standard deviations.

2.2.6. Quantification of protein binding (Bradford assay)

To determine the amount of protein in loading, rinsing, or eluent solutions, 30 μ L of permeate was added to 1.5 mL of a solution of Coomassie reagent, and the mixture was shaken a few times and allowed to react for 10 min at room temperature. The UV/Vis absorbance spectra of these solutions were then obtained with a Perkin-Elmer UV/Vis (model Lambda 40) spectrophotometer. Calibration curves for the absorbances of lysozyme, Con A or His U solutions at 595 nm were prepared using a series of protein solutions (concentration range of 0 to 0.3 mg of protein per mL) that were mixed with Coomassie reagent in a 30 μ L to 1.5 mL ratio. All spectra were measured against a Coomassie reagent blank.

2.2.7. Protein separation from a cell extract and determination of protein purity

His-tagged *myo*--inositol-1-phosphate synthase (MIPS) was over-expressed in *E.coli* cells by the research group of Professor James Geiger. The cells were lysed with sonication in 20 mM, pH 8 phosphate buffer that contained 10 mM imidazole and 300 mM NaCl, and centrifuged at 4

^oC. Supernatant (5 mL) was pumped thorough the poly(MES)-NTA-Ni²⁺-modified nylon membrane at room temperature at a flow rate of 1.5 mL/min. Subsequently the membrane was rinsed with 20 mL washing buffer II at pH 8 followed by 20 mL washing buffer III (pH 8, 20 mM phosphate buffer with 45 mM imidazole and 0.15 M NaCl), and the bound protein was eluted with 10 mL (2 mL fractions) of 20 mM, pH 8 phosphate buffer with 0.5 M NaCl and 0.5 M imidazole. The purity of the eluted protein was determined by sodium dodecyl sulfate-polyacrylamide gel electrophoresis (SDS-PAGE). A 4-20% gradient gel obtained from Bio-Rad was used, and the protein bands were visualized using standard silver staining ³⁴ or Coomassie blue staining protocols. ³⁵

2.2.8. Determination of hydraulic permeability

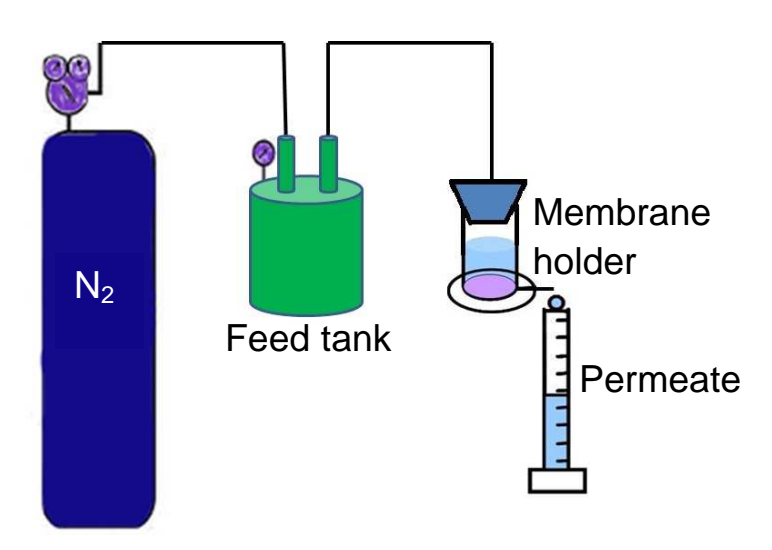


Figure 2.2. Apparatus for measuring hydraulic permeability of the membrane.

A pressurized feed tank connected to a sealed teflon membrane holder (similar to an amicon cell) was used to determine the pure water and buffer permeabilities before and after

modification of the membrane (Figure 2.2). The feed tank was filled with water or buffer, the system was pressurized with N_2 to 0.68 atm (10 psig), and permeate was collected over defined time periods. Three measurements of permeate flux were recorded for 3 different membranes with each modification, and the reported values are the averages of these data.

2.2.9. Determination of the amount of Cu^{2+} in the membrane

A calibration curve was created by measuring the absorbance of $CuSO_4$ standard solutions in 50 mM EDTA (pH 7.4) using a Perkin-Elmer UV/Vis (model Lambda 40) spectrophotometer, and a sample solution was obtained by eluting Cu^{2+} from poly(MES)-NTA- Cu^{2+} -coated membranes with 7.0 mL of 50 mM EDTA (pH 7.4). The amount of Cu^{2+} in the solution was calculated from its absorbance at 733 nm using the calibration curve.

2.3. Results and Discussion

2.3.1. Synthesis and characterization of polymer brushes in nylon membranes

Based on prior work in our group²⁹ and preliminary studies on polymerization from macroinitiators adsorbed on Au-coated wafers (see the appendix), we developed methods to grow polymer brushes from adsorbed macroinitiators in membranes. To create initiation sites, we simply pass a macroinitiator solution through the unmodified membrane and rinse the system with water. Hydrophobic interactions between the backbones of the macroinitiator and the nylon membranes presumably provide strong adsorption of the macroinitiator. After a subsequent 5-min polymerization by pumping a MES/catalyst solution through the membrane, ATR-IR spectra

clearly show a carbonyl peak at 1740 cm⁻¹ (Figure 2.3 (b)), consistent with the presence of poly(MES) in the membrane.

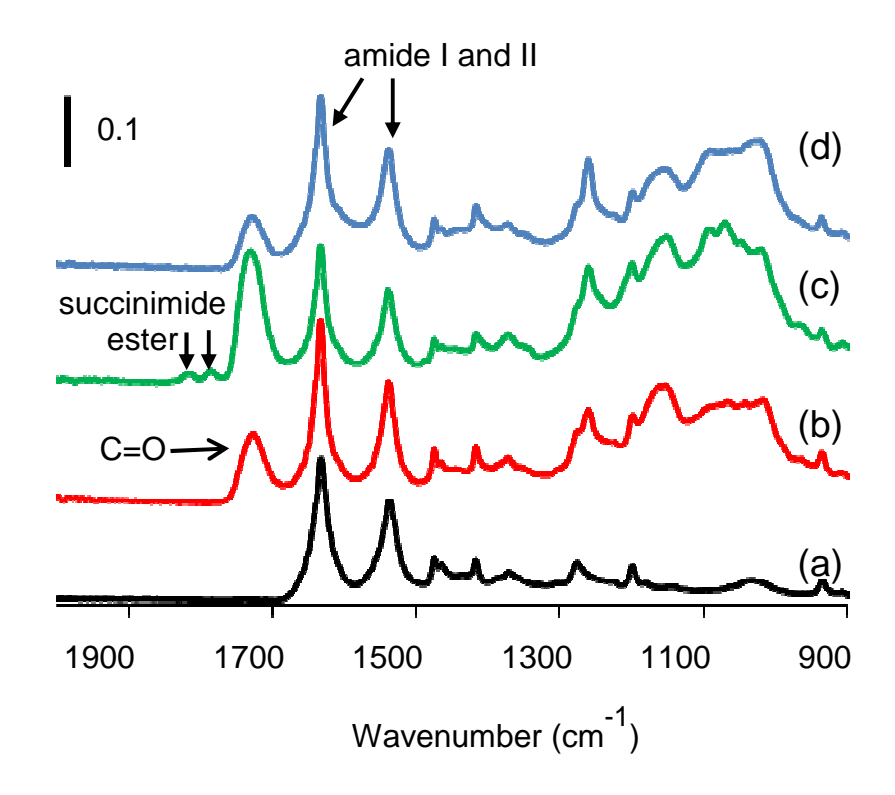


Figure 2.3. ATR-FTIR spectra of a hydroxylated nylon membrane before (a) and after the following modifications: (b) formation of poly(MES) brushes in the pores of the membrane; (c) activation of the poly(MES) with NHS/EDC; and (d) reaction with aminobutyl-NTA.

Remarkably, the macroinitiator adsorption is sufficiently robust to allow reuse of poly(MES)-modified membranes at least 5 times for protein adsorption (Figure 2.4). (We discuss protein binding studies in much more detail below.)

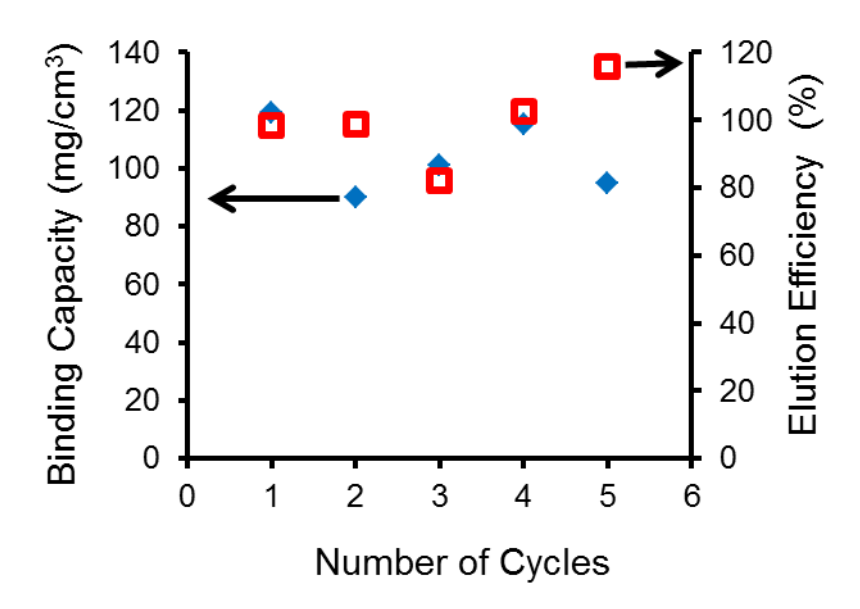


Figure 2.4. Binding capacities (blue diamonds) and elution efficiencies (red hollow squares) for 5 cycles of lysozyme adsorption and elution on a single hydroxylated nylon membrane modified with poly(MES). Flow rate- ~ 1 mL/min; Feed concentration- 0.3 mg/mL; elution buffer- 1 M KSCN in 20 mM phosphate buffer, pH 7.4, Elution efficiency is the amount of protein in the eluent divided by the amount of adsorbed protein as determined from the breakthrough curve.

Activation of the carboxylic acid groups of poly(MES) followed by reaction with aminobutyl NTA and complexation of a metal ion (Figure 2.1) lead to polymer brushes containing immobilized metal ion complexes capable of binding protein. ATR-IR spectra confirm the derivatization process (Figure 2.3). The IR spectrum of the bare nylon membrane (Figure 2.3 (a), all spectra were obtained with an air background) contains dominant amide I and amide II peaks at 1630 and 1533 cm⁻¹, respectively. Reaction of the —COOH groups of poly(MES) with a mixture of EDC and NHS in water converts these groups to succinimidyl esters that give rise to absorption bands at 1810 and 1779 cm⁻¹ and also increase the absorption around 1730 cm⁻¹ (Figure 2.3 (c)). Subsequent reaction of the EDC/NHS-activated poly(MES)

with aminobutyl-NTA results in a loss of the absorbances due to the succinimidyl esters (Figure 2.3 (d)). Additionally, a new absorbance at 1680 cm⁻¹ results from a combination of carboxylate groups of NTA and amide bonds formed between poly(MES) and NTA. However, this signal is not distinct because of the large amide peaks in this region. An additional broad absorbance around 1600 cm⁻¹ could stem from carboxylate groups of either NTA or hydrolyzed active esters. Reflectance FTIR spectra of films on Au better demonstrate the absorbances due to NTA. After exposing the brush to Cu²⁺, there is no observable change in the IR spectrum. However, the membrane appears blue, and elemental analysis demonstrates the presences of Cu²⁺ (see below).

SEM images also provide evidence for the polymerization and derivatization process (Figure 2.5). The SEM image of the bare nylon membrane (1.2 μ m pore size, Figure 2.5 (a)) contains many open pores. After a 5 min polymerization of MES the structure appears less porous, presumably because poly(MES) coats much of the membrane (Figure 2.5 (b)). Derivatization of the poly(MES) with NTA-Ni²⁺/Cu²⁺ leads to more extensive coverage of membrane pores (Figure 2.5 (c)).

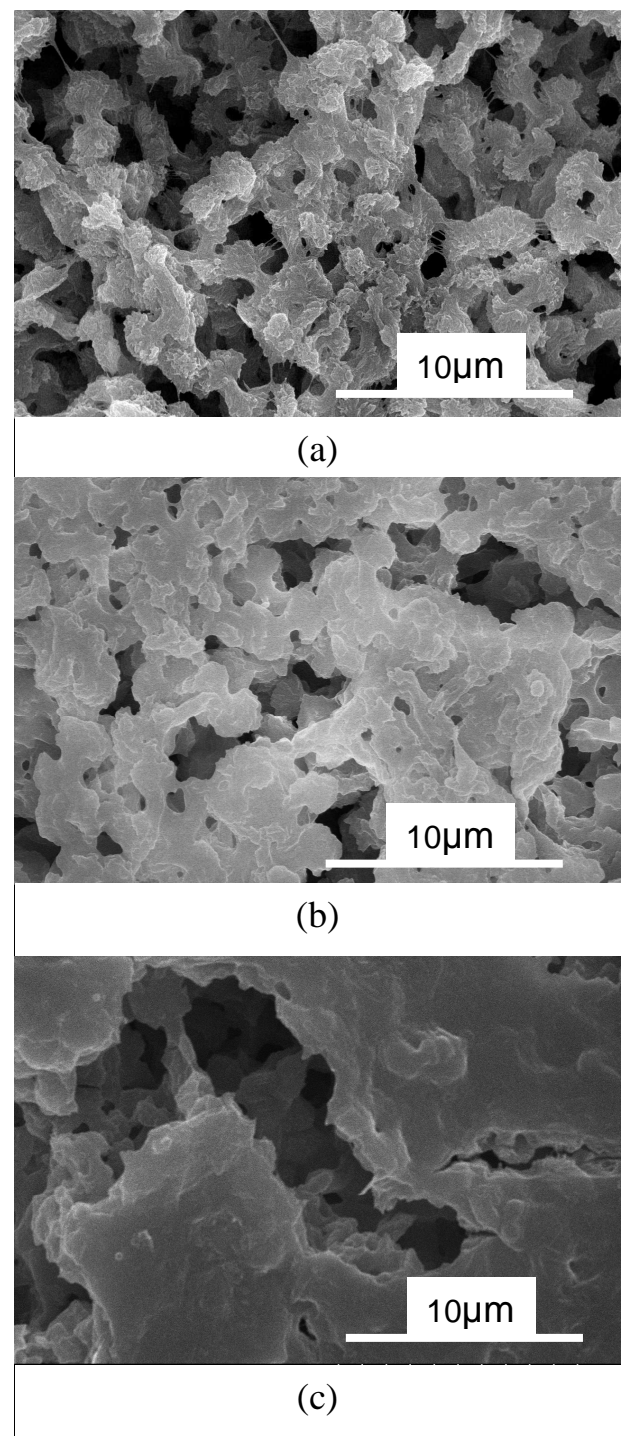


Figure 2.5. SEM images of (a) a bare nylon membrane with nominal 1.2 μm pores, (b) a similar membrane modified with poly(MES), and (c) a membrane coated with poly(MES)-NTA-Cu²⁺ polymer brushes.

Because the amount of polymer in the membranes is low and ATR-IR spectra are qualitative, monitoring the growth of poly(MES) in the membrane is difficult. We can, however, readily determine the amount of Cu²⁺ that binds to membranes modified with poly(MES)-NTA brushes. Figure 2.6 shows that the amount of Cu²⁺ captured in these membranes increases rapidly with the time allotted for polymerization of MES from the macroinitiator. However, after 30 min of polymerization, the Cu²⁺-binding capacity reaches a plateau at 25 mg of Cu²⁺ per cm³ of membrane. The initial increase reflects growth of polymer in the membrane, whereas the subsequent plateau may stem from termination of polymerization or steric hindrance to Cu²⁺ binding.

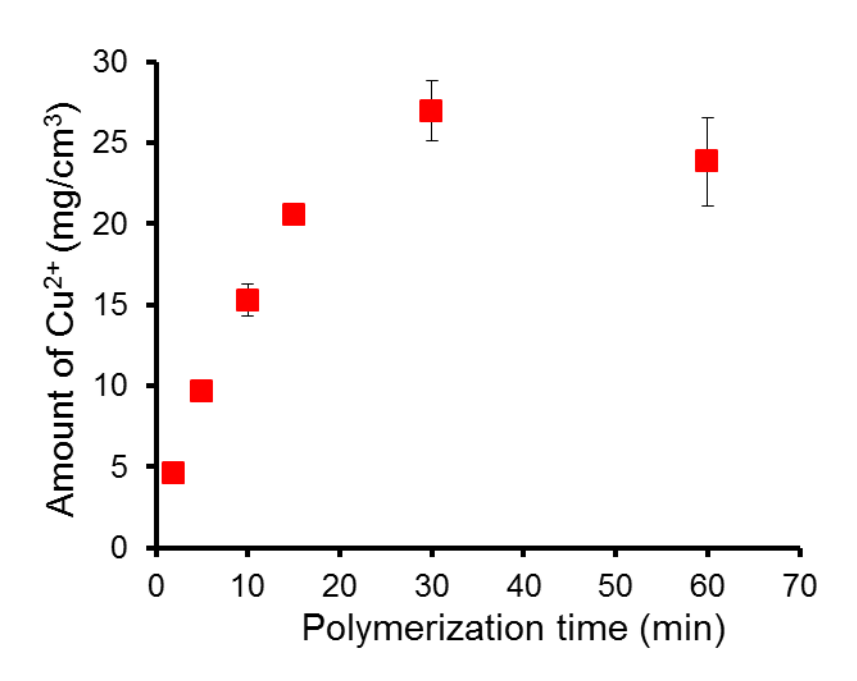


Figure 2.6. Cu²⁺ binding capacities of poly(MES)-NTA-modified nylon membranes as a function of polymerization time. Poly(MES) was grown from adsorbed macroinitiator.

As we show below, 5 min of MES polymerization is sufficient to achieve maximum protein binding. After modification with NTA, the membranes modified with a 5-min polymerization time bind 10 ± 0.4 mg of Cu^{2+} per cm³ of membrane. Assuming every NTA binds one Cu^{2+} ion and every carboxylic acid group of poly(MES) reacts with one aminobutyl NTA molecule, this amount of Cu^{2+} implies 35 mg of poly(MES) (before derivatization) per cm³ of the membrane (the membrane volume, 0.035 cm³ includes both porous and nonporous regions). For comparison, maximum protein binding when growing poly(MES) brushes from trichlosilane initiator-modified nylon membranes requires 1 h of polymerization, and Cu^{2+} analysis suggests that this system contains 110 mg poly(MES)/cm³ of membrane.

2.3.2. Membrane Permeability

Effective membrane adsorbers should have both a high binding capacity and a reasonably high permeability. At 0.68 atm of transmembrane pressure, a bare hydroxylated nylon membrane with a 1.2 μ m nominal pore size has a pure water hydraulic permeability of 118 \pm 1 mL/(cm² min atm), but this value drops to 85 \pm 4 mL/(cm² min atm) after adsorption of the macroinitiator and a 5-min polymerization of MES. The polymer brushes presumably decrease pore diameters and reduce permeability. Because permeability is proportional to pore diameter raised to the fourth power, even thin films cause a significant drop in flux. After immobilization of aminobutyl NTA, the hydraulic water permeability decreases to 69 \pm 4 mL/(cm² min atm) due to the increase in brush thickness. Complexation of Cu²⁺ or Ni²⁺ by NTA does not significantly

alter the permeability (76 \pm 6 mL/(cm² min atm)). Notably, however, even after growth of poly(MES) for 5 min, derivatization with aminobutyl NTA, and formation of the NTA-metal ion complex, the pure water flux only decreases by 35%.

For nylon membranes modified with poly(MES) brushes grown from trichlorosilane initiators, the water permeability is only 21 ± 4 mL/(cm² min atm), 1/4 of that for the macroinitiator-based modification. The trichlorosilane-based system requires longer polymerization times (1 h versus 5 min) to achieve binding capacities similar to those of the macroinitiator-based membranes, and the longer time results in more polymerization and smaller pore diameters. After derivatization with NTA-metal ion complexes, the trichlorosilane-based modification still gives 4-fold lower flux than growth of brushes from the macroinitiator and subsequent derivatization.

Figure 2.7 shows the water permeability of nylon membranes as a function of the time allowed for MES polymerization from adsorbed macroinitiators. The permeability decreases continuously with polymerization time, and after 30-45 min of polymerization, the macroinitiator-based membranes have a permeability similar to membranes modified with the trichlorosilane initiator and a 1-h polymerization. This suggests that 30-45 min of polymerization from the macroinitiator gives the same amount of poly(MES) in the membrane as the 1-h polymerization from the trichlorosilane initiator, which is consistent with Cu^{2+} binding capacities. A 30 min polymerization from the macroinitiator leads to binding of 27 ± 2 mg of Cu^{2+} per cm³ of membrane, whereas 1 h polymerization from immobilized trichlorosilane initiators gives 29 ± 4 mg/cm³. We speculate that the poly(MES) chains are more separated

and swollen when grown from the macroinitiator (at least initially), so binding a given amount of protein requires less polymer brush, which leads to a lower hydraulic resistance.

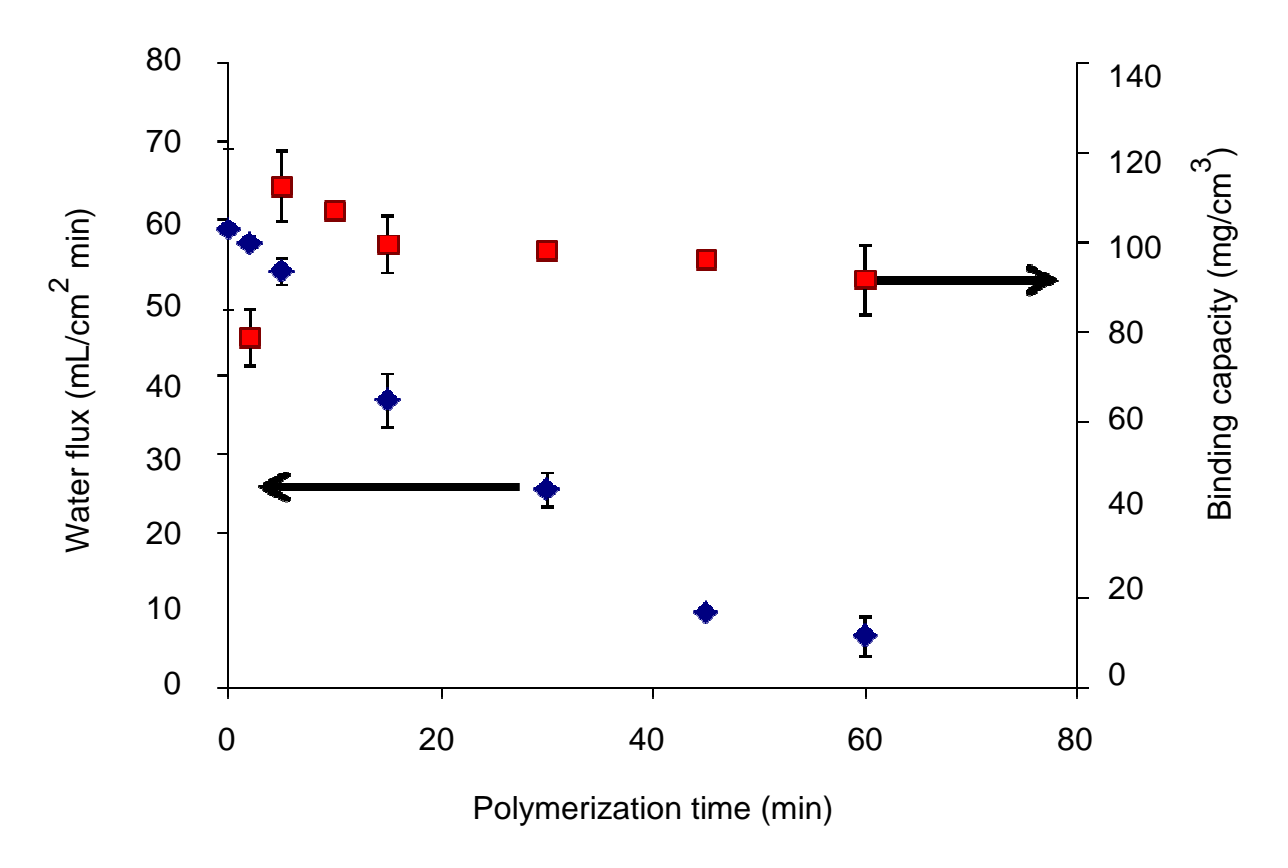


Figure 2.7. Evolution of the lysozyme binding capacity (red squares) and hydraulic permeability (blue diamonds) of nylon membranes with the time allowed for growth of poly(MES) brushes. Hydraulic permeability was obtained at a pressure of 0.68 atm, and binding amounts were determined from breakthrough curves during passage of 15 mL of 0.3 mg/mL lysozyme solution through the membrane.

Because protein binding typically occurs in buffers and not pure water, we also examined the permeability of membranes to pH 7.4, 20 mM phosphate buffer. By deprotonating the acid groups of polymer brushes, buffers can effect a dramatic increase in brush swelling and decrease flux. $^{36-38}$ At 0.68 atm, the macroinitiator-based, poly(MES)-modified nylon membrane exhibits a buffer permeability of 37 ± 3 mL/(cm² min atm), about 1/2 the initial pure water permeability.

However, after passing buffer through the membrane, the pure water permeability drops to $18 \pm 3 \text{ mL/(cm}^2 \text{ min atm})$. In subsequent measurements, the buffer permeability is still $37 \pm 3 \text{ mL/(cm}^2 \text{ min atm})$ and the pure water permeability remains $18 \pm 3 \text{ mL/(cm}^2 \text{ min atm})$. After synthesis, pure water may not be sufficient to deprotonate the brush, so the water flux is higher than the buffer flux. In contrast, after deprotonation in buffer, the brush likely remains ionized in pure water so hydraulic permeability decreases. Compared to pure water, the high ionic strength (50 mM) of the buffer collapses deprotonated brushes somewhat, so flux is higher in the buffer than pure water once deprotonation occurs. Relative to the buffer solution, flux increases 1.5-fold in 0.1 M NaCl, further indicating that the brushes collapse at high ionic strength to enhance permeability. The buffer flux through trichlorosilane-based poly(MES)-modified membranes (8 $\pm 3 \text{ mL/(cm}^2 \text{ min atm})$) is 4- to 5-fold less than that of macroinitiator based poly(MES) modified membranes.

2.3.3. Lysozyme Binding

Lysozyme binds to poly(MES) by ion exchange and provides a convenient, inexpensive probe of how protein binding varies with polymerization time in poly(MES)-modified membranes. Figure 2.7 shows lysozyme binding determined from breakthrough curves for a series of membranes prepared using different MES polymerization times. The lysozyme binding increases when going from a 2-min to a 5-min polymerization, presumably because of more binding sites in thicker brushes. However, with further polymerization the brushes likely become more crowded so the interior adsorption sites are less accessible to proteins and binding does not increase. Longer brushes may even block protein access to relatively small pores and

decrease binding. The trend in Figure 2.7 is very different from that for the amount of Cu²⁺ bound by poly(MES)-NTA (Figure 2.6) because Cu²⁺ is much smaller than proteins.

Nevertheless, binding 113 ± 8 mg lysozyme/cm³ of membrane with only 5 min of polymerization is comparable to 1 h polymerization using a similar membrane and a trichlorosilane initiator (118 ± 8 mg/cm³). Remarkably, the macroinitiator method allows membrane modification in much less time (10 min as opposed to 2 h for initiator attachment prior to rinsing, and 5 min as opposed to 1 h for polymerization) than the trichlorosilane initiator method and gives the same binding and a 4-fold greater permeability. The binding determined from lysozyme elution from the poly(MES)-modified membrane (5-min polymerization from the macroinitiator) is 108 ± 13 mg/cm³, comparable to that measured from break through curves.

We note that the binding amounts reported in this section resulted from passing only 15 mL of 0.3 mg/mL lysozyme solution through the membrane, which is not sufficient to completely fill all binding sites. We maintained this procedure to compare Figure 2.7 with similar data reported for the trichlorosilane system. Figure 2.8 shows the breakthrough curves for the macroinitiator-based system. In the remainder of the manuscript, binding capacities are those at saturation, unless mentioned otherwise.

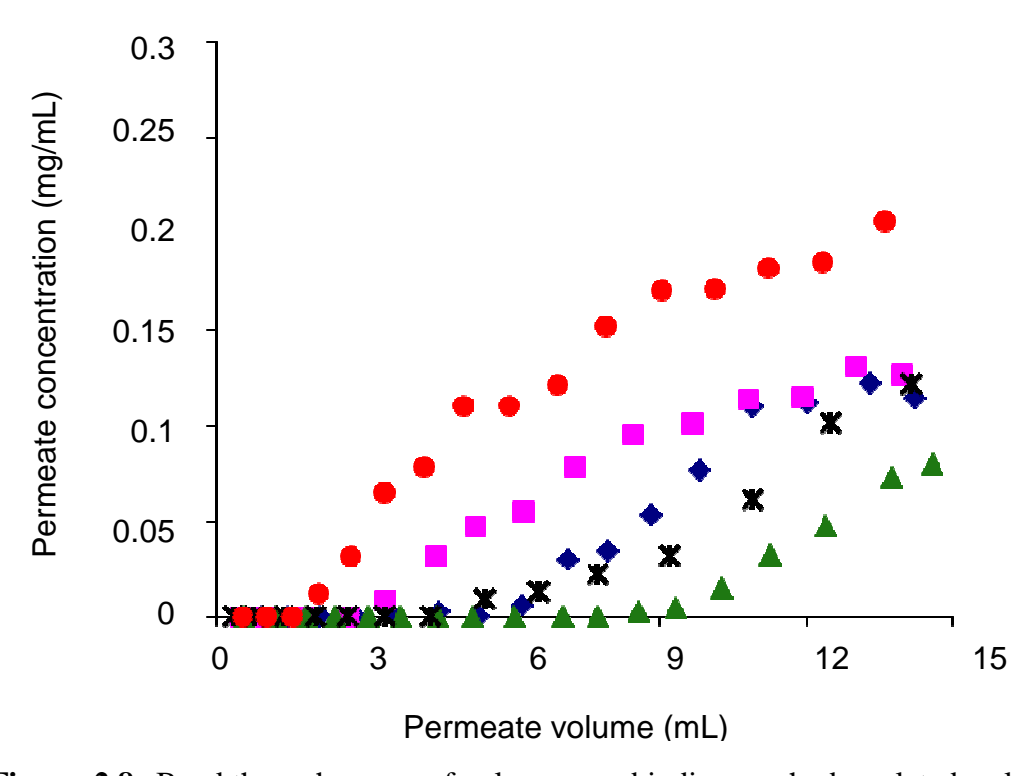


Figure 2.8. Breakthrough curves for lysozyme binding on hydroxylated nylon membranes containing poly(MES) grown for 2 min (red circles), 5 min (green triangles), 10 min (black stars), 15 min (blue diamonds), 1 hr (pink squares). The curves obtained for 30 min and 45 min were similar to that of a 1 hr polymerization and, hence, not shown in the graph. Flow rate -1 mL/min; feed solution concentration -0.3 mg/mL.

The performance of the macroinitiator (the ability to initiate polymerization) diminishes with time. ²¹ In Figure 2.9, we compare lysozyme binding for 2 poly(MES) modified membranes, one with MES grown from a fresh macroinitiator (used within a week of its synthesis, binding of 119 mg lysozyme/cm³), and a second membrane modified with a 6 month old macroinitiator (binding of 96 mg lysozyme/cm³). The results suggest that initiation efficiency declines as the macroinitiator ages. All experiments in this manuscript were performed

with macroinitiator used within 10 months of synthesis. Note that these binding capacities are also not at the saturation.

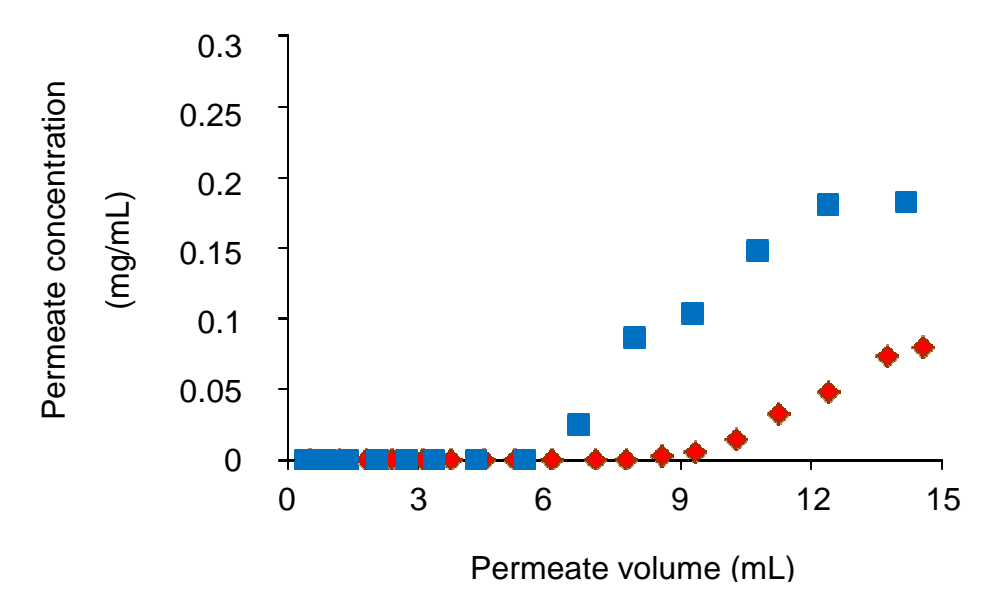


Figure 2.9. Breakthrough curves for lysozyme binding to hydroxylated nylon membranes containing poly(MES) grown from adsorbed macroinitiator which was < 1 month old (red diamonds) and about 6 months old (blue squares).

2.3.4. Protein binding capacity as a function of flow rate

Membrane adsorbers are particularly attractive for rapid separations because radial diffusion distances are short, and convection brings proteins to binding sites. Moreover, rapid flow rates can occur with only modest pressure drops. ^{13,14} We compared the breakthrough curves for lysozyme binding to poly(MES)-modified membranes at flow rates of 1 and 30 mL/min. These flow rates correspond to linear velocities of 19 cm/h and 570 cm/h, and residence times of 1000 msec and 35 msec, respectively. (Note that these residence times assume a membrane porosity of 50%, whereas the linear velocity is that above the membrane.) As Figure 2.10 shows, the breakthrough curves are essentially independent of the flow rate over this range, so a 30-fold increase in linear velocity does not lead to early breakthrough and a change in

the dynamic binding capacity. Thus, neither diffusion nor binding kinetics limit protein binding at these linear velocities, and adsorption occurs in less than 35 msec. The membrane geometry likely determines the shape of the breakthrough curves, as breakthrough will occur sooner for large pores than smaller ones.

Recommended linear velocities through typical commercial gels are 150 cm/h³⁹ (compared to 570 cm/h for membranes), and the binding capacity for His-tagged proteins in such resin-packed columns is about 2-fold less than the membranes in this study (40-50 mg/mL of His-tagged protein compared to 85 mg/cm³ in the membrane). Thus the brush-modified membranes have the potential to greatly increase the rate of protein binding.

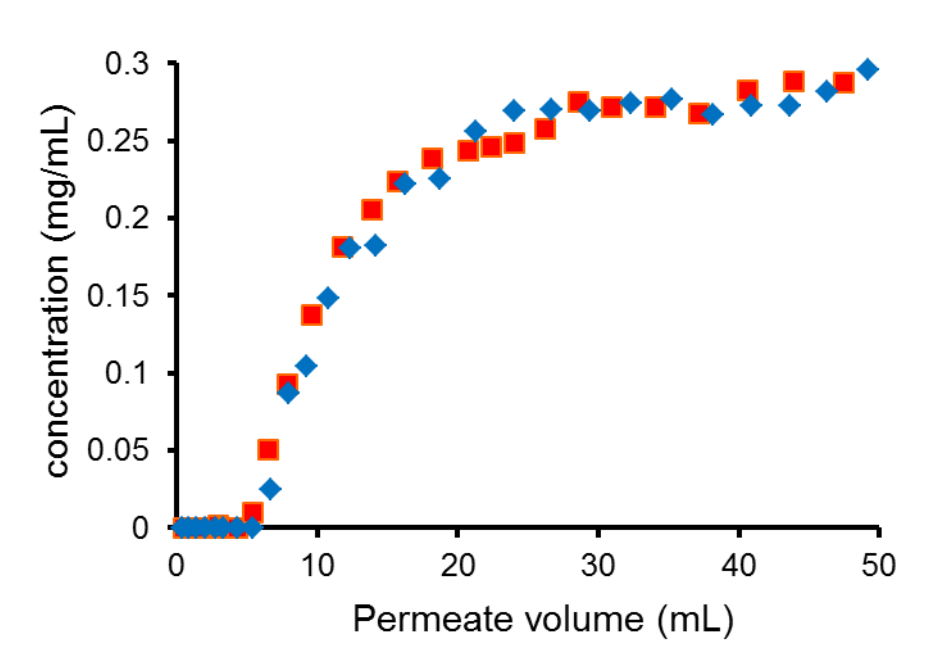


Figure 2.10. Breakthrough curves for the passage of 0.3 mg/mL lysozyme through a poly(MES)-modified nylon membrane at flow rates of 1 mL/min (blue diamonds) and 30 mL/min (red squares). Similar curves were obtained for two different membranes.

2.3.5. Scaling up poly(MES)-modified membranes

The high permeability of membranes modified using macroinitiators should permit the use of membrane stacks to increase binding capacity without creating high pressure drops. ⁴⁰ To test this concept, we polymerized MES for 5 min in 5 different membranes and stacked these membranes in a membrane holder (Figure 2.11). The pure water flux through this stack was $5 \pm 0.06 \text{ mL/(cm}^2 \text{ min atm})$, which is ~20-fold less than the flux through a single membrane ($85 \pm 4 \text{ mL/(cm}^2 \text{ min atm})$). The flux was 1/4 of the expected value, possibly because misalignment between pores in adjacent spongy membranes leads to high pressure drops between membranes.

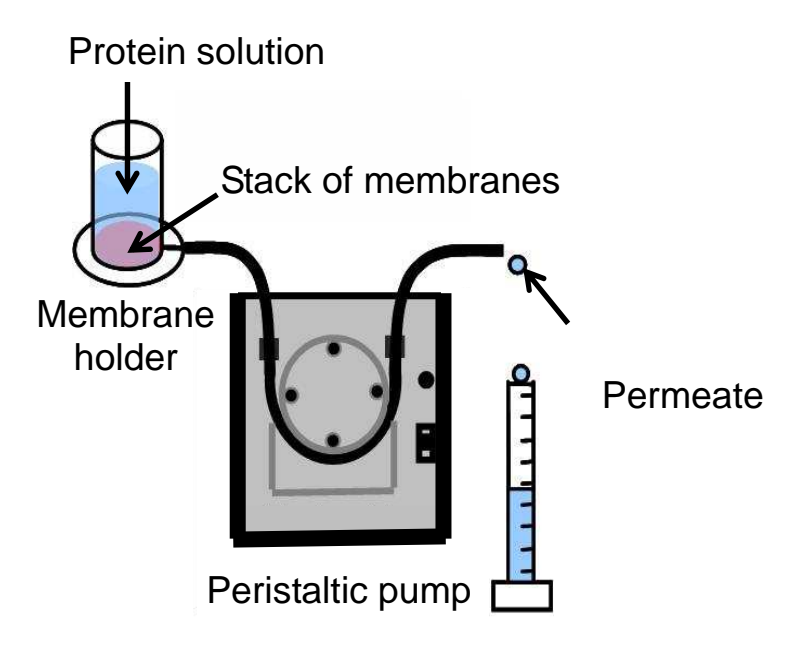


Figure 2.11. Apparatus used to measure the binding capacity of a stack of polymer brush modified membranes.

The lysozyme binding capacity of the membrane stack was $76 \pm 8 \text{ mg/cm}^3$ or about 30 % less than individual membranes. This also might result from blocked inlets or outlets of some pores due to stacking. Nevertheless, the binding capacity of the stack of 5 membranes is still 3.5-fold more than the capacity of a single membrane, and the linear velocity through the membrane (~175 cm/hr at 0.68 atm) is comparable to the recommended flow rate for commercial columns. Placing small spacers between the membranes might increase both binding capacity and permeability.

We produced stacks of 5 membranes in two different ways. In one case, we modified the membranes individually prior to stacking, and in the second variation, we stacked 5 membranes in the holder prior to modification. Both methods yield comparable binding and permeability, suggesting that simultaneous modification of many membranes can occur without a loss of polymerization efficiency.

Scale up can also occur by simply increasing the diameter of the membrane. To demonstrate this effect, we modified a 3.8 cm diameter membrane and compared its performance to 2 cm-diameter membranes (3.6-fold increase in surface area). The water flux through the larger membrane is 60 ± 3 mL/(cm² min atm), slightly less than that obtained with the 2 cm diameter system (85 \pm 4 mL/(cm² min atm)). Within experimental uncertainty, the volumenormalized lysozyme binding capacity measured for the larger membrane (105 \pm 14 mg/cm³) is the same as for the smaller system. Overall, the 3.8 cm-diameter membrane binds 3.3-fold more protein than 2 cm-diameter membranes, and the pressure drops for the two systems differ by only

~20%. Thus increasing the membrane area provides a viable alternative for scaling up separations, as expected.

2.3.6. HisU binding to poly(MES)-NTA-Ni²⁺-modified membranes

Affinity purification methods rely on specific interactions between immobilized ligands and affinity tags appended to the protein of interest. Polyhistidine is the most commonly used tag in recombinant protein purification, ⁴¹ and we employ HisU as a model His-tagged protein to determine the binding capacity of poly(MES)-NTA-Ni²⁺-modified nylon membranes. Figure 2.12 shows the breakthrough curve for HisU binding to a poly(MES)-NTA-Ni²⁺-modified nylon membrane along with similar curves for Con A binding to poly(MES)-NTA-Cu²⁺ and lysozyme binding to poly(MES). Integration of the differences between the feed and the permeate concentrations in the breakthrough curves gives binding capacities of 88 ± 4 , 86 ± 10 and $122 \pm$ 9 mg/cm³ for HisU, Con A and lysozyme, respectively. The permeate flow rate for this analysis was initially set at 1 mL/min but declined to 0.8 - 0.9 mL/min at the end of the experiment due to the protein loading. (The peristaltic pump could not maintain the flow rate at higher pressure drops.) The similar shapes of the break through curves for all 3 proteins again suggest that the geometrical inhomogeneity of the pore structure in the spongy nylon membrane defines the shape of the curve, rather than binding kinetics or diffusion limitations. The similarity in the curves occurs in spite of the variation in protein size (HisU - 10.7 kDa; Lysozyme - 14.3 kDa; Con A – 104 kDa) and the binding mechanism (HisU and Con A – affinity binding; lysozyme – ion exchange).

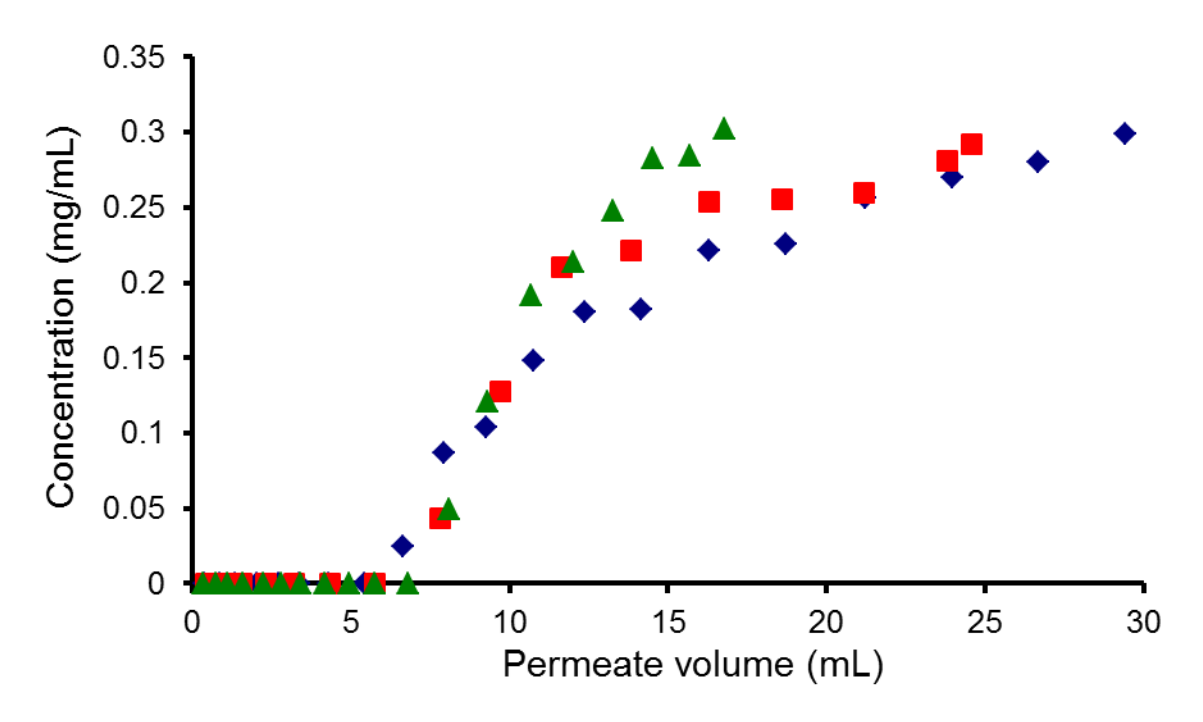


Figure 2.12. Breakthrough curves for adsorption of lysozyme (blue diamonds), HisU (green triangles) and Con A (red squares) in nylon membranes modified with poly(MES) (lysozyme), poly(MES)-NTA-Ni²⁺ (HisU) or poly(MES)-NTA-Cu²⁺ (Con A) brushes. The feed solution contained 0.3 mg protein/mL, and the flow rate was between 0.8 and 1.0 mL/min.

After obtaining the breakthrough curve of HisU, we washed the poly(MES)-NTA-Ni²⁺-HisU membrane with washing buffer II (20 mL) followed by 20 mL of phosphate buffer and eluted the protein with 5-10 mL of elution buffer containing 0.5 M imidazole and 0.5 M NaCl. Bradford assay of the eluent gives a binding capacity of 96 ± 7 mg/cm³, consistent with the binding capacity value from the breakthrough curve. This binding capacity is 4- to 6-fold higher than those reported for affinity membranes in the literature ^{19,42-45} and about twice that of commercial IMAC resins (40-50 mg/mL of resin). Elution of Con A with phosphate buffer (pH 6) containing 50 mM EDTA, and lysozyme with phosphate buffer (pH 7.4) containing 1 M

potassium thiocyanate gives membrane binding capacities of 88 ± 2 and 136 ± 4 mg/cm³, respectively, again confirming the binding capacity obtained from break through curve analysis and demonstrating efficient elution.

2.3.7. Con A binding to a monolayer of NTA-Cu²⁺ and other poly(MES)-NTA-Cu²⁺ brushes

A major premise of this work is that polymer brushes greatly increase the binding capacities of membrane adsorbers. To help demonstrate this premise, we deposited NTA complexes in a nylon membrane by linking aminobutyl NTA to a poly(acrylic acid)-terminated polyelectrolyte film (Figure 2.13). Covalent attachment of NTA to this surface uses the same reaction as attachment to poly(MES), but the structure of the polyelectrolyte film should only yield approximately a monolayer of NTA.

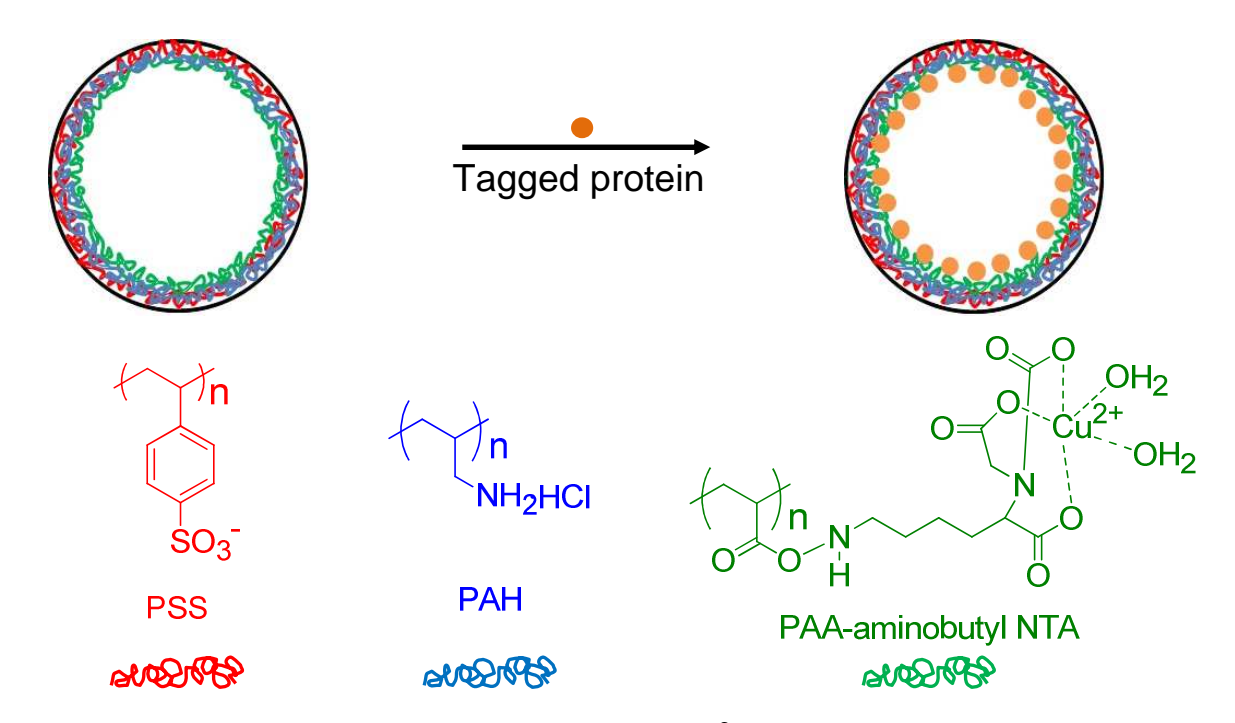


Figure 2.13. Formation of a monolayer of NTA-Cu²⁺ from a polyelectrolyte multilayer adsorbed within a membrane pore.

Figure 2.14 shows the breakthrough curve obtained for the monolayer of NTA-Cu²⁺ along with the breakthrough curves for Con A binding to poly(MES)-NTA-Cu²⁺ modified membranes prepared using both the macroinitiator (5-min polymerization) and the trichlorosilane initiator (1-h polymerization). The Con A binding capacities determined from the curves are 23 ± 8 , 76 ± 6 and 86 ± 10 mg of Con A per cm³ of membrane for the monolayer, trichlorosilane-based brush and macroinitiator-based brush, respectively. Within experimental error, the capacities determined from the eluate analysis (17 ± 7 , 80 ± 8 and 88 ± 3 mg/cm³) were the same. Breakthrough curves and the eluent analyses reveal that binding to the brushes is about 4 times higher than the monolayer, clearly showing the advantage of growing polymer brushes within the pores of the membrane.

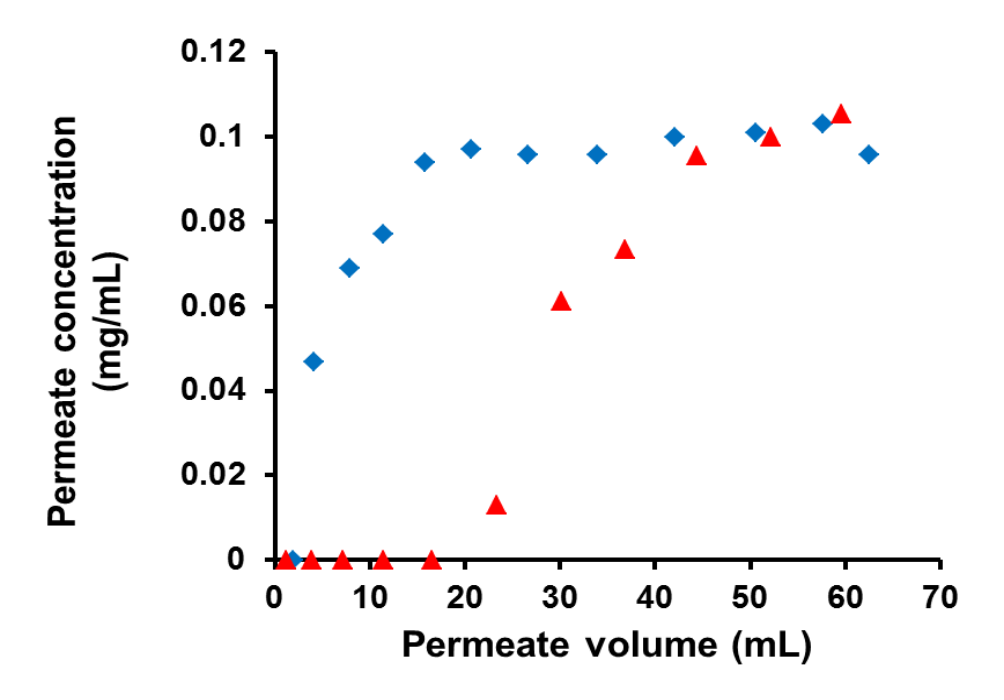


Figure 2.14. Breakthrough curves for binding of Con A to a monolayer of NTA-Cu²⁺ (blue diamonds), a macroinitiator-based poly(MES)-NTA-Cu²⁺-modified membrane (green triangles) and a trichlorosilane initiator-based poly(MES)-NTA-Cu²⁺-modified membrane (red squares). The feed solution concentration was 0.1 mg/mL.

The amount of copper present in the NTA monolayer-containing membrane is 2.2 ± 0.3 mg/cm³, or 4- to 5-fold less than the amount of Cu^{2+} in the macroinitiator-based poly(MES)-NTA- Cu^{2+} system (10 ± 0.4 mg/cm³). Thus the ratio of Cu^{2+} to protein is around 10:1 for both poly(MES)-NTA- Cu^{2+} and the monolayer of NTA- Cu^{2+} . In contrast, the trichlorosilane-based poly(MES)-NTA- Cu^{2+} contains much more copper (29 ± 4 mg/cm³)²¹ and has about a 3-fold lower ratio (3:1) of protein to Cu^{2+} than the macroinitiator system. As films increase in thickness, access to Cu^{2+} complexes apparently decreases.

Bovine serum albumin (BSA) is commonly used to examine protein binding to Cu²⁺ complexes. BSA binding to the macroinitiator-based system was quite low (~ 30 mg/cm³), and we were unable to reproduce the BSA binding capacities reported earlier for the trichlorosilane based system, ²¹ even though lysozyme and HisU binding were reproducible. Since SDS-PAGE of BSA showed a number of bands, we selected Con A rather than BSA for this work.

2.3.8. Purification of His-tagged MIPS and HisU from cell extracts and protein mixtures

The above studies reveal the high binding capacity of membranes modified with poly(MES)-NTA-Ni²⁺, but do not address selectivity. To demonstrate that membranes can isolate His-tagged protein from complex cell extracts, we purified His-tagged MIPS that was over-expressed in *E. coli*. Figure 2.15 (a) shows the SDS-PAGE analysis of the cell extract (lane 1) and the eluate from a membrane loaded with the cell extract and rinsed with buffers (lane 2). Remarkably, the eluate contains a single detectable band. The total time for purification of 5 mL

of cell extract was about 13 min, including 3 min and 20 sec to flow the extract through the membrane at 1.5 mL/min, 4 min (each) to rinse the membrane with washing buffer II and III at 5 mL/min, and 1 min and 20 sec for elution at 1.5 mL/min.

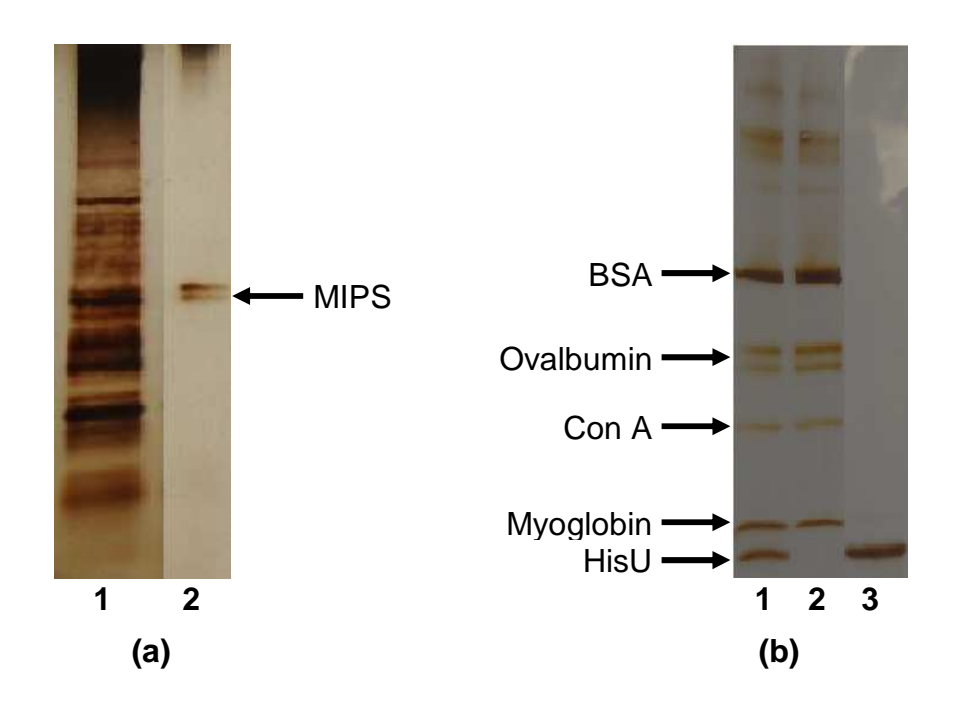


Figure 2.15. SDS-PAGE analysis (silver staining) of (a) an extract from E. *Coli* containing over expressed His-tagged MIPS (lane 1) and His-tagged MIPS purified from the cell extract using a poly(MES)-NTA-Ni²⁺-modified membrane (lane 2); (b) a mixture of BSA, ovalbumin, Con A, myoglobin and HisU (lane 1), the same solution after passing through the membrane (lane 2) and the eluent from the membrane (lane 3).

In addition to selectivity, high protein recoveries are vital when purifying tagged proteins. Unfortunately, in most purification of overexpressed recombinant proteins from cell lysates, ignorance of the initial protein concentration prevents calculation of recovery. Thus, to determine recovery with a poly(MES)-NTA-Ni²⁺-modified nylon membrane, we prepared a protein mixture containing BSA, ovalbumin, Con A, myoglobin and HisU in equal amounts (0.05 mg/mL of each in 20 mM phosphate buffer). This mixture (10 mL) was passed through the

poly(MES)-NTA-Ni²⁺ modified membrane at 1.5 mL/min, followed by rinsing with washing buffer II and phosphate buffer, and elution of the bound protein with 2 mL of phosphate buffer containing 0.5 M imidazole and 0.5 M NaCl. SDS-PAGE of the permeate loading solution suggests selective and complete removal of the HisU (Figure 2.15 (b) – lane 2), whereas similar analysis of the eluent shows a single band for HisU (Figure 2.15 (b) – lane 3). The high purity of the eluted protein allowed quantitation using a Bradford assay, and the eluted protein recovery on a single membrane was a remarkable 94 ± 4 %. Overall, less than 10% of the protein was lost in the loading, rinsing and elution steps.



Figure 2.16. Extract from E. *Coli* containing spiked HisU (lane 1), flow through from the membrane (lane 2), elution from membrane (lane 3) and HisU standard solution (lane 4).

As a more stringent test of recovery, we obtained a crude *Escherichia coli* cell extract void of His-tagged protein, diluted the extract 1:1 with phosphate buffer, spiked it with 2.5 mg of HisU and passed this solution through a poly(MES)-NTA-Ni²⁺-modified membrane. Following rinsing with washing buffer II and phosphate buffer, we eluted the bound protein with a phosphate buffer containing 0.5 M imidazole and 0.5 M NaCl. Gel electrophoresis confirmed

the purity of the eluted protein (Figure 2.16 – lane 3), and a Bradford assay of the eluate gave a recovery of 91 ± 2 % for this membrane. The high recovery occurs even when the total HisU binding (2.5 mg) approaches the membrane capacity ($\sim 3 \text{ mg}$).

2.3.9. Polymer growth and protein binding in other polymeric membranes

Macroinitiator adsorption and MES polymerization occur in aqueous solutions, so growth of poly(MES) brushes should be possible in a wide range of polymeric membranes. To examine the versatility of this method, we attempted to grow poly(MES) in PES, PVDF, nonhydroxylated nylon, and regenerated cellulose membranes and studied lysozyme binding to these brushes. We could not modify the regenerated cellulose because it became very fragile after exposure to water. Figures 2.17 (a), (b), and (c) show the ATR-IR spectra of PES, PVDF and non hydroxylated nylon membranes, respectively, before and after growth of poly(MES). After polymerization, all of the spectra contain a strong carbonyl absorbance that confirms the presence of poly(MES) in the membranes. We slightly modified the membrane modification procedure in these cases to include deposition of a layer of PSS prior to the attachment of the macroinitiator to the membrane. PSS sticks well to many surfaces and provides a negatively charged substrate for macroinitiator adsorption.²⁹ Also, we added the polymerization catalyst directly to the monomer/solvent mixture during the degassing process to avoid the use of any DMF. DMF may damage membranes, particularly PES. On hydroxylated nylon membranes, this altered procedure yields a lysozyme binding capacity of 119 mg/cm³, showing that the changes to the process do not affect the polymer brush growth or protein binding. The lysozyme binding capacities obtained from breakthrough curves for PES, PVDF and nonhydroxylated nylon membranes were 65 mg/cm³, 64 mg/cm³ and 115 mg/cm³ respectively. Thus, the completely aqueous polymerization can modify a wide variety of polymeric membranes, but it may be most effective on nylon. Binding capacity will vary with membrane geometry as well as the effectiveness of poly(MES) growth.

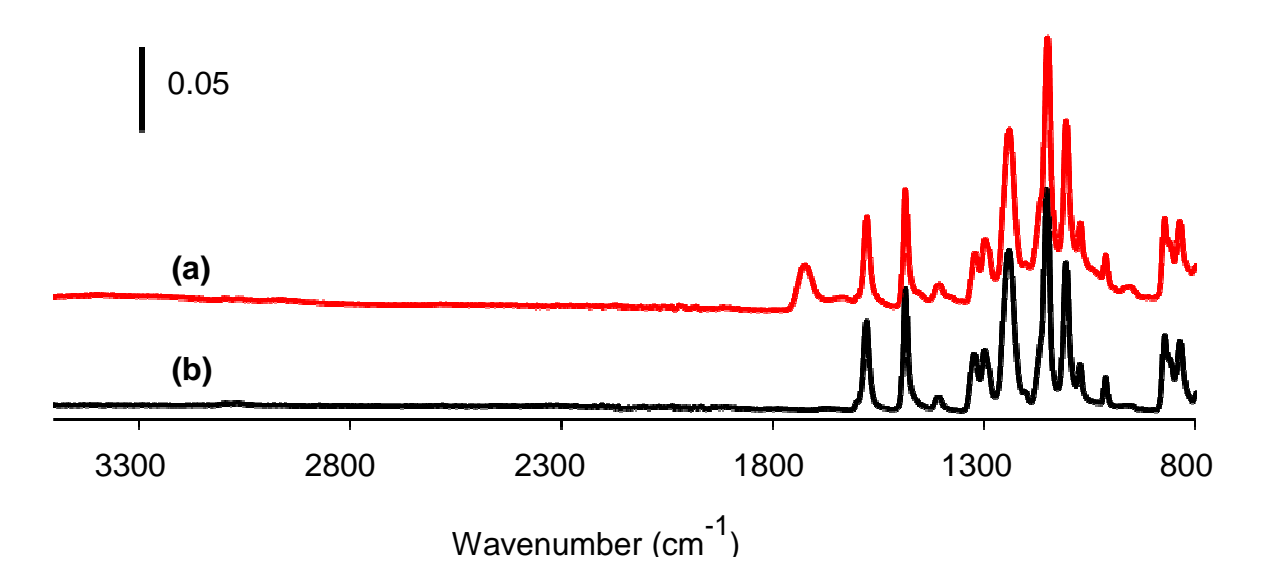


Figure 2.17 (a). ATR-FTIR spectra of PES membrane before (a) and after (b) growth of poly(MES) brushes.

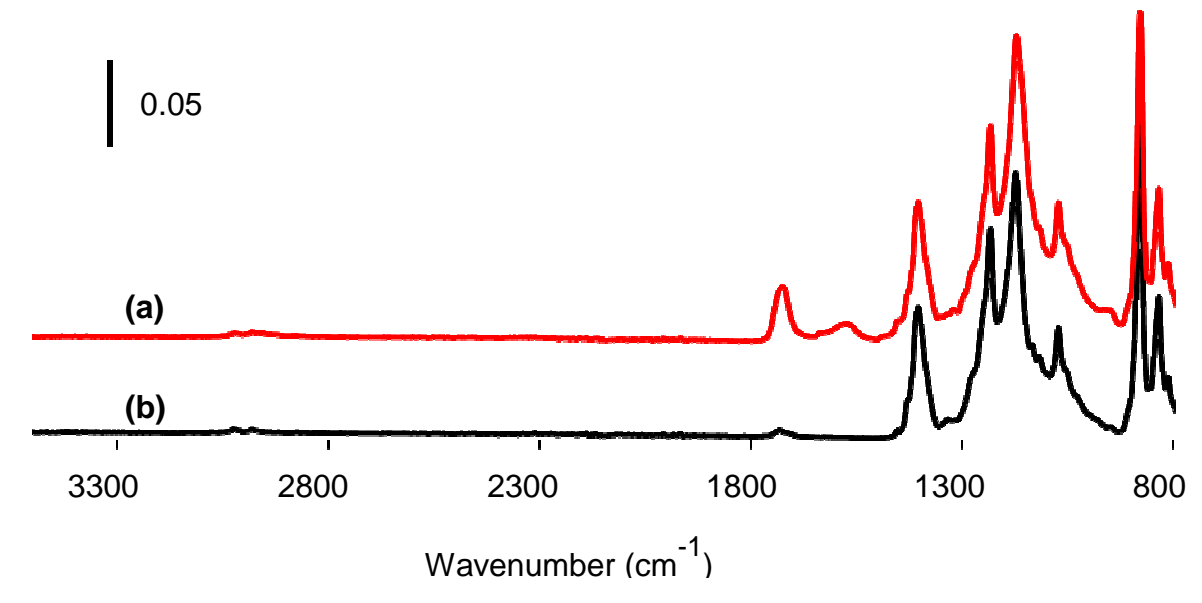


Figure 2.17 (b). ATR-FTIR spectra of PVDF membrane before (a) and after (b) growth of poly(MES) brushes.

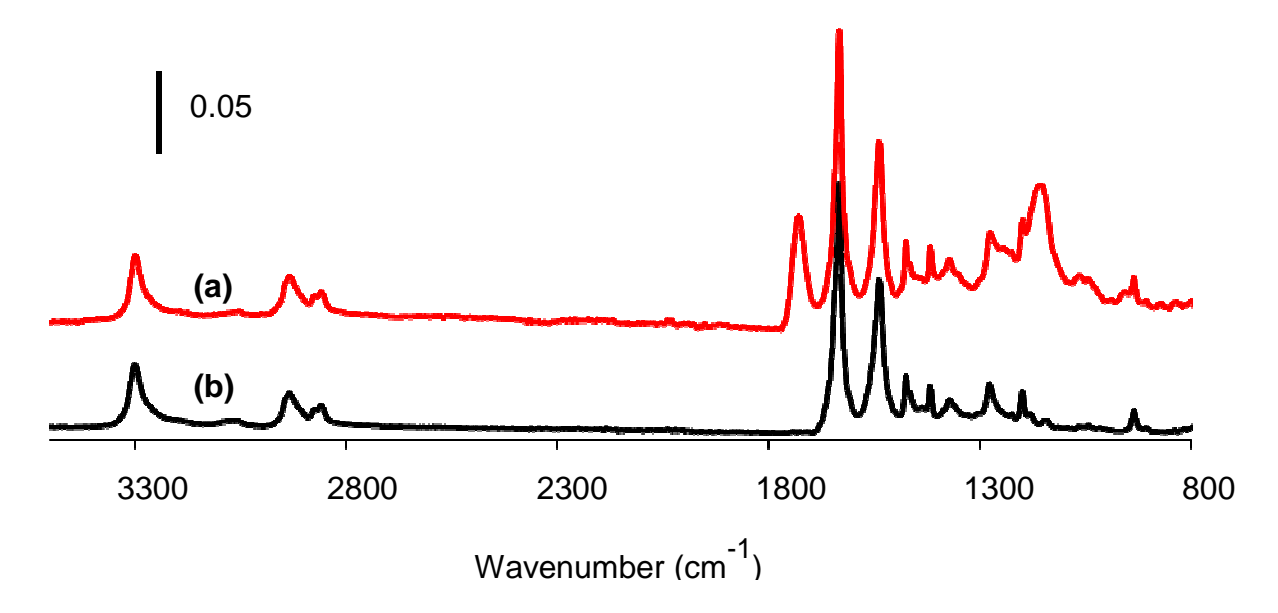


Figure 2.17 (c). ATR-FTIR spectra of a non-hydroxylated nylon membrane before (a) and after (b) growth of poly(MES) brushes.

2.4. Conclusions

Polymerization of MES from immobilized macroinitiators in porous membranes is a rapid method (10 min of initiator attachment and 5 min of polymerization) for synthesizing high-capacity, protein-binding membranes that are highly permeable. Poly(MES)-modified nylon membranes bind 122 ± 9 mg/cm³ of lysozyme, and after further derivatization to poly(MES)-NTA-Ni²⁺ the membranes bind 88 ± 4 mg/cm³ of HisU. Lysozyme capture in these membranes can occur during a ~35 ms residence time, and the HisU binding capacity is twice as high as commercial resin packed columns. Additionally poly(MES)-NTA-Ni²⁺-modified membranes purify His-tagged MIPS directly from cell extracts in less than 15 min using a simple peristaltic pump. Remarkably, the recovery of HisU from a cell extract is ~ 90 %. Scale up of the protein separation can occur both by stacking several membranes and increasing the membrane

diameter. The polymerization method is completely aqueous and thus compatible with nylon (hydroxylated and non-hydroxylated), PES, PVDF and presumably other polymeric membranes.

REFERENCES

2.5. References

- (1) Pavlou, A. K.; Reichert, J. M. *Nature Biotechnology* **2004**, 22, 1513-1519.
- (2) Wurm, F. M. *Nature Biotechnology* **2004**, 22 1393-1398.
- (3) Clarke, W.; Hage, D. S. Separation and Purification Reviews 2003, 32, 19-60.
- (4) Kawai, T.; Saito, K.; Lee, W. Journal of Chromatography B **2003**, 790, 131-142.
- (5) Bhut, B. V.; Husson, S. M. *Journal of Membrane Science* **2009**, *337*, 215-223.
- (6) Ghosh, R. *Journal of Chromatography A* **2002**, 952, 13-27.
- (7) Brandt, S.; Goffe, R. A.; Kessler, S. B.; O'Connor, J. L.; Zale, S. E. *Nature Biotechnology* **1988**, *6*, 779 -782.
- (8) Thommes, J.; Etzel, M. *Biotechnology Progress* **2007**, *23*, 42-45.
- (9) Roper, D. K.; Lightfoot, E. N. Journal of Chromatography A 1995, 702, 3 26.
- (10) Lightfoot, E. N.; Moscariello, J. S. *Biotechnology and Bioengineering* **2004**, 87, 259–273.
- (11) Sun, L.; Dai, J. H.; Baker, G. L.; Bruening, M. L. *Chemistry of Materials* **2006**, *18*, 4033-4039.
- (12) Zeng, X.; Ruckenstein, E. Biotechnology Progress 1999, 15 1003–1019.
- (13) Thommes, J.; Kula, M.-R. *Biotechnology Progress* **1995**, *11*, 357-367.
- (14) Saxena, A.; Tripathi, B. P.; Kumar, M.; Shahi, V. K. *Advances in Colloid and Interface Science* **2009**, *145*, 1-22.
- (15) Smuleac, V.; Bachas, L.; Bhattacharyya, D. *Journal of Membrane Science* **2010**, *346*, 310-317.
- (16) Van Reis, R.; Zydney, A. Journal of Membrane Science 2007, 297, 16-50.
- (17) Müller, W. Journal of Chromatography A **1990**, 510, 133-140.
- (18) Gautrot, J. E.; Huck, W. T. S.; Welch, M.; Ramstedt, M. ACS Applied Materials & Interfaces 2010, 2, 193-202.
- (19) Yang, Q.; Ulbricht, M. *Macromolecules* **2011**, *ASAP*.

- (20) Jain, P.; Sun, L.; Dai, J. H.; Baker, G. L.; Bruening, M. L. *Biomacromolecules* **2007**, 8, 3102-3107.
- (21) Jain, P.; Vyas, M. K.; Geiger, J. H.; Baker, G. L.; Bruening, M. L. *Biomacromolecules* **2010**, *11*, 1019-1026.
- (22) Dai, J. H.; Bao, Z. Y.; Sun, L.; Hong, S. U.; Baker, G. L.; Bruening, M. L. *Langmuir* **2006**, 22, 4274-4281.
- (23) He, D.; Ulbricht, M. Journal of Membrane Science 2008, 315, 155-163.
- (24) Bhut, B. V.; Wickramasinghe, S. R.; Husson, S. M. *Journal of Membrane Science* **2008**, 325, 176-183.
- (25) Singh, N.; Chen, Z.; Tomer, N.; Wickramasinghe, S. R.; Soice, N.; Husson, S. M. *Journal of Membrane Science* **2008**, *311*, 225-234.
- (26) Ulbricht, M.; yang, H. Chemistry of Materials **2005**, 17, 2622-2631.
- (27) Bhut, B. V.; Christensen, K. A.; Husson, S. M. *Journal of Chromatography A* **2010**, *1217*, 4946-4957.
- (28) Cvullen, S. P.; Liu, X.; Mandel, I. C.; Himpsel, F. J.; Gopalan, P. *Langmuir* **2008**, *24*, 913-920.
- (29) Jain, P.; Dai, J.; Grajales, S.; Saha, S.; Baker, G. L.; Bruening, M. L. *Langmuir* **2007**, *23*, 11360-11365.
- (30) Matyjaszewski, K.; Miller, P. J.; Shukla, N.; Immaraporn, B.; Gelman, A.; Luokala, B. B.; Siclovan, T. M.; Kickelbick, G.; Vallant, T.; Hoffmann, H.; Pakula, T. *Macromolecules* **1999**, *32*, 8716-8724.
- (31) Chen, X. Y.; Armes, S. P. Advanced Materials (Weinheim, Germany) 2003, 15, 1558.
- (32) Jain, P.; Dai, J. H.; Baker, G. L.; Bruening, M. L. *Macromolecules* **2008**, *41*, 8413-8417.
- (33) Dai, J.; Baker, G. L.; Bruening, M. L. Analytical Chemistry **2006**, 78, 135-140.
- (34) Wray, W.; Boulikas, T.; Wray, V. P.; Hancock, R. *Analytical Biochemistry* **1981**, *118*, 197-203.
- (35) Bertolini, M. J.; Tankersley, D. L.; Schroeder, D. D. *Analytical Biochemistry* **1976**, *71*, 6-13.
- (36) Ito, Y.; Inaba, M.; Chung, D.-J.; Imanishi, Y. *Macromolecules* **1992**, 25, 7313-7316.

- (37) Zhang, Z. B.; Zhu, X. L.; Xu, F. J.; Neoh, K. G.; Kang, E. T. *Journal of Membrane Science* **2009**, *342* 300–306.
- (38) Wang, M.; An, Q.-S.; Wu, L.-G.; Mo, J.-X.; Gao, G.-J. *Journal of Membrane Science* **2007**, 287, 257-263.
- (39) http://www.gelifesciences.com/aptrix/upp01077.nsf/Content/Products?Open Document&parentid=525604&moduleid=165902&zone=Labsep (Dynamic binding capacity Approx. 40 mg histidine-tagged protein/ml medium; Max. linear flow rate 600 cm/h) (accessed February 23rd 2011)
- (40) Lin, S.-Y.; Suen, S.-Y. Journal of Membrane Science 2002, 204, 37-51
- (41) Garberc-Porekar, V.; Menart, V. Chemical Engineering & Technology **2005**, 28, 1306-1014.
- (42) Kawakita, H.; H., M.; Nomura, K.; Uezu, K.; Akiba, I.; Tsuneda, S. *Journal of Porous Materials* **2007**, *14*, 387-391.
- (43) Bayramoglu, G.; Celik, G.; Arica, M. Y. Colloids and Surfaces A 2006, 287, 75-85.
- (44) Ma, Z. W.; Masaya, K.; Ramakrishna, S. *Journal of Membrane Science* **2006**, 282, 237-244.
- (45) Nova, C. J. M.; Paolucci-Jeanjean, D.; Belleville, M. P.; Barboiu, M.; Rivallin, M.; Rios, G. *Journal of Membrane Science* **2008**, *321* 81–89.
- (46) http://www.qiagen.com/products/protein/purification/qiaexpressproteinpurification system/ni-ntaagarose.aspx?ShowInfo=1 (Binding capacity Approx. 50 mg histidine-tagged protein/mL medium) (accessed February 23, 2011)

Chapter 3. Protein Binding to Polymer

Brushes with a Reduced Areal Chain Density

3.1. Introduction

Porous membranes are attractive for protein purification because convective mass transport rapidly brings proteins to adsorption sites and overcomes diffusion limitations on binding rates. Convective flow may also decrease non-specific adsorption and increase protein purity. However, when compared to packed-bed columns membranes show low binding capacities. Thus, much current research focuses on modifying membranes with polymer brushes to increase the number of protein-binding sites. 6-9

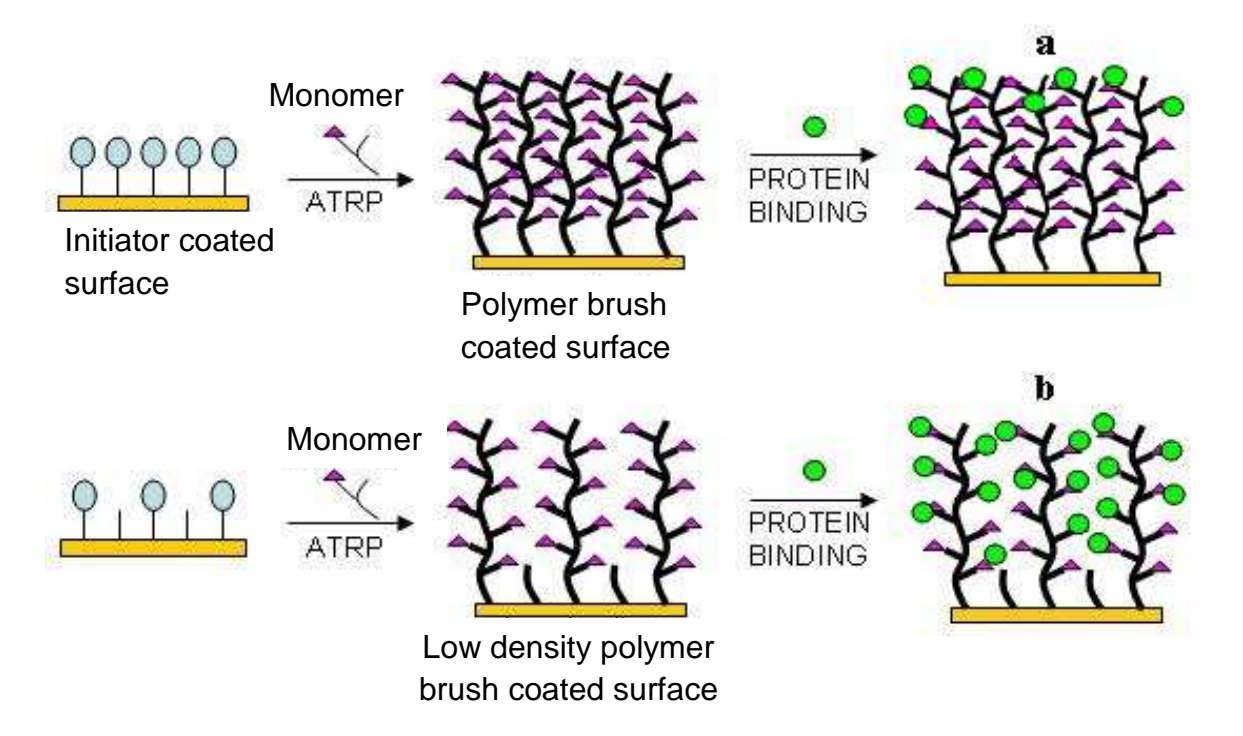
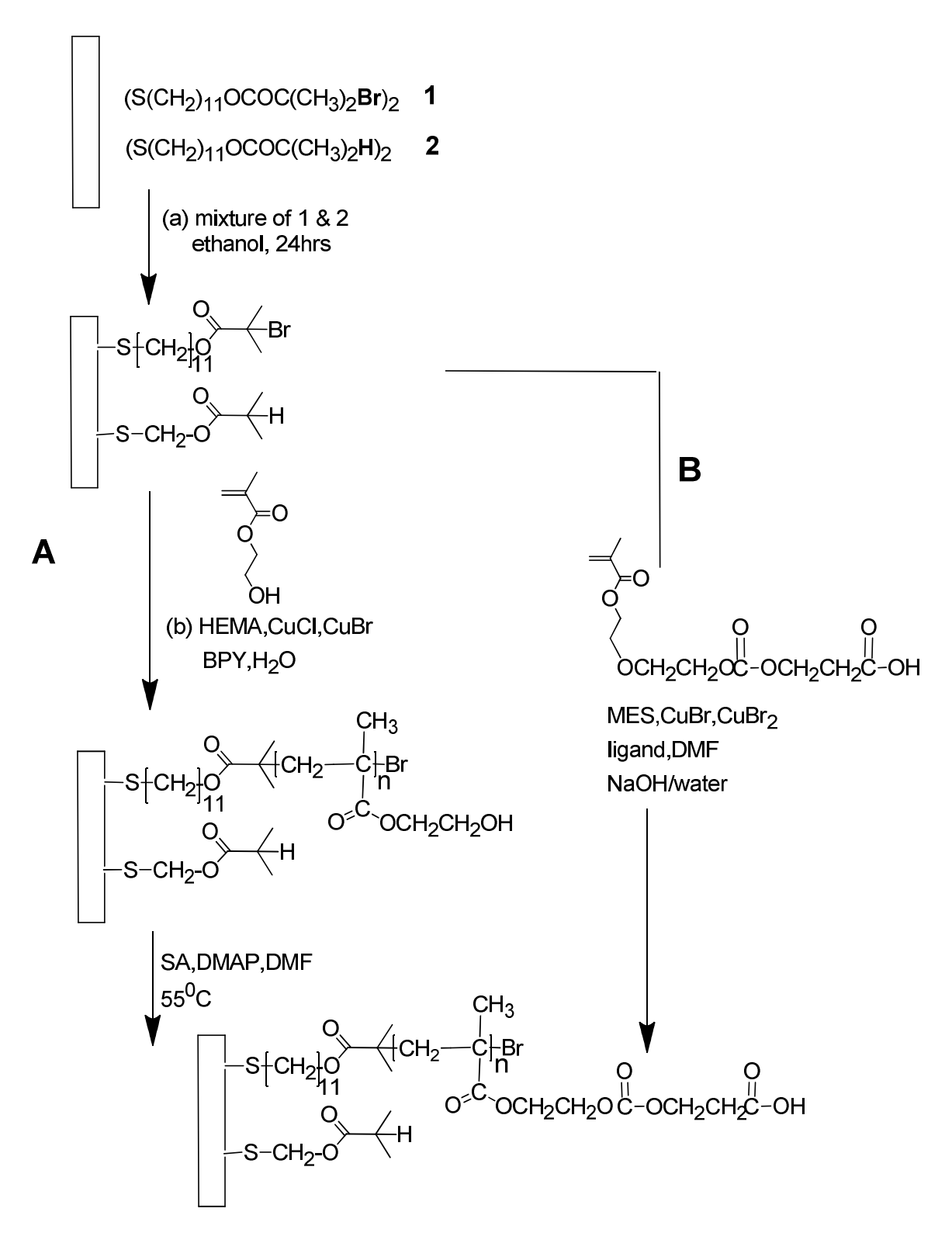


Figure 3.1. Enhanced protein binding to reduced density polymer brushes (b) compared to regular polymer brushes (a).

Control over the density and functionality of polymer brushes should facilitate their application in a number of areas. ¹⁰⁻¹³ For example dense polymer brushes can potentially serve as anticorrosion coatings, ¹⁴ etch masks ¹⁵ and lithographic films. ^{15,16} In contrast, applications such as biomolecule immobilization for sensing and separation require less dense polymer brushes. As Figure 3.1 suggests, lower densities of polymer chains may greatly enhance protein binding to polymer brushes. Several studies reported ways to control the areal chain density of polymer brushes. ¹⁷⁻²⁰

This chapter examines two strategies to reduce the areal chain density in polymer brushes and potentially increase their protein-binding capacity. The first method relies on diluting initiators in a self-assembled monolayer to decrease the number of sites available for chain growth. Bao and coworkers successfully decreased the density of thiol initiators on Au and silane initiators on SiO₂ using a mixture of initiator and an inert analog, and I employ a similar approach. Scheme 3.1 shows the active initiator, 1, and the inactive spacer or diluent molecule, 2. I grew reduced density polymer-brushes from monolayers containing various ratios of 1 and 2 to investigate the effect of chain density on protein binding. A larger chain spacing might increase brush swelling to enhance the protein binding capacity, and Bao et al reported that widely spaced brushes exhibit a 20-fold increase in swelling compared to dense polymer films.



Scheme 3.1. Synthesis of reduced density polymer-brushes from monolayers containing initiator (1) and diluent (2) molecules. Polymerization of MES (reaction **B**) and polymerization of HEMA followed by reaction with succinic anhydride (SA) (reaction **A**) yield poly(acid) brushes with nominally the same formula but different chain spacing.

Our second strategy to reduce initiator density relies on derivatizing monomers prior to polymerization rather than after brush formation. In this approach we compared two synthetic pathways to poly[(2-methacryloyoxyethy)succinate] (poly(MES)) films. The first path includes polymerization of (2-hydroxyethyl methacrylate) (HEMA) from a surface and subsequent reaction of this polymer brush with SA, whereas the more direct route is simple polymerization of MES. Although the two methods yield the same polymer formula, the spacing of the chains should be very different. Derivatization of poly(HEMA) with succinic anhydride (poly(HEMA-SA)) will increase the size of polymer side chains and make the brushes more crowded, whereas direct polymerization of poly(MES) should yield more widely separated polymer chains because long side chains are present during brush formation (Scheme 3.1-compare reactions A and B). In fact, poly(MES) films and poly(HEMA-SA) have very different binding capacities. In the case of ~50 nm-thick films, the poly(MES) brushes bind about 180 nm of lysozyme, while poly(HEMA-SA) captures only 80 nm of lysozyme.

3.2. Experimental

3.2.1. Materials

11-mercaptoundecanol (97%, MUD), 2-bromoisobutyryl bromide (98%, BIBB), 2,2'-dipyridyl, CuCl (99%), K₂CO₃, Na₂HPO₄, SA, NaHCO₃, *N*-(3-dimethylaminopropyl)-*N*'-ethylcarbodiimide hydrochloride (EDC), *N*-hydroxysuccinimide (NHS), dimethylformamide (DMF, anhydrous, 99.8%), CuBr (99.999%), CuBr₂ (99%), MES inhibited with 750 ppm monomethyl ether hydroquinone, TWEEN-20 surfactant, bovine serum albumin (BSA), lysozyme, ethylenediamine tetraacetic acid, 1,1,4,7,10,10-hexamethyltriethylenetetramine (HMTETA), 4-dimethylaminopyridine (DMAP), 2-methyl propionyl chloride and *Na*:*Na*-

Bis(carboxymethyl)-L-lysinehydrate (aminobutyl nitrilotriacetic acid, NTA) were used as received (unless specified) from Sigma Aldrich. CuSO₄·5H₂O (CCI), NaH₂PO₄ (CCI), Na₂HPO₄ (CCI) and NaOH (Spectrum) were also used received. Tris[2-(dimethylamino)ethyl]amine (Me₆(TREN) was obtained from both Sigma Aldrich and ATRP solutions. HEMA (Aldrich) was purified before use by passage through a column of activated basic alumina (Spectrum). Buffers were prepared using analytical grade chemicals and deionized (Milli-Q, 18.2 M Ω cm) water. Synthesis of the initiator (1, Scheme 1) and the diluent (2, Scheme 1) molecules was performed using a published procedure. 13,17 Both compounds were stored under nitrogen for future use

3.2.2. Preparation of initiator-modified Au substrates

Ethanolic solutions containing 1 mM initiator, $\mathbf{1}$, or diluent, $\mathbf{2}$, were mixed in appropriate ratios, and Au-coated Si wafers (200 nm of sputtered Au on 20 nm of sputtered Cr on Si wafers) were cleaned with UV-ozone for 15 min and immersed in these solutions for 24 h. Subsequently, the wafers were rinsed sequentially with ethanol and water, and dried under a stream of N_2 . These initiator-modified substrates were then transferred to a N_2 -filled glove bag where polymerization was carried out at room temperature.

3.2.3. Polymerization of MES and HEMA on Au substrates

Polymerization mixtures were prepared as described before. ^{9,23} Briefly, 10 mL of a mixture of neat MES monomer and 1 M aqueous NaOH (1:1, v/v) was first degassed with three freeze-pump-thaw (FPT) cycles. A 1 mL solution of DMF containing CuBr (2 mM), CuBr₂ (1 mM), and Me₆TREN or HMTETA (6 mM) was similarly degassed, and in a N₂-filled glove bag,

this solution of catalyst was mixed with the monomer/NaOH solution. Polymerization from the initiator-modified Au wafer occurred by immersing the wafer in the polymerization mixture in a N₂ glove bag for the desired time. Following the polymerization, the Au wafer was taken out of the glove bag, sonicated in DMF for 10 min and rinsed with ethanol and water.

Polymerization of HEMA from the immobilized initiator was performed as described previously²² by immersing the wafer in a degassed solution containing 15 mL of purified HEMA, 15 mL water, 82.5 mg (0.825 mmol) of CuCl, 54 mg (0.24 mmol) of CuBr₂, and 320 mg (2.04 mmol) of 2,2'-bipyridyl for defined time periods in a nitrogen filled glove bag. After polymerization, the wafer was sonicated in DMF for 10 min and rinsed with ethanol (20 mL), deionized water (20 mL), and acetone (20 mL).

In cases where error bars are reported, 2 Au wafers were individually tested, and the average data is reported. Error bars are standard deviations.

3.2.4. Polymer brush derivatization and protein immobilization

The functionalization of the poly(MES) side chains for protein binding occurred as reported previously. ²³ Briefly, the carboxylic acid groups of the poly(MES)-modified substrates were activated using an aqueous solution containing NHS (0.1 M) and EDC (0.1 M) for 1 h. This was followed by sequentially rinsing with 20 mL of deionized water and 20 mL of ethanol. The substrate was then immersed in an aqueous solution of NTA (0.1 M, pH 10.2) and rinsed with 20 mL of water. Finally, the NTA-Cu²⁺ complex was formed by immersing the film-coated wafer in an aqueous 0.1 M CuSO₄ solution for 2 h followed by rinsing with water followed by ethanol (20 mL each). The substrate was dried with N₂ prior to protein binding. In the case of

poly(HEMA) brushes, the derivatization was also performed as reported before. The poly(HEMA)-coated wafers were immersed in a DMF solution containing SA (10 mg/mL) and DMAP (15 mg/mL) for 3hrs at 55 °C followed by rinsing with DMF (20 mL), deionized water (20 mL) and ethanol (20 mL). These poly(HEMA-SA) brushes were further modified to form NTA- Cu²⁺ complexes as was done for poly(MES) brushes.

For lysozyme binding, poly(MES) and poly(HEMA-SA) brushes were immersed in a 1 mg/mL solution of lysozyme in phosphate buffer (20 mM, pH 7.4) for 18 hrs. The films were then rinsed with 20 mL of washing buffer (phosphate buffer containing 0.1% Tween-20, pH 7.4) followed by 20 mL of phosphate buffer and 20 mL of ethanol. The protein-containing substrates were dried under a stream of N₂. To immobilize BSA, poly(MES)-NTA-Cu²⁺-modified Au substrates were immersed in a solution of 1 mg/mL BSA in phosphate buffer for 18 h. The films were then rinsed with 20 mL washing buffer followed by 20 mL of phosphate buffer and 20 mL ethanol and dried under a steam of N₂.

3.2.5. Quantification of protein binding

To quantify the amount of protein bound to polymer brushes on Au-coated Si wafers, the method reported by Dai and co-workers²⁴ was employed. Briefly, a calibration curve was obtained by plotting the ellipsometric thickness of spin-coated BSA or lysozyme films against the reflectance FTIR absorbance of their amide I band.^{22,24} The amide absorbance of lysozyme or BSA adsorbed to poly(MES) or poly(MES)-NTA-Cu²⁺ films was then compared to the calibration curve to obtain the thickness added due to protein adsorption. These results were confirmed by ellipsometric studies that examined the difference in film thickness due to protein

binding. Before characterizing the poly(MES) and poly(MES)-NTA- Cu^{2+} films by reflectance FTIR spectroscopy and ellipsometry, the films were immersed in phosphate buffer (pH 7.4) for 15 min followed by rinsing with 20 mL of ethanol and drying under a stream of N_2 to account for any variations in the film absorbance due to pH changes.

3.3. Results and Discussion

3.3.1. Polymerization of MES and HEMA on Au wafers with controlled initiator density

Scheme 1 shows polymerization of HEMA (A) and MES (B) from diluted initiator monolayers, and subsequent reaction of the poly(HEMA) with SA. Variation of the ratio of 1 and 2 in the monolayer-forming solution affords control over the immobilized initiator density and in turn the brush density. As Figure 3.2 shows, poly(MES) films grown from monolayers containing 50 % and 100 % initiator show similar thicknesses, as would be expected because steric constraints do not allow polymerization from every initiator in a self-assembled monolayer. In fact, consistent with previous studies the thickness as a function of initiator density drops most steeply when the initiator density is small (<10 %) and a large fraction of the initiators give rise to growing chains. Figure 3.2 also reveals that the relative thickness per initiator (normalized thickness) increases ~5-fold on going from 25 % to 1 % or 0.1 % initiator. Presumably this reflects a much higher initiation efficiency at low initiator densities and not a large increase in chain molecular weight. 17,25 Bao and coworkers reported similar trends for poly(HEMA) and poly(methacryllic acid). Based on these results, I selected 1% and 5% initiator densities for comparison of protein binding with films grown from monolayers with 100% initiator density.

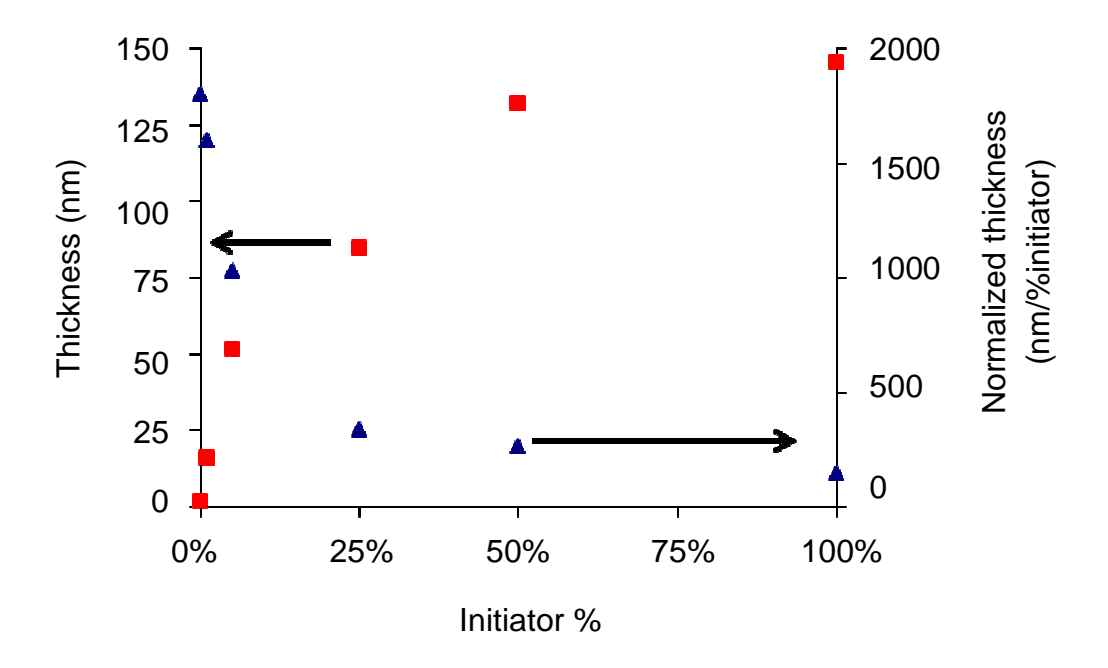


Figure 3.2. Thickness (■) and normalized film thickness (▲) (measured thickness divided by the percentage of initiator in the monolayer) of poly(MES) brushes grown from complete and diluted initiator monolayer on Au -coated wafers. Catalyst system CuBr (2 mM), CuBr₂ (1 mM), and HMTETA (6 mM). The polymerization time was 2 h.

Ideally, we would like to compare protein binding for films of the same thickness grown from monolayers with different fractions of initiator, so we examined film thickness as a function of polymerization time from different monolayers. Figure 3.3 shows results for polymerization of MES from Au wafers modified with monolayers containing 1 %, 5 % and 100 % initiator. When HMTETA served as the ligand in the ATRP ligand system (Figure 3.3 (a)), films grew quickly from monolayers with 1% and 5% initiator, but growth essentially stopped after 1 h, suggesting that significant termination occurs in this case. Interestingly, with 100%

initiator the film thickness increased almost linearly with polymerization time over 8 h. The high initial density of initiators in these films may make their growth less susceptible to termination.

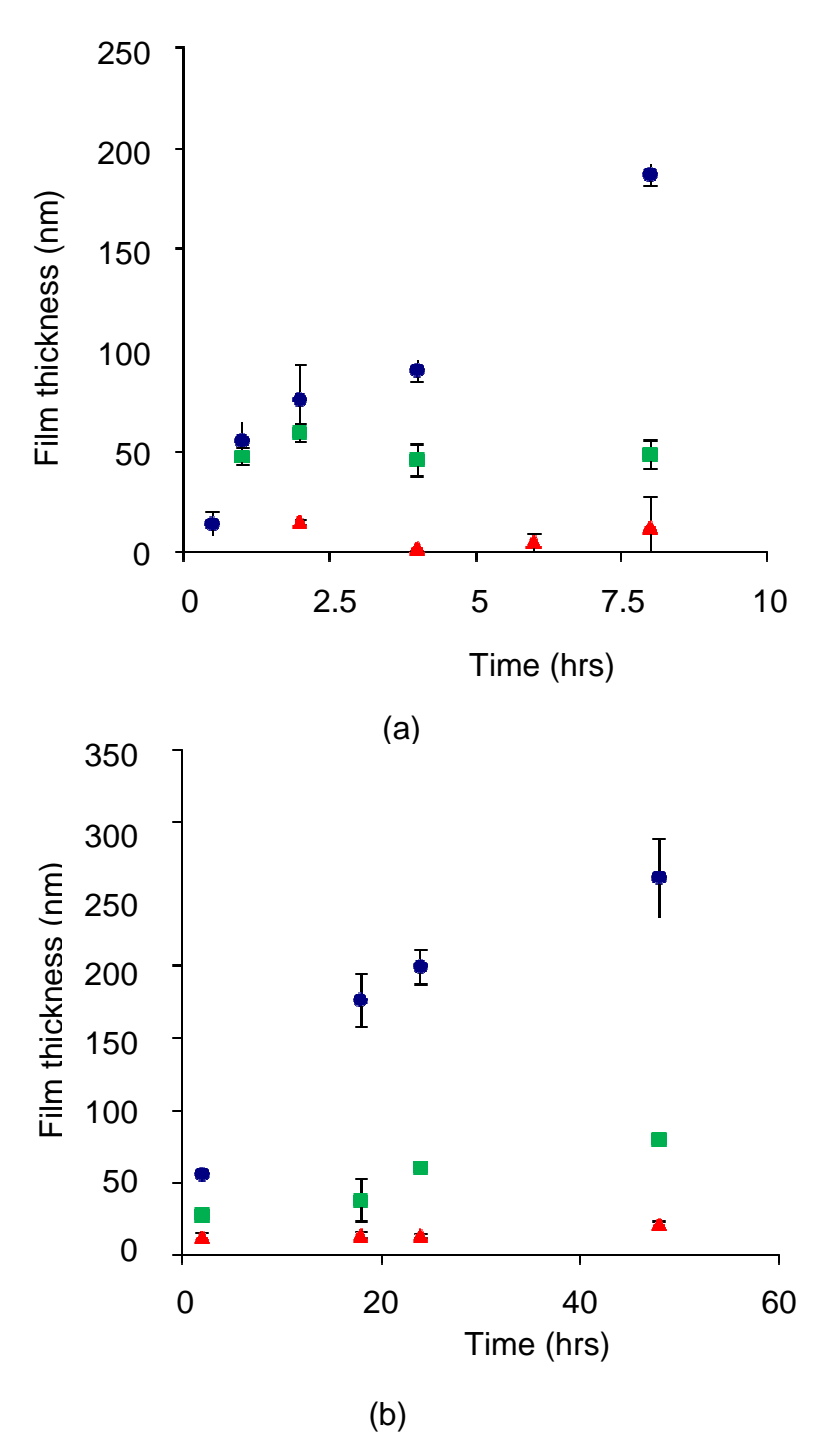


Figure 3.3. Evolution of ellipsometric film thickness with time for polymerization of MES using Me₆(TREN) (b) and HMTETA (a) as the catalyst ligands. Films were grown from monolayers containing 100% (\bullet), 5% (\blacksquare), 1% (\blacktriangle) initiator.

With a catalyst ligand, $ME_6(TREN)$, 23 that typically yields more controlled ATRP, the monolayers with 1% and 5% initiator give slower initial growth but a more constant growth with time (Figure 3.3 (b)). This is consistent with the use of $ME_6(TREN)$ leading to a high fraction of dormant chains (low radical concentration) during polymerization. However, even after 48 h of polymerization, the maximum thickness of films grown from 1 % initiator was only 15 nm.

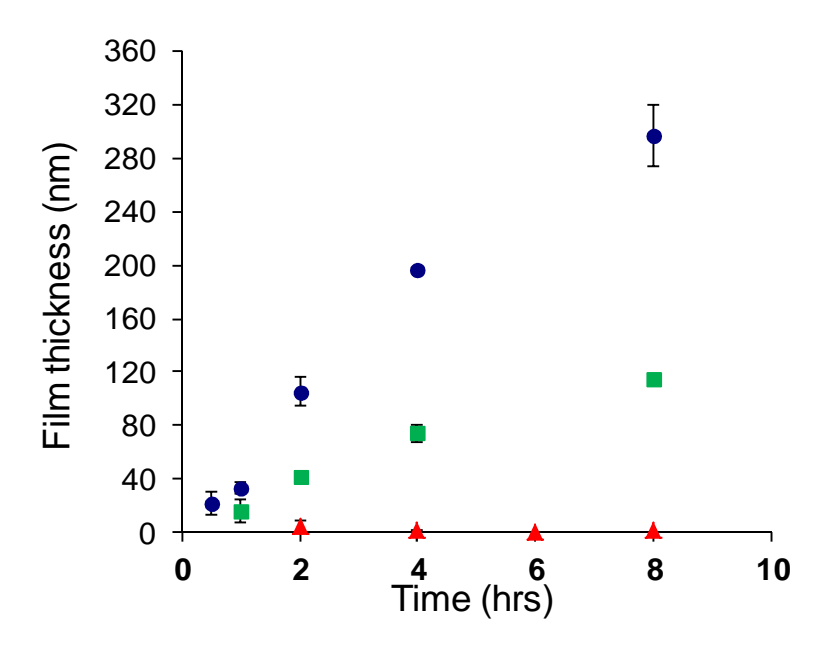


Figure 3.4. Evolution of ellipsometric film thickness with time for polymerization of HEMA. Polymerization occurred from monolayers containing 100% (●), 5% (■), and 1% (▲) initiator. Catalyst system CuCl (0.825 mmol), CuBr₂ (0.24 mmol) and 2,2'-bipyridyl (2.04 mmol).

We also wish to compare poly(MES) films with poly(HEMA) coatings reacted with SA, and this requires study of the kinetics of HEMA polymerization from monolayers containing different fractions of initiator. Compared to MES, HEMA shows a relatively controlled polymerization when using bipyridine as the catalyst ligand (Figure 3.4) and monolayers

containing 100% and 5% initiator. However, with a 1 % initiator density, the poly(HEMA) thickness was 1-2 nm irrespective of the duration of polymerization. Again, the small number of initiators in the 1% monolayer may make these films especially susceptible to termination, particularly by small amounts of impurities.

3.3.2. Protein binding as a function of chain areal density

This study aimed to reduce the chain areal density in polymer brushes and increase the rate and capacity (normalized to thickness) of protein binding to these brushes. Our hypothesis is that when the chain density decreases, film swelling will increase and expose more sites for protein immobilization. To investigate the effect of chain density on protein binding, we determined the amount of protein bound to polymer brushes of similar thickness but grown from monolayers with different initiator fractions. With poly(MES), the maximum polymer brush thicknesses for films grown from monolayers with 1 %, 5 %, and 100 % initiator were 15 nm, 50 nm and 250 nm, respectively. Thus, to compare the protein binding by the reduced density films with that of the high density polymer films, we chose 15 nm-thick films grown from each type of initiator monolayer. Poly(HEMA) was not suitable for this study because the maximum thickness of films grown from 1% initiator was only 1-2 nm.

Poly(MES) films capture lysozyme via ion-exchange, whereas BSA binds to poly(MES)-NTA-Cu²⁺ brushes through metal ion affinity interaction. Accordingly, we modified 15 nm thick poly(MES) films with NTA-Cu²⁺ complexes to form BSA-binding brushes. Wafers coated with poly(MES) and poly(MES)-NTA-Cu²⁺ brushes were immersed in 1 mg/mL solutions of lysozyme and BSA, respectively, in 20 mM phosphate buffer (pH 7.4) for 18 h. After removal of the film from the solution, rinsing, and drying, reflectance FTIR spectroscopy was used to

determine the amount of protein bound to the films following the method reported by Dai and co-workers. As Figure 3.5 shows, regardless of the initiator fraction (1 %, 5 % or 100 %) 15 nm thick (before derivatization) films bind similar amounts of protein, about 80 nm (40 monolayers) of 1985 o

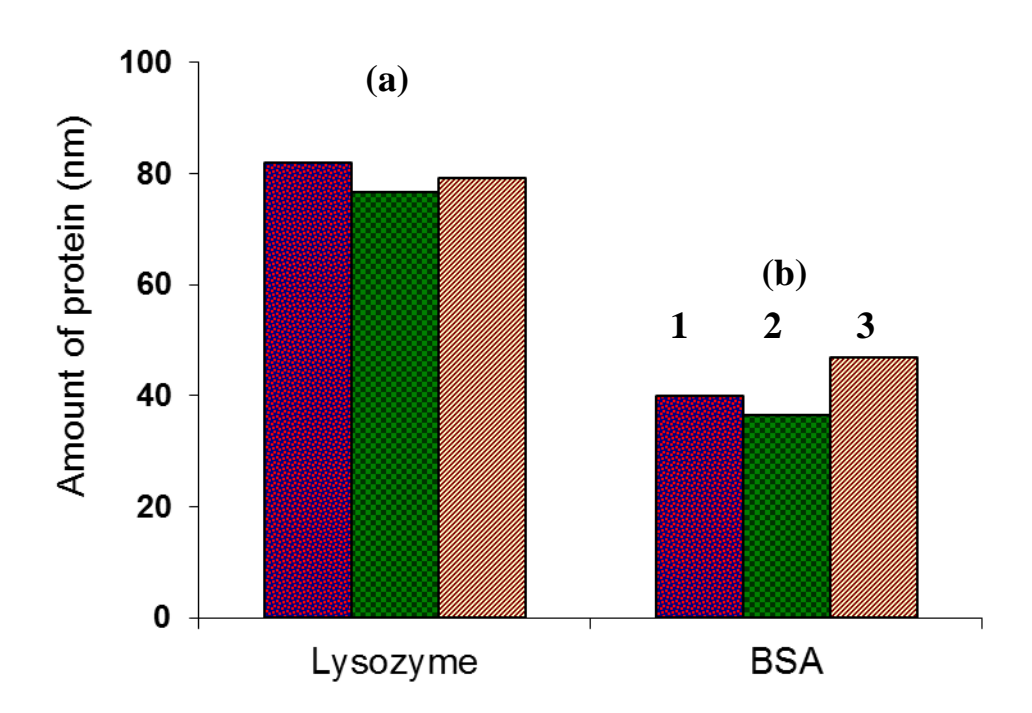


Figure 3.5. Lysozyme (a), and BSA (b) binding capacities of 15 nm-thick poly(MES) (lysozyme) or poly(MES-NTA-Cu $^{2+}$) (BSA) brushes grown from monolayers containing 1% (1), 5% (2) and 100 % (3) initiator. Binding occurred from a 1 mg/mL solution for 18 h. The protein binding is the thickness of a spin-coated film with the same amount of protein as that sorbed in the film.

Because the maximum thickness of poly(MES) grown from a 1% initiator monolayer was 15 nm, we could only study protein binding to thicker brushes with films polymerized from 5 % and 100 % initiator. In this case, we determined the binding of lysozyme to 50 nm thick poly(MES) and poly(HEMA)-SA brushes. (The poly(HEMA-SA) thickness of 50 nm is that after reaction with SA, and for BSA binding both types of brushes were derivatized with NTA-Cu²⁺ complexes.) As Figure 3.6 shows, the binding capacities of all types of polymer brushes do not change significantly when polymerization occurs from 5% rather than 100% initiator. This suggests that although chain density may differ, swelling is independent of initiator density. The longer chains that result from fewer initiators collapse to give the same polymer density as in films with a higher chain density.

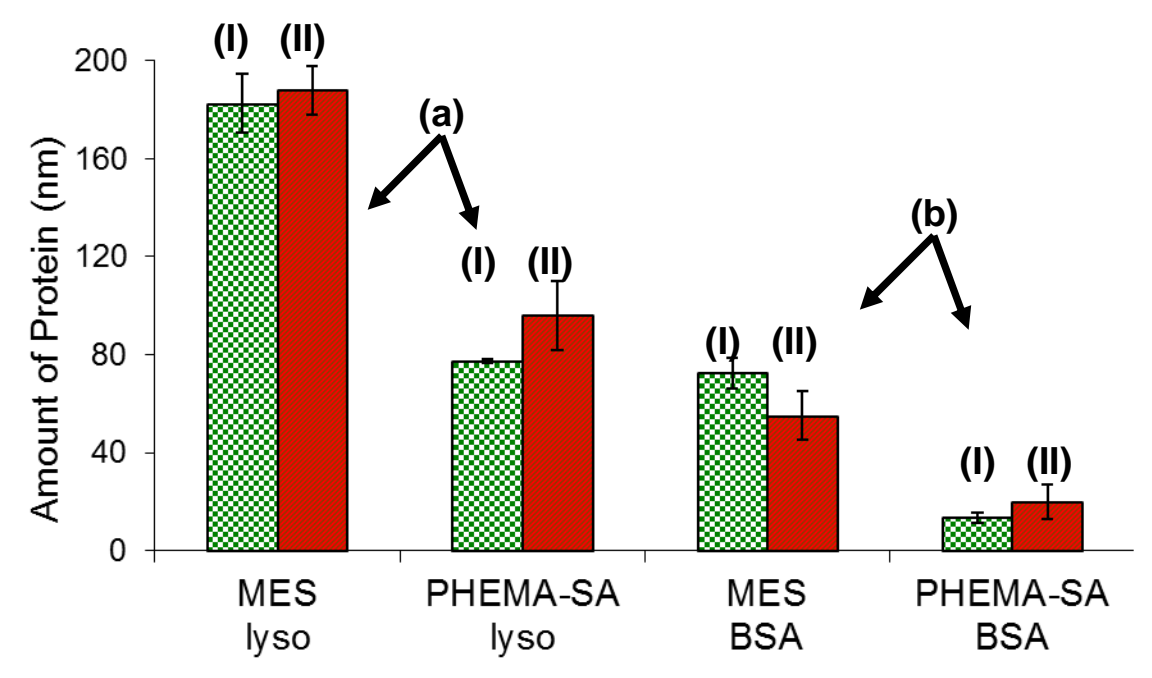


Figure 3.6. Amount of lysozyme (a), and BSA (b) bound to 50 nm poly(MES) (1,3) and 50 nm poly(HEMA)-SA (2,4) brushes grown from monolayers containing 5% (I) and 100% (II) initiator densities. For BSA binding poly(MES) and poly(HEMA-SA) films were derivatized with NTA-Cu²⁺. Binding occurred from a 1 mg/mL protein solution for 18 h. The protein binding is the thickness of a spin-coated film with the same amount of protein as that sorbed in the film.

The most interesting and useful observation from this preliminary study is that in all cases poly(MES) brushes and their NTA-Cu²⁺ derivatives bind 2- to 5-fold more protein than poly(HEMA-SA) brushes, even though the films have nominally the same chemical formula. With polymerization from a 100% initiator monolayer a 50 nm poly(MES) film binds 180 nm of lysozyme, whereas 50 nm poly(HEMA)-SA brushes bind 80 nm of lysozyme. The direct polymerization of poly(MES) should yield more widely separated polymer chains than reaction of poly(HEMA) with SA, because with poly(MES) long side chains are present during brush formation to separate chains (Scheme 3.1). Evidently, compared with poly(HEMA-SA) the higher accessibility of the less crowded poly(MES) leads to much larger protein binding.

Crowding should be most apparent with films grown from 100 % initiator and derivatized with NTA-Cu²⁺. Binding of BSA to the NTA-Cu²⁺ films should be an especially good indicator of steric constraints because the molecular mass of BSA (67 kDa) is nearly 5-times greater than the molecular mass of lysozyme (14 kDa). Remarkably, for films grown from 100% initiator, binding of BSA to poly(MES-NTA-Cu²⁺) is 5-fold greater than binding of BSA to poly(HEMA-SA-NTA-Cu²⁺). These results strongly suggest that binding to poly(MES) brushes is greater than binding to poly(HEMA-SA) because of less crowding in the film.

3.4. Conclusion

This study aimed to increase the capacity and rate of protein binding to polymer brushes by decreasing the areal density of polymer chains. We initially reduced the chain density by including a diluent molecule in initiator monolayers. However, 15 nm-thick poly(MES) brushes grown from 1% or 100% initiator in the monolayer show similar protein binding capacities.

Thicker (50 nm) films also showed similar protein binding with poly(MES) or poly(HEMA) films grown from monolayers with 5% and 100% initiator.

In a second method to examine the effect of areal chain density on protein binding to polymer brushes, we compared poly(MES) brushes with poly(HEMA) derivatized with SA. Both brushes have the same repeat unit, but derivatization of poly(HEMA) with SA will result in more crowded brushes. Direct polymerization of poly(MES) provides more widely separated polymer backbones because longer side-chains are present during brush formation. Protein-binding studies show as much as 2.25-fold greater lysozyme adsorption to poly(MES) than to poly(HEMA-SA). Derivatization of poly(MES) and poly(HEMA-SA) with NTA-Cu²⁺ to capture BSA leads to even greater difference in protein binding by the two types of polymer brushes. For 50 nm thick poly(MES) and poly(HEMA)-SA brushes, BSA binding was 80 nm and 15 nm respectively (~5 fold high for poly(MES)) with films derivatized with NTA-Cu²⁺. Increased brush crowing due to insertion of NTA-Cu²⁺ likely has a greater effect on the already crowded poly(HEMA-SA) than on poly(MES).

REFERENCES

3.5. References

- (1) Kawai, T.; Saito, K.; Lee, W. *Journal of Chromatography B* **2003**, 790, 131-142.
- (2) Bhut, B. V.; Husson, S. M. *Journal of Membrane Science* **2009**, *337*, 215-223.
- (3) Thommes, J.; Etzel, M. *Biotechnology Progress* **2007**, 23, 42-45.
- (4) Steve Brandt; Randal A. Goffe; Stephen B. Kessler; O'Connor, J. L.; Zale, S. E. *Nature Biotechnology* **1988**, *6*, 779 782.
- (5) Roper, D. K.; Lightfoot, E. N. Journal of Chromatography A 1995, 702, 26.
- (6) Van Reis, R.; Zydney, A. Journal of Membrane Science 2007, 297, 16-50.
- (7) Müller, W. *Journal of Chromatography A* **1990**, *510*, 133-140.
- (8) Yang, Q.; Ulbricht, M. *Macromolecules* **2011**, *ASAP*.
- (9) Jain, P.; Vyas, M. K.; Geiger, J. H.; Baker, G. L.; Bruening, M. L. *Biomacromolecules* **2010**, *11*, 1019-1026.
- (10) Matyjaszewski, K.; Miller, P. J.; Shukla, N.; Immaraporn, B.; Gelman, A.; Luokala, B. B.; Siclovan, T. M.; Kickelbick, G.; Vallant, T.; Hoffmann, H.; Pakula, T. *Macromolecules* **1999**, *32*, 8716-8724.
- (11) Edmondson, S.; Huck, W. T. S. Journal of Materials Chemistry 2004, 14, 730-734.
- (12) De Vos, W. M.; Kleijn, J. M.; De Keizer, A.; Stuart, M. A. C. Angewandte Chemie International Edition 2009, 48, 5369-5371.
- (13) Shah, R. R.; Merreceyes, D.; Husemann, M.; Rees, I.; Abbott, N. L.; Hawker, C. J.; Hedrick, J. L. *Macromolecules* **2000**, *33*, 597-605.
- (14) Bantz, M. R.; Brantley, E. L.; Weinstein, R. D.; Moriarty, J.; Jennings, G. K. *Journal of Physical Chemistry B* **2004**, *108*, 9787-9794.
- (15) Zhou, F.; Liu, W. M.; Hao, J. C.; Xu, T.; Chen, M.; Xue, Q. J. *Advanced Functional Materials* **2003**, *13*, 938-942.
- (16) Von werne, T. A.; Germack, D. S.; Hagberg, E. C.; Sheares, V. V.; Hawker, C. J.; Carter, K. R. *Journal of the American Chemical Society* **2003**, *125*, 3831-3838.
- (17) Bao, Z. Y.; Bruening, M. L.; Baker, G. L. *Macromolecules* **2006**, *39*, 5251-5258.
- (18) He, D.; Ulbricht, M. Journal of Membrane Science 2008, 315, 155-163.

- (19) Yang, Q.; Kaul, C.; Ulbricht, M. Langmuir 2009, 26, 5746-5752.
- (20) Wu, T.; Efimenko, K.; Vlcek, P.; Subr, V.; Genzer, J. *Macromolecules* **2003** *36*, 2448-2453.
- (21) Jones, D. M.; Brown, A. A.; Huck, W. T. S. Langmuir 2002, 18 1265-1269.
- (22) Jain, P.; Sun, L.; Dai, J. H.; Baker, G. L.; Bruening, M. L. *Biomacromolecules* **2007**, 8, 3102-3107.
- (23) Jain, P.; Dai, J. H.; Baker, G. L.; Bruening, M. L. *Macromolecules* **2008**, *41*, 8413-8417.
- (24) Dai, J. H.; Bao, Z. Y.; Sun, L.; Hong, S. U.; Baker, G. L.; Bruening, M. L. *Langmuir* **2006**, 22, 4274-4281.
- (25) Kim, J. B.; Bruening, M. L.; Baker, G. L. Journal of the American Chemical Society **2000**, 122, 7616-7617.
- (26) Tsuneda, S.; Shinano, H.; Saito, K.; Furusaki, S.; Sugo, T. *Biotechnology Progress* **1994**, *10*, 76-81.
- (27) Carter, D. C.; He, X. M.; Munson, S. H.; Twigg, P. D.; Gernert, K. M.; Broom, M. B.; Miller, T. Y. *Science* **1989**, *244*, 1195-1198.

Chapter 4. Attempts to Synthesize Affinity

Membranes that Isolate Maltose Binding

Protein-Fusion Proteins

4.1. Introduction

Rapid increases in recombinant protein synthesis for fundamental studies and therapeutic applications demand efficient purification methods for a wide variety of proteins. Affinity-based isolation, the most popular and convenient way to capture target proteins from complex biological fluids, usually relies on specific interactions between a binding tag on the protein and a complementary ligand immobilized on a support. In a typical purification, the target protein selectively binds to ligands in a matrix while the other components pass through the matrix. Rinsing removes residual impurities, and recovery of the target protein occurs through elution using a competitive binder or other conditions that dissociate the protein-ligand complex.

Affinity tags are crucial to these separations as they allow selective capture of proteins from crude cell extracts without pretreatment to remove cellular materials. Equally important, these tags give rise to generalized protocols to purify different proteins. 1,5 Common affinity tags include polyhistidine (His₆), 6,7 maltose binding protein (MBP), 8 glutathione-S-transferase (GST), 9 calmodulin-binding peptide 10 and streptavidin. 11 His₆ is the most popular affinity tag because it allows rapid purification by binding to Ni²⁺ complexes on a stationary phase. 12,13

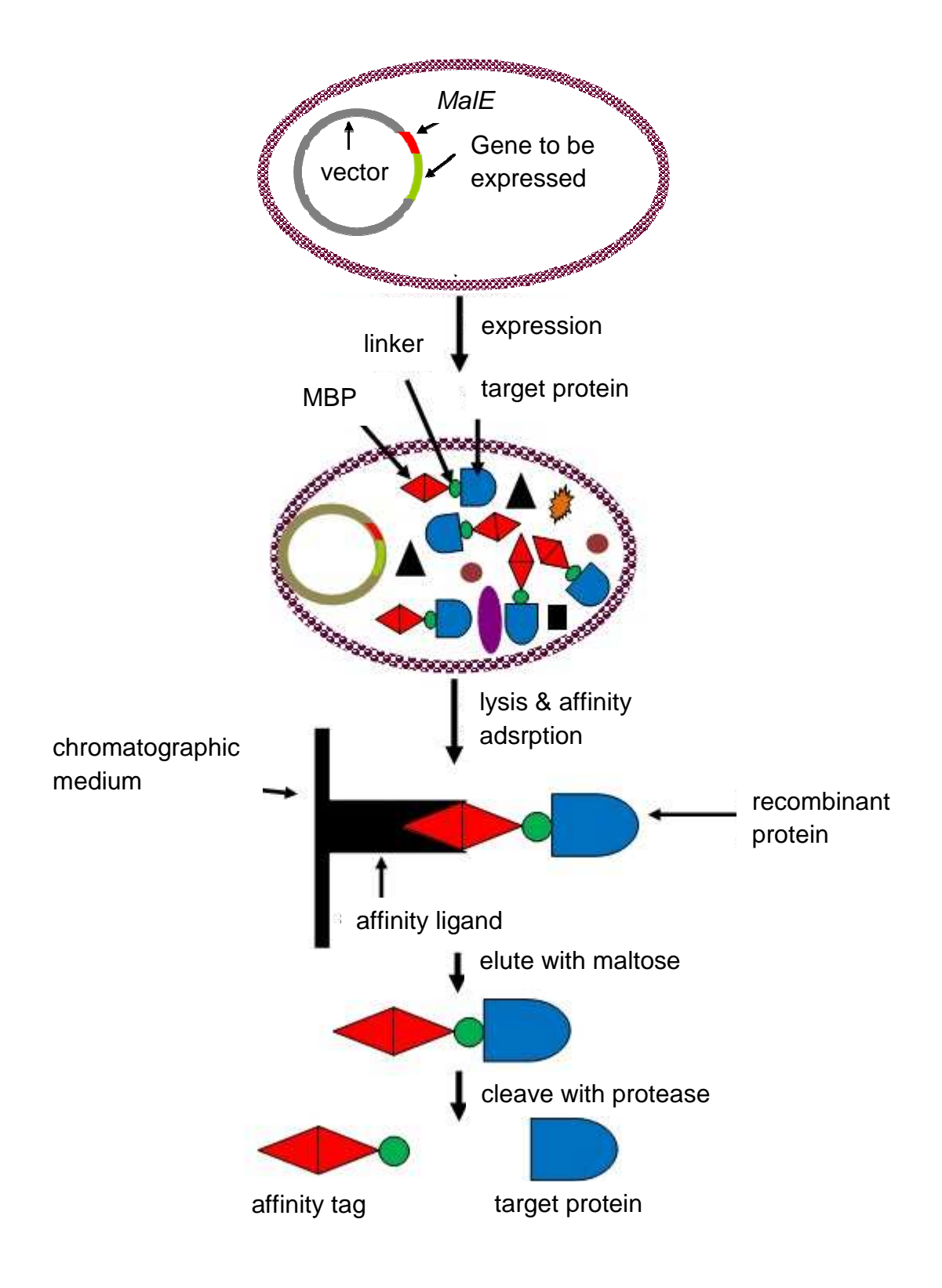


Figure 4.1. Expression and purification of MBP-tagged fusion protein. MalE is the gene that encodes MBP.

However, some proteins and peptides cannot be directly synthesized in a stable form within a cell, and in such cases the target is produced as part of a fusion protein. The fusion partner should be expressed at high levels within the cell and would be especially beneficial if it facilitated the purification of the fusion protein. One of the fusion partners most widely used in *Escherichia coli* is MBP, which facilitates isolation of the fusion protein in a single adsorption step. Additionally purification with this tag occurs under physiological conditions including mild elution (generally 10 mM maltose). Moreover MBP improves folding of the target protein to increase solubility. This becomes especially important when the target is a heterologous eukaryotic protein expressed in bacterial cells. Figure 4.1 shows expression of an MBP fusion protein and purification with an affinity medium.

Purifications of MBP-tagged protein generally employ crossed-linked amylose resins. ¹⁷ Commercially available resin from New England Biolabs is a composite of amylose and agarose with a binding capacity of 6-8 mg of fusion protein per mL of binding medium. ¹⁸ The maltose transport system in *Escherichia coli* mediates the entry of maltodextrins into the cell and MBP recognizes not only maltose but also maltodextrins up to at least maltoheptaose. Sigma Aldrich produces maltoheptaose agarose resins that exhibits a binding capacity of 6 mg/mL of resin. ¹⁹ GE Life Sciences claims that their dextrin sepharose medium binds about 7-16 mg/mL of MBP-fusion proteins. ²⁰

Microporous membranes could potentially provide faster separations than columns because flow through membrane pores can prevent diffusion limitations in MBP binding. Fast separations are particularly attractive for large-scale separations. ^{8,21,22} Cattoli and Sarti showed

that microporous cellulose membranes modified with amylose bind an MBP fusion protein (51 kDa total molecular weight) with a capacity of 0.55 mg/mL at a flow rate of 70 cm/h. 8

In this work we attempt to immobilize maltose on polymer-brush modified porous membranes to create materials that isolate MBP fusion proteins (Figure 4.2). The brushes should present a high protein-binding capacity due to their multiple binding sites, and the membrane based system should provide fast and efficient purification. Preliminary studies show successful attachment of maltose to polymer brushes on gold surfaces, but MBP binding to the brushes was not seen. Future studies should examine the suitability of maltoheptaose- or dextrin-modified polymer brushes for MBP binding.

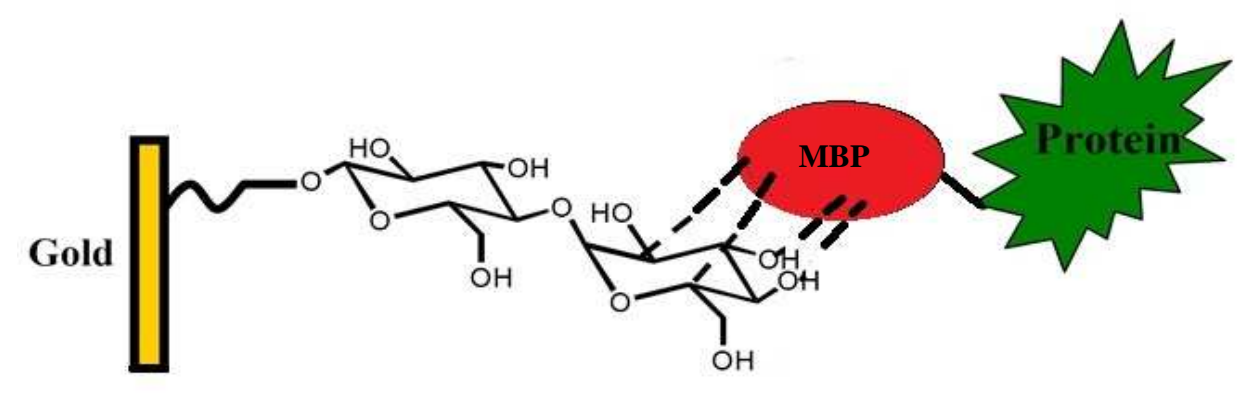


Figure 4.2. Binding of MBP-tagged protein to polymer brushes attached to a gold coated silicon substrate.

4.2. Experimental

4.2.1. Materials

11-mercaptoundecanol (97%, MUD), 2-bromoisobutyryl bromide (98%), glycidyl methacrylate (GMA), 2,2'-dipyridyl, Copper(I) chloride (99%), Copper(II) bromide (99%), sodium azide, and sodium ascorbate (NaAsc) were purchased from Sigma Aldrich and used as obtained. Copper sulfate (CCI) and maltose (Fischer Scientific) were also used as received. MBP was purchased from Abcam, and disulfide initiator [(S(CH₂)₁₁OCOC(CH₃)₂Br)₂] was

synthesized according to literature procedure. ²³ Buffers were made using analytical grade chemicals and deionized (Milli -Q, 18.2 $M\Omega$ cm) water.

4.2.2. Formation of azide-modified poly(GMA) brushes on \mathbf{Au}^{23-25}

Au-coated wafers (200 nm of sputtered Au on 20 nm of sputtered Cr on Si wafers) were cleaned with UV/ozone (Boekel model 135500) for 15 min and immersed in a 1 mM ethanolic solution of disulfide initiator for 24 h followed by sequential rinsing with ethanol and water and drying under a stream of nitrogen. The wafer was transferred to a nitrogen-filled glove bag for polymerization. A polymerization solution of GMA (5 mL, 36.7 mmol) in methanol (4 mL) and water (1 mL) was degassed using 3 freeze-pump-thaw cycles. Copper(I) chloride (36.4 mg, 0.368 mmol), copper(II) bromide (3.9 mg, 0.017 mmol) and 2,2'-dipyridyl (141 mg, 0.904 mmol) were added to the monomer solution, which was degassed again. The mixture was stirred for 5 min to dissolve all solids and was transferred to a N_2 filled glove bag where the initiator-coated wafer was immersed in the solution for 3 h of polymerization. The wafer was then washed with methanol followed by water (20 mL of each), and dried under a stream of N_2 . These wafers were subsequently immersed in 0.1 M sodium azide in water at 40 $^{\circ}$ C for 48 h, and the wafers were rinsed with water and dried in nitrogen.

4.2.3. Synthesis of propargyl maltose 26,27

Propargyl maltose was kindly synthesized following a literature procedure ^{26,27} by Somnath Bhattacharjee. Briefly, acetic anhydride (6 mL) was mixed with maltose (2 g) and sodium acetate (0.2g), and the mixture was refluxed for 2 h at 140 °C. The solution was cooled to room temperature, poured into ice water to obtain a yellow oil layer that was then

recrystallized in methanol to obtain acetyl maltose. The acetyl maltose (1 g) was dissolved in dichloromethane (20 mL) and cooled to 0-5 °C before addition of propargyl alcohol (0.13 mL). Boron trifluoride/ether (0.55 mL) was added dropwise to the above mixture, which was stirred for 1 h at 0-5 °C and then at room temperature for another 4 h. K₂CO₃ was added to neutralize the excess acid, and the solution was continuously stirred for 30 minutes. The mixture was filtered to remove unreacted solid, and the filtrate was concentrated to obtain a solid, which was purified using column chromatography (ethyl acetate: hexane 1:1). 1-propargyl-acetyl maltose (0.3 g) was dissolved in methanol (5mL) and cooled to 0-5 °C. A solution of sodium methoxide in methanol (1M) was added to the mixture drop wise and stirred at room temperature while the reaction was monitored with TLC. After completion, the mixture was neutralized with Amberlite IR-120 ion exchange resin, filtered and concentrated to obtain a white solid. The solid was dried in vacuum and used without further purification.

4.2.4. Click chemistry to react propargyl maltose with azide groups on Au

Propargyl maltose (1g) was dissolved in a water-methanol (1:1 V/V) mixture prior to addition of copper sulfate (0.024g) and sodium ascorbate (0.074g). An azide-modified polymer brush on a Au-coated wafer was immersed in the mixture, which was stirred at 25°C for 48 h. The wafer was washed with methanol and water and dried in nitrogen.

4.2.5. Protein immobilization

For MBP protein binding studies, the Au coated wafer containing maltose-modified polymer brushes was immersed in a 0.2-1 mg/mL solution of MBP protein in 20 mM phosphate buffer (pH 8) for 18 h at 4 °C. The film was then rinsed with the same buffer followed by 20 mL ethanol and dried in nitrogen.

4.2.6. Characterization of Au surface modification and protein binding

Polymerization, each step of derivatization of the side chain of the polymer, and protein binding to the functionalized polymer brush were characterized using reflectance Fourier Transform Infrared (FTIR) Spectroscopy (Nicolet 6700 spectrophotometer containing a PIKE grazing angle (80 °) accessory) and with a rotating analyzer Ellipsometer (model M-44, J.A. Woollam, at an incident angle of 75 °, assuming a film refractive index of 1.5). A UV/ozone cleaned Au coated wafer was used as the background, and ellipsometric measurements were performed on at least on 3 spots on the film surface.

4.3. Results and discussion

Scheme 4.1 outlines the growth of poly(GMA) brushes on Au-coated Si wafers and the derivatization of these brushes to attach maltose for later binding of MBP-fusion proteins. ^{23,25} Figure 4.3 shows the reflectance FTIR spectra obtained after polymerization of GMA and subsequent derivatization of the poly(GMA) brushes on the Au-coated surface. In Figure 4.3 (a), the peak at 1740 cm⁻¹ stems from the carbonyl groups of poly(GMA) and confirms brush growth. The ellipsometric thickness of the poly(GMA) films is 27 nm after 3 h of polymerization. Immersing the wafer in 0.1M sodium azide results in the appearance of a peak at 2100 cm⁻¹ due to azide groups and a broad peak around 3500 cm⁻¹ corresponding to hydroxyl groups (Figure 4.3 (b)). These absorbances confirm opening of the epoxide ring to create an azide and alcohol. Subsequent exposure of the film to propargyl maltose dissolved in a water/methanol mixture along with copper sulfate and sodium ascorbate results in nearly complete disappearance of the azide peak (Figure 4.3 (c)).

Scheme 4.1. Polymerization of poly(GMA) brushes from initiators on a Au-coated wafer, derivatization of the brushes with azide groups, and attachment of maltose to the brushes through "click" chemistry.

In addition, the strong broad band ranging from 850 to 1350 cm⁻¹ shows the various vibrations of the C-O-C skeletal structure of the immobilized maltose. The broad band around 3500 cm⁻¹ representing free OH groups increases in intensity, further confirming maltose immobilization. The increase in the ellipsometric thickness from 27 nm for poly(GMA) brushes to 45 nm after maltose immobilization, also corroborates the maltose immobilization, but the thickness increase is less than one might expect from the molecular masses of the polymer repeat units for poly(GMA) before (140 g/mole) and after (567 g/mole) complete derivatization.

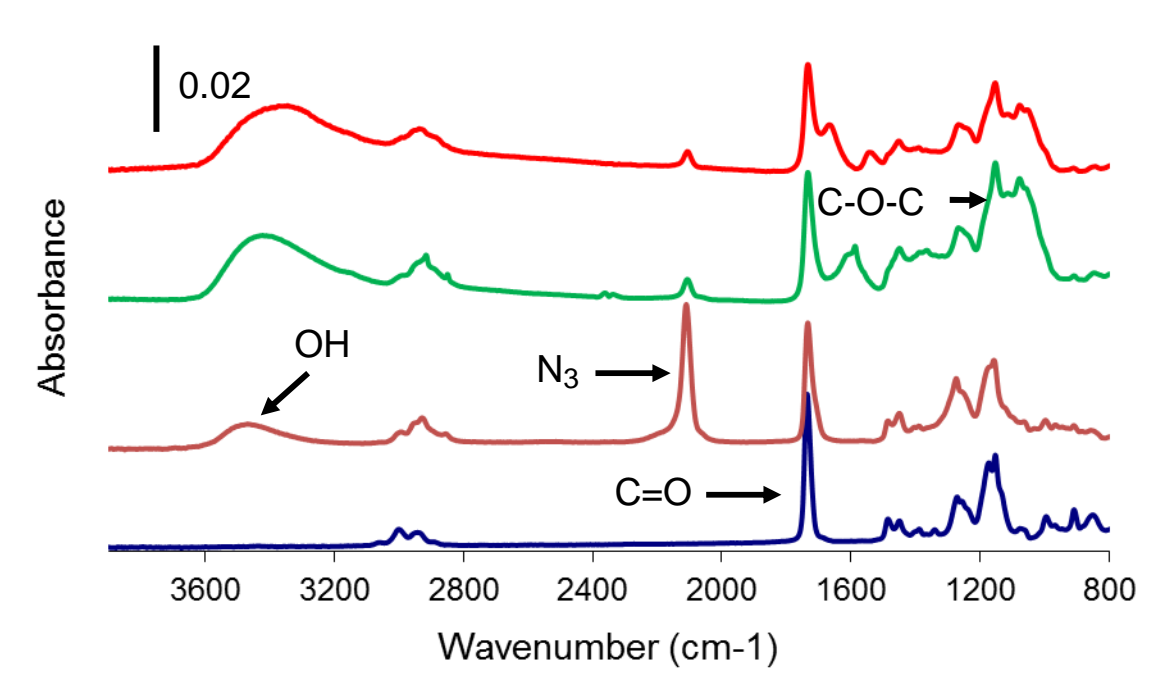


Figure 4.3. Reflectance-FTIR spectra of (a) poly(GMA) brushes on Au-coated wafers and the same brushes after (b) reaction with sodium azide, (c) immobilization of maltose during exposure to a propargyl maltose solution, and (d) immersion in a solution of cellular extract with MBP-tagged protein.

A control experiment was performed by immersing the azide modified wafer into a solution void of propargyl maltose but containing copper sulfate and NaAsc. This wafer did not

show the appearance of a broad band ranging from 850 to 1350 cm⁻¹ and an increase around 3500 cm⁻¹, which indicates that the immobilization of maltose results from a click reaction between propargyl maltose and the azide group on the polymer brush.

To examine whether the poly(GMA) brushes modified with maltose can bind MBP, we immersed the fully derivatized brushes in a solution containing 0.2 mg/mL MBP (43 kDa) in phosphate buffer (pH 8) for 18 hours at 4 °C. Following rinsing with phosphate buffer and drying in stream of nitrogen, the reflectance FTIR spectrum of the film showed no changes due to protein binding. Moreover, the ellipsometric film thickness did not increase after immersion of the film in an MBP solution. The same experiment with a higher concentration (1 mg/mL) of MBP yielded the same result.

However, when we immersed the maltose-modified poly(GMA) brushes in a cell extract that contained MBP-tagged-ADP glucose pyrophosphorylase (100 kDa) (the cell extract was kindly provided by Dr. Geiger and his lab²⁸), amide I and II stretches at 1660 cm⁻¹ and 1550 cm⁻¹, respectively, appeared suggesting binding of protein to the modified polymer brush (Figure 4.3 (d)). Additionally, the ellipsometric film thickness increased by 9 nm after incubation in the cell lysate and rinsing. However, we cannot confirm whether the binding is due to the MBP-tagged protein or other proteins with affinity for carbohydrates (see below).

Lectins are a group of proteins with unique affinity towards different carbohydrates, and Concanavalin A (Con A), the most common lectin, binds specifically to mannosyl and glycosyl residues of sugars. ²⁹ We incubated Au wafers modified with the maltose-containing polymer brush in a 1 mg/mL solution of Con A in phosphate buffer for 18 h at room temperature.

Following rinsing and drying the reflectance FTIR spectrum of the film showed clear amide I and II bands, demonstrating binding of Con A to the modified polymer brush. The ellipsometric thickness of the polymer brush increased by 20 nm, corroborating Con A binding. These results also provide evidence for successful immobilization of maltose to the poly(GMA). A control experiment was performed by immersing a maltose modified wafer in a phosphate buffer void of Con A. This wafer showed no observable changes on the FTIR spectrum.

As mentioned in the introduction, current MBP-tagged protein purifications occur using resins with a binding capacity of around 6 mg/mL bed volume. Based on the relatively high binding capacities of ~80 mg His-tagged protein/mL of membrane adsorber, we think that membranes can offer high capacities relative to commercial resins for binding of lectins or MBP-tagged protein as well. Nevertheless, we have not clearly demonstrated that maltose-containing brushes can bind MBP-tagged proteins. Binding of lectins should be possible.

4.4. Conclusions

This preliminary study shows successful attachment of maltose to polymer brushes via click chemistry and the subsequent binding of proteins to the maltose-containing polymer brushes. Unfortunately immobilized maltose failed to bind MBP, but Con A binds to these brushes in significant amounts.

REFERENCES

4.5. References

- (1) Arnau, J.; Lauritzen, C.; Petersen, G. E.; Pedersen, J. *Protein Expression and Purification* **2006**, *48*, 1-13.
- (2) Kawai, T.; Saito, K.; Lee, W. *Journal of Chromatography B* **2003**, 790, 131-142.
- (3) Steve Brandt; Randal A. Goffe; Stephen B. Kessler; O'Connor, J. L.; Zale, S. E. *Nature Biotechnology* **1988**, *6*, 779 782.
- (4) Shi Wei; Zhang Fengbao; Zhang Guoliang *Journal of Chromatography A* **2005**, *1081*, 156-162.
- (5) Lichty, J. J.; Malecki, J. L.; Agnew, H. D.; Michelson-Horowitz, D. J.; Tan, S. *Protein Expression and Purification* **2005**, *41*, 98-105.
- (6) Hochuli, E.; Dobeli, H.; Schacher, A. *Journal of Chromatography* **1987**, 411, 177-184.
- (7) Stiborova, H.; Kostal, J.; Mulchandani, A.; Chen, W. *Biotechnology and Bioengineering* **2003**, 82, 605-611.
- (8) Cattoli, F.; Sarti, G. C. Biotechnology Progress 2002, 18, 94-100.
- (9) Smith, D. B.; Johnson, K. S. Gene **1988**, 67, 31-40.
- (10) Stofko-Hahn, R. E.; Carr, D. W.; Scott, J. D. Febs Letters 1992, 302, 274-278.
- (11) Skerra, A.; Schmidt, T. G. M. Biomolecular Engineering 1999, 16, 79-86.
- (12) Suen, S. Y.; Liu, Y. C.; Chang, C. S. Journal of Chromatography B 2003, 797, 305-319.
- (13) Everson, R. J.; Parker, H. E. bioinorganic Chemistry 1974, 4, 15-20.
- (14) Srinivasan, U.; Bell, J. A. *Journal of Biotechnology* **1998**, 62, 163-167.
- (15) Guan, C. D.; Li, P.; Riggs, P. D.; Inouye, H. Gene **1988**, 67, 21-30.
- (16) Ferenci, T.; Klotz, U. Febs Letters 1978, 94, 213-217.
- (17) Malhotra, A.; Richard, R. B. a. M. P. D. In *Methods in Enzymology*; Academic Press, 2009; Vol. Volume 463, pp 239-258.
- (18) http://www.neb.com/nebecomm/products/productE8021.asp (Binding Capacity 6 8 mg MBP-fusion protein / ml bed volume) (accessed March 21, 2011)

- (19) http://www.sigmaaldrich.com/etc/medialib/docs/Sigma/Datasheet/4/m9676dat. Par.0001.File.tmp/m9676dat.pdf (Maltoheptaose agarose resin binds a minimum of 6 mg of maltose binding protein per ml of packed resin) (accessed March 21, 2011)
- (20) http://www.gelifesciences.com/aptrix/upp00919.nsf/Content/78BDD97E3689F1 FFC1257628001D4242/\$file/28913633AB.pdf (Dextrin Sepharose chromatographic medium dynamic binding capacity 7-16 mg/ml medium) (accessed March 21, 2011)
- (21) Zou, H.; Luo, Q.; Zhou, D. Journal of Biochemical and Biophysical Methods 2001, 49, 199-240.
- (22) Ghosh, R. Journal of Chromatography A **2002**, 952, 13-27.
- (23) Shah, R. R.; Merreceyes, D.; Husemann, M.; Rees, I.; Abbott, N. L.; Hawker, C. J.; Hedrick, J. L. *Macromolecules* **2000**, *33*, 597-605.
- (24) Edmondson, S.; Huck, W. T. S. Journal of Materials Chemistry 2004, 14, 730-734.
- (25) Slater, M.; Snauko, M.; Svec, F.; Frechet, J. M. J. *Analytical Chemistry* **2006**, 78, 4969-4975.
- (26) Guo, Z. M.; Lei, A. W.; Zhang, Y. P.; Xu, Q.; Xue, X. Y.; Zhang, F. F.; Liang, X. M. *Chemical Communications (Cambridge, United Kingdom)* **2007**, 2491-2493.
- (27) El-Boubbou, K.; Gruden, C.; Huang, X. *Journal of the American Chemical Society* **2007**, *129*, 13392.
- (28) Jin, X.; Ballicora, M. A.; Preiss, J.; Geiger, J. H. *The EMBO Journal* **2005**, 24, 694-704.
- (29) Tang, J.; Liu, Y.; Yin, P.; Yao, G.; G., Y.; Deng, C.; Zhang, X. *Proteomics* **2010**, *10*, 2000-2014.

Chapter 5. Conclusions and Future Work

5.1. Conclusions and Future work

Chapter 2 described a simple, rapid and completely aqueous procedure for growth and functionalization of polymer brushes in nylon, PES and PVDF membranes. MES polymerization from macroinitiators immobilized within the pores of polymeric membranes is a rapid method (10 min of initiator attachment and 5 min of polymerization) for synthesizing high capacity protein-binding membranes with a relatively high water permeability. Poly(MES)-modified nylon membranes bind 122 ± 9 mg/cm³ of lysozyme and after further derivatization to poly(MES-NTA-Cu²⁺) or poly(MES-NTA-Ni²⁺), these membranes capture 86 ± 10 mg/cm³ of Con A and 88 \pm 4 mg/cm³ of His U. Poly(MES-NTA-Ni²⁺)- and poly(MES-NTA-Cu²⁺)modified nylon membranes have a pure water permeability of 85 ± 4 mL/(cm² min atm). Remarkably, protein capture can occur during a 35 ms residence time in the membrane. Additionally poly(MES)-NTA-Ni²⁺-modified membranes facilitate purification of His-tagged MIPS from cell extracts in less than 15 min. The fraction of total HisU recovered during elution was at least 90 %. We also showed that stacking several membranes and increasing membrane diameter are viable means for scaling up protein purification. The method for membrane modification is completely aqueous and applicable to a wide range of membranes including hydroxylated and non-hydroxylated nylon, PES and PVDF.

This work should be expanded to include purification of His-tagged protein from more complex cell extracts. The presence of surface clusters of histidine residues and also tryptophan and cysteine residues in contaminant proteins can lead to nonspecific binding to metal

complexes. ¹⁻³ For example, proteins like lipocalin, ⁴ glucosamine-6-phosphate synthase, ⁵ and peptidoylproline cis-trans isomerase ⁶ show affinity for Ni²⁺ binding sites in IMAC columns and elute along with the His-tagged protein of interest. Because the brush-modified membranes also employ Ni²⁺ complexes, however, this challenge may be difficult to overcome. In some cases hydrophobic interactions between the resin and proteins lead to non-specific binding to IMAC columns. For example, Hsp 60 has affinity towards the resins and gets co-purified with the over expressed protein. ⁷ Purification of proteins like small nuclear RNA activating protein complex ⁸ and GroEL-GroES chaperonin complex in a single-step is difficult because highly abundant, "sticky" proteins in the cell extract bind to the resin material. ⁷ Relative to IMAC resins, both flow through the membrane pores and the hydrophilicity of polymer brushes could decrease the binding of unwanted proteins. Investigation of whether membranes can improve protein purity in these cases is an important area for future research.

To fully demonstrate the utility of brush-modified membranes for protein purification, we need to compare the performance (purity, separation time, operating pressure) of membranes and columns for both large and small scale separations. Large-scale purification will require larger membranes and perhaps membrane stacking. In the opposite case of small samples with $100~\mu L$ volumes, reducing the membrane's effective surface will allow elution in volumes as small as $10\text{--}20~\mu L$. Xu et al. recently demonstrated membrane holders that treat such small-volume samples. The high binding capacity of the membranes is very important in this case because the membrane volume will be small. 1,10--12

Chapter 3 presented research aimed at increasing protein binding capacity and enhancing binding kinetics by reducing the areal density of chains in polymer brushes. Larger spacings between polymer chains may increase brush swelling to make protein-binding sites more accessible. In a first method, we achieved reduced chain areal densities in polymer brushes by diluting the initiators and reducing areal density of potential polymerization sites. We choose initiator fractions as low as 1% and 5% of a self-assembled monolayer and compared the protein binding to brushes grown from these surfaces with binding to polymer brushes grown from monolayers with 100% initiator. Unfortunately, monolayers with low initiator densities exhibited very slow growth rates, and the amount of polymerization was small even after long polymerization times. This resulted in a maximum film thickness of only 15 nm with 1% initiator monolayers, and these brushes showed similar protein binding capacities to a 15 nm-thick brush grown from 100 % initiator monolayers.

In a second method we varied the chain density by creating poly(MES) brushes through two different routes. In one scheme we polymerized HEMA and subsequently derivatized the side chains with SA, and in a direct route we polymerized MES. Derivatization of poly(HEMA) with SA will result in more crowded brushes, whereas direct polymerization of poly(MES) provides more widely separated polymer chains because longer side-chains are present during brush formation. Direct polymerization of MES yields significantly greater protein-binding capacities. For 50 nm thick poly(MES) and poly(HEMA-SA) brushes on Au-coated substrates, the lysozyme binding capacities were 180 nm and 80 nm, respectively (~2 fold high for poly(MES)) and BSA binding capacities were 80 nm and 15 nm, respectively (~5 fold high for poly(MES)).

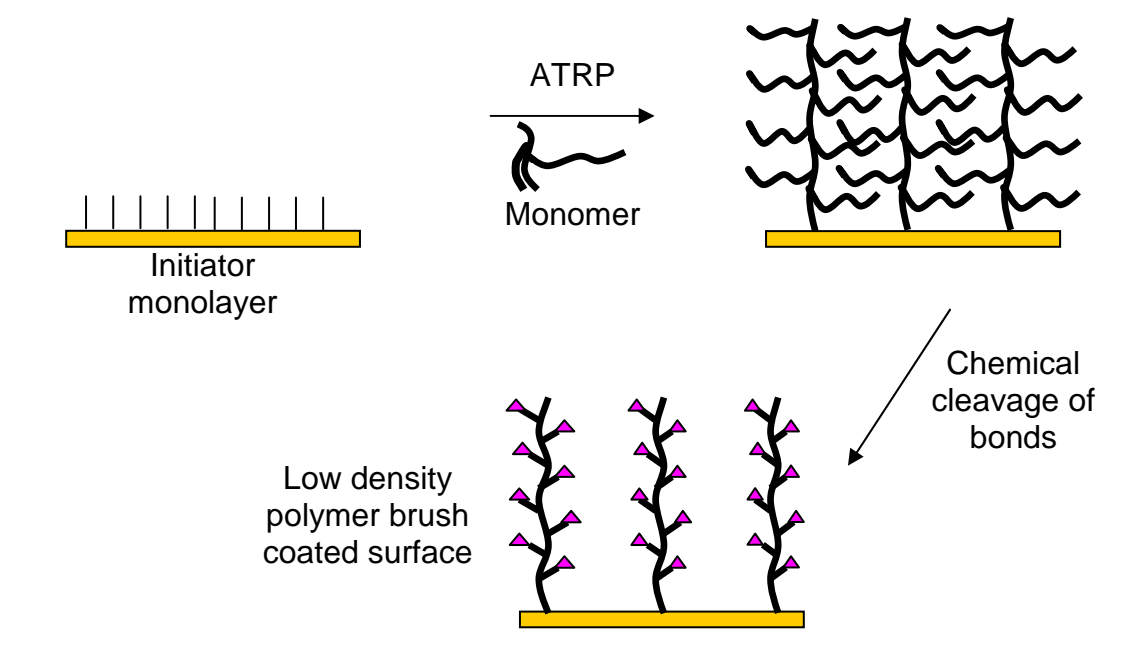


Figure 5.1. Synthesis of reduced-density polymer-brushes using monomers with long side chain and subsequent side chain hydrolysis. Triangles represent carboxylic acid.

Future studies could focus on further reducing brush density by synthesizing polymer brushes with long, cleavable side chains. Removal of the side chains after polymerization should lead to a low areal chain density (Figure 5.1). Figure 5.2 shows the structure of one possible monomer. The tertiary esters should hydrolyze under mild, acidic conditions but remain stable under aqueous polymerization conditions.

Figure 5.2. Proposed structure of a cleavable monomer (poly(ethyleneglycol)-bis-acrylate).

One concern is that after hydrolysis the brushes might collapse to restrict access to interior binding sites. Cross-linking of the films may help to avoid this problem. In that case

the rigidity of the polymer brushes can be increased by cross-linking them with an appropriate reagent. The choice and percentage of cross-linker is crucial as cross-linking might result in a reduction of binding capacity. ¹³

Chapter 4 describes an attempt to capture MBP-tagged recombinant protein from cell extracts using polymer brushes derivatized with maltose. We successfully attached maltose to polymer brushes via click chemistry and observed some Con A binding to these films (20 nm of Con A binds to a 25 nm-thick film). However, MBP does not bind to these films. Future work could examine whether immobilization of oligomers such as maltaheptaose or dextrin will lead to brushes that bind MBP-tagged proteins.

REFERENCES

5.2. References

- (1) Arnau, J.; Lauritzen, C.; Petersen, G. E.; Pedersen, J. *Protein Expression and Purification* **2006**, *48*, 1-13.
- (2) Porath, J. Trends in Analytical Chemistry 1988, 7, 254-259.
- (3) Porath, J. Protein Expression and Purification 1992, 3, 263-281.
- (4) David, G.; Blondeau, K.; Schiltz, M.; Penel, S.; Lewit-Bentley, A. *Journal of Biological Chemistry* **2003**, 278, 43728-43735.
- (5) Obmolova, G.; Badet-Denisot, M.-A.; Badet, B.; Teplyakov, A. *Journal of Molecular Biology* **1994**, *242*, 703-705.
- (6) Hottenrott, S.; Schumann, T.; Pluckthun, A.; Fischer, G.; Rahfeld, J. U. *Journal of Biological Chemistry* **1997**, 272, 15697-15701.
- (7) Bolanos-Garcia, V. M.; Davies, O. R. *Biochimica Et Biophysica Acta-General Subjects* **2006**, *1760*, 1304-1313.
- (8) Hanzlowsky, A.; Jelencic, B.; Jawdekar, G.; Hinkley, C. S.; Geiger, J. H.; Henry, R. W. *Protein Expression and Purification* **2006**, *48*, 215-223.
- (9) Xu, F.; Wang, W.-H.; Tan, Y.-J.; Bruening, M. L. *Analytical Chemistry* **2010**, 82, 10045–10051.
- (10) Pavlou, A. K.; Reichert, J. M. *Nature Biotechnology* **2004**, 22, 1513-1519.
- (11) http://www.gelifesciences.com/aptrix/upp00919.nsf/Content/78BDD97E3689F1 FFC1257628001D4242/\$file/28913633AB.pdf (Dextrin Sepharose chromatographic medium dynamic binding capacity 7-16 mg/ml medium) (accessed on March 21, 2011)
- (12) Jain, P.; Vyas, M. K.; Geiger, J. H.; Baker, G. L.; Bruening, M. L. *Biomacromolecules* **2010**, *11*, 1019-1026.
- (13) He, D.; Ulbricht, M. *Journal of Membrane Science* **2008**, *315*, 155-163.

APPENDIX

Poly(MES) Brushes Grown from

Macroinitiators on Au-coated Si

A.1. Experimental

A.1.1. Polymerization of MES on Au-coated wafers

Au-coated wafers (200nm of sputtered Au on 20nm of sputtered Cr on Si wafers) were cleaned with UV/ozone (Boekel model 135500) for 15 min, immersed overnight in 5 mM 3mercaptopropionic acid (MPA) in ethanol, and rinsed with ethanol to form a monolayer of MPA. This substrate was then immersed in a solution of macroinitiator (2 mg/mL in water) for 10 min, rinsed with water (20 mL) and dried in a stream of N2. In some cases a bilayer of poly(sodium 4styrene sulfonate) (PSS, Mw ~ 70 000, deposited from a 0.02 M solution containing 0.5 M NaCl) and poly(diallyldimethylammonium chloride) (PDADMAC, Mw ~ 150 000, deposited from a 0.02 M solution containing 0.5 M NaCl) was deposited on the MPA-modified Au surface prior to macroinitiator adsorption. (Polymer concentrations are given with respect to the repeating unit.) For macroinitiator multilayer films on gold, macroinitiator and PSS layers were deposited alternatively macroinitiator/PSS films. disulfide initiator, to form Α [(S(CH₂)₁₁OCOC(CH₃)₂Br)₂] (synthesized following a published procedure ¹), was attached to the gold wafer surface by immersing the clean wafer in a 1 mM ethanolic solution of the initiator for 24 h followed by sequential rinsing with ethanol and water and drying under stream of N₂.

Poly((2-methacryloyoxyethyl) succinate) (poly(MES)) brushes were grown from initiator-modified, Au-coated wafers. The polymerization mixture was prepared as described

before.^{2,3} Briefly 10 mL of a mixture of neat MES monomer and 1 M aqueous NaOH (1:1, v/v) was first degassed with three freeze-pump-thaw cycles. A 1 mL solution of DMF containing CuBr (2 mM), CuBr₂ (1 mM), and Me₆TREN (6 mM) was similarly degassed, and in a N₂-filled glove bag, this solution of catalyst was mixed with the monomer/NaOH solution. Polymerization on the initiator-modified Au surface occurred by immersing the wafer in the polymerization mixture in a N₂ glove bag for the desired time. Following the polymerization, the Au wafer was taken out of the glove bag, sonicated in DMF for 10 min and rinsed with ethanol and water. The sonication step was performed only for the disulfide-based substrate to avoid possible removal of the adsorbed macroinitiator from the surface.

A.1.2. Derivatization of poly(MES) and protein binding

Functionalization of the poly(MES) side chain for protein binding occurred as reported previously. ^{2,3} Briefly, the carboxylic acid groups of the poly(MES)-modified Au wafers were activated by immersing the substrate in an aqueous solution containing NHS (0.1 M) and EDC (0.1 M) for 1 h. This was followed by sequentially rinsing with 20 mL of deionized water and 20 mL of ethanol. These wafers were then immersed in an aqueous solution of aminobutyl NTA (0.1 M, pH 10.2) for 1 h, and subsequently rinsed with 20 mL of water. Finally, the NTA-Cu²⁺ complex was formed by immersing the substrate in an aqueous 0.1 M CuSO₄ solution for 2 h followed by rinsing with water followed by ethanol (20 mL each). The substrate was dried with N₂ prior to protein binding.

For lysozyme binding studies Au wafers with poly(MES) brushes were immersed in a 1 mg/mL solution of lysozyme in 20 mM phosphate buffer (pH 7.4) for 18 h. The films were then

rinsed with 20 mL washing buffer (20 mM phosphate buffer with 0.1% Tween 20, pH 7.4) followed by 20 mL phosphate buffer and 20 mL ethanol. Films were dried under a stream of N_2 .

To immobilize bovine serum albumin (BSA), poly(MES)-NTA-Cu $^{2+}$ -modified Au substrates were immersed in a solution of 1 mg/mL BSA in phosphate buffer for 18 h. The films were then rinsed with washing buffer (20 mM phosphate buffer with 150 mM NaCl and 0.1% Tween-20, pH 7.4) followed by 20 mL of phosphate buffer and 20 mL ethanol and were dried under a steam of N₂.

A.1.3. Characterization of polymer brush growth, derivatization and protein binding

Polymer film growth and subsequent modifications on Au substrates were confirmed with reflectance Fourier transform infrared spectroscopy (FTIR) (Nicolet 6700 IR spectrophotometer containing a PIKE grazing angle (80 °) accessory) and ellipsometry (rotating analyzer ellipsometer, model M-44, J.A. Woollam) at an incident angle of 75 °, assuming a film refractive index of 1.5). Ellipsometric measurements were performed on at least three spots on a film.

A.1.4. Quantification of protein binding

To quantify the amount of protein bound to polymer brushes on Au coated Si wafers, the method reported by Dai and co-workers was employed. Briefly, a calibration curve was obtained by plotting the ellipsometric thickness of spin-coated BSA or lysozyme films against the reflectance FTIR absorbance of their amide I band. The amide absorbance of lysozyme or BSA adsorbed to poly(MES) or poly(MES)-NTA-Cu²⁺ films was then compared to the

calibration curve to obtain the thickness added due to protein adsorption. These results were confirmed by the increase in ellipsometric thickness after protein binding. To avoid pH-induced changes in film spectra, before characterization by reflectance FTIR spectroscopy and ellipsometry, poly(MES)-NTA-Cu²⁺ films were immersed in phosphate buffer (pH 7.4) for 15 min followed by rinsing with 20 mL of ethanol and drying under a stream of N₂.

A.2. Results and Discussion

A.2.1. Polymer brush growth and characterization

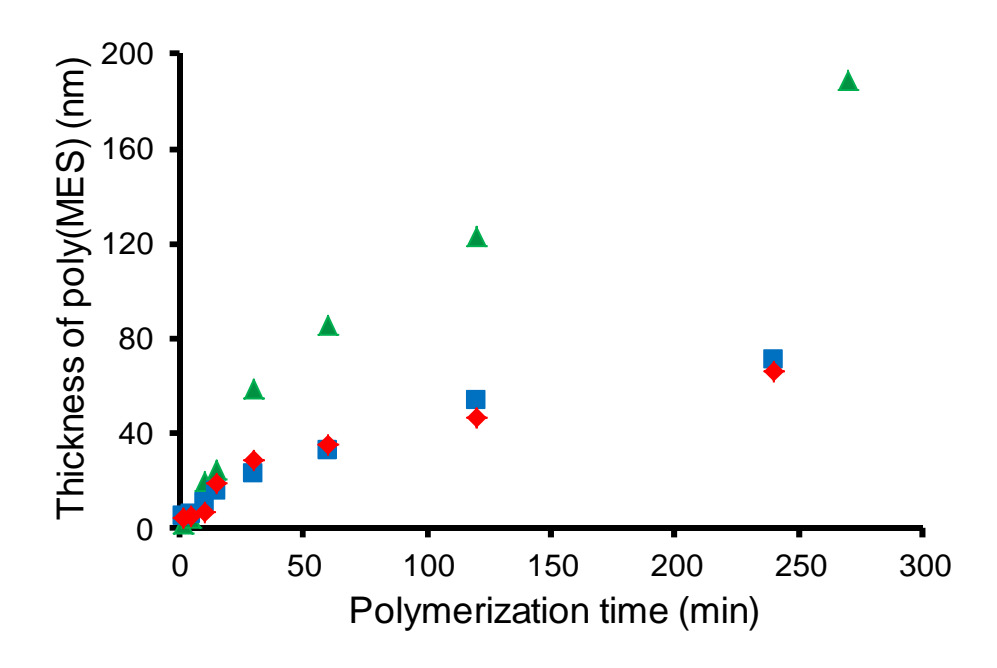


Figure A.1. Evolution of ellipsometric thickness with time for surface-initiated polymerization of MES on Au-coated Si. Polymerization occurred using a disulfide initiator (green triangles) or a macroinitiator adsorbed on either a MPA-modified surface (blue squares) or a MPA-(PDADMAC/PSS)₂ film (red diamonds). The ATRP system contained CuBr (2 mM), CuBr₂ (1 mM), and Me₆TREN (6 mM), along with 2.35 M MES.

To investigate polymerization kinetics, we first grew poly(MES) brushes from Au-coated wafers modified with either a monolayer of disulfide initiator or a film containing the macroinitiator. The disulfide initiator adsorbed directly to the Au whereas the macroinitiator adsorption occurred either on MPA-modified Au or on an MPA-(PDADMAC/PSS)₂ film.

Figure A.1 shows ellipsometric thickness as a function of time for growth of poly(MES) with different initiation systems. After a few minutes, the brushes grow much more rapidly from the disulfide initiator system than from the macroinitiator films, and poly(MES) is as much as 3-fold thicker when grown from the disulfide initiator. This difference may stem from lower initiator densities in the macroinitiator film than in the disulfide monolayer, but our previous study showed similar thicknesses for poly(HEMA) grown from the different initiators. MES polymerizes more rapidly than HEMA² and may be subject to higher rates of termination, which could lead to a greater dependence of film thickness on initiator density. Macroinitiator films on MPA-modified and MPA-(PDADMAC/PSS)₂-modified Au surfaces show similar polymerization rates, suggesting that the initiator density is similar for these two systems.

A.2.2. Protein binding to poly(MES) and its derivatives on Au surfaces

Figure A.2 shows FTIR spectra of poly(MES) brushes on Au-coated Si before and after derivatization. A clean, Au-coated wafer served as the background. For the native poly(MES), the peak at 1740 cm⁻¹ (Figure A.2 (a)) corresponds to the ester carbonyl. Immersing the surface in a 0.1 M EDC, 0.1 M NHS aqueous solution converts the carboxylic acid group to a succinimide ester that exhibits absorption maxima at 1817 and 1786 cm⁻¹ and an increase in the absorption around 1750 cm⁻¹ (Figure A.2 (b)). After reacting the activated poly(MES) with

aminobutyl NTA, the succinimidal ester peaks disappear and the carbonyl ester peak decreases (Figure A.2(c)). The new peak at 1680 cm⁻¹ likely results from a combination of absorbance due to carboxylate groups of NTA and amide bonds formed between poly(MES) and NTA. The broad peak around 1600 cm⁻¹ could stem from carboxylate groups of either NTA or hydrolyzed active esters. After exposing the brush to Cu²⁺, there is no observable change in the IR spectrum but elemental analysis (described in chapter 2) demonstrates the presences of Cu²⁺.

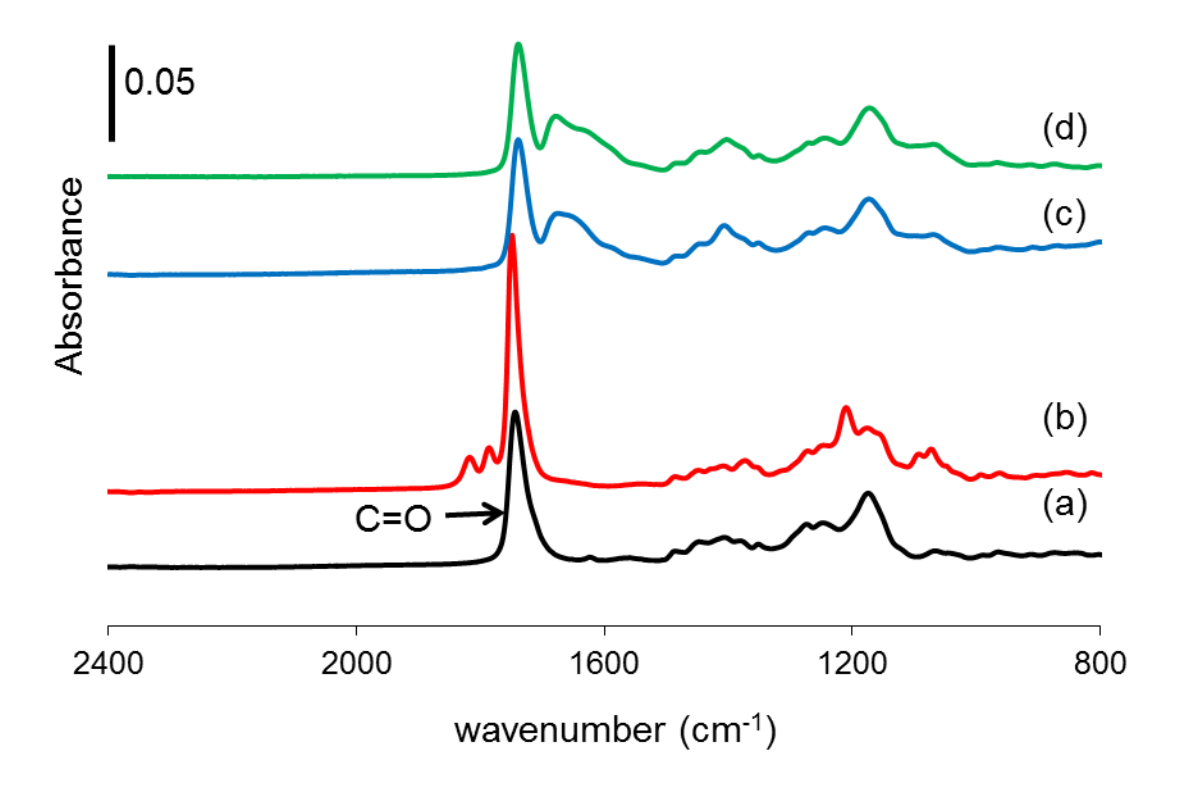


Figure A.2. Reflectance FTIR spectra of a poly(MES) brush grown from a macroinitiator adsorbed on MPA-modified Au. The spectra show the film before (a) and after the following modifications: activation with NHS/EDC (b); reaction with aminobutyl NTA (c) and complexation of Cu²⁺ by NTA (d).

Protein binding studies demonstrate the utility of these polymer brushes. I examined adsorption of two different proteins, lysozyme, which binds through ion exchange to poly(MES)

brushes and BSA, which binds through metal affinity interactions to poly(MES) brushes derivatized with NTA-Cu²⁺. For protein binding we immersed the polymer films on Au-coated Si in a 1 mg/mL solution of protein in 20 mM phosphate buffer at pH 7.4 for 18 h. After removal of the wafer from the solution and rinsing with buffers, reflectance FTIR spectroscopy allowed determination of the amount of bound protein using a procedure previously developed by Dai and co-workers⁴.

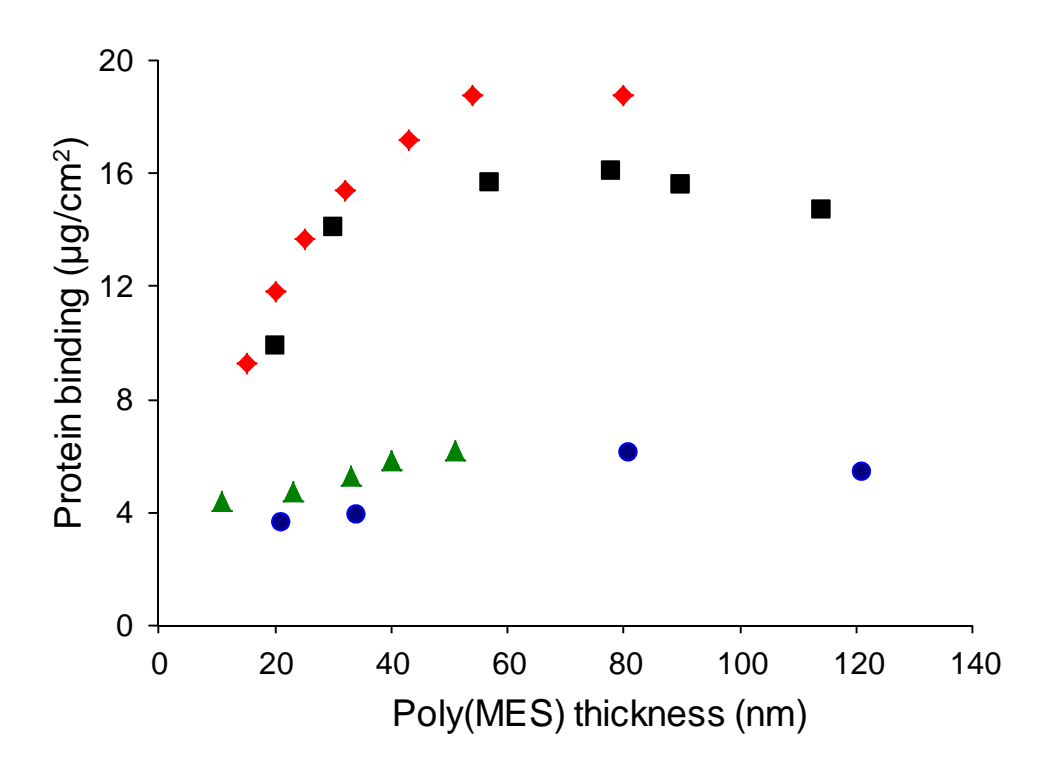


Figure A.3. Comparison of protein binding on polymer brushes grown from disulfide initiator and a macroinitiator as a function of poly(MES) film thickness. The symbols correspond to lysozyme binding to poly(MES) films grown from disulfide initiators (black squares) or macroinitiators (red diamonds) and BSA binding to NTA-Cu²⁺-derivatized poly(MES) grown from disulfide initiators (blue circles) or macroinitiators (green triangles).

The trends in lysozyme binding to polymer films grown from macroinitiator and disulfide initiators are essentially the same. The binding capacities initially increase with brush thickness, suggesting the adsorption occurs both on the surface and the interior of the brushes. For thicker films, however, steric hindrance likely decreases access to binding sites deep within the film. Binding of the larger BSA to more crowed poly(MES)-NTA-Cu²⁺ films does not increase greatly with film thickness, indicating that accessibility is limited to near the top of the film.

A.2.3. Effect of multilayers of initiator on polymerization and protein binding

To determine whether adsorption of multilayers of initiator increases polymer growth and subsequent protein binding, we deposited macroinitiator/(PSS/macroinitiator) $_n$ films on an MPA-modified Au surface.

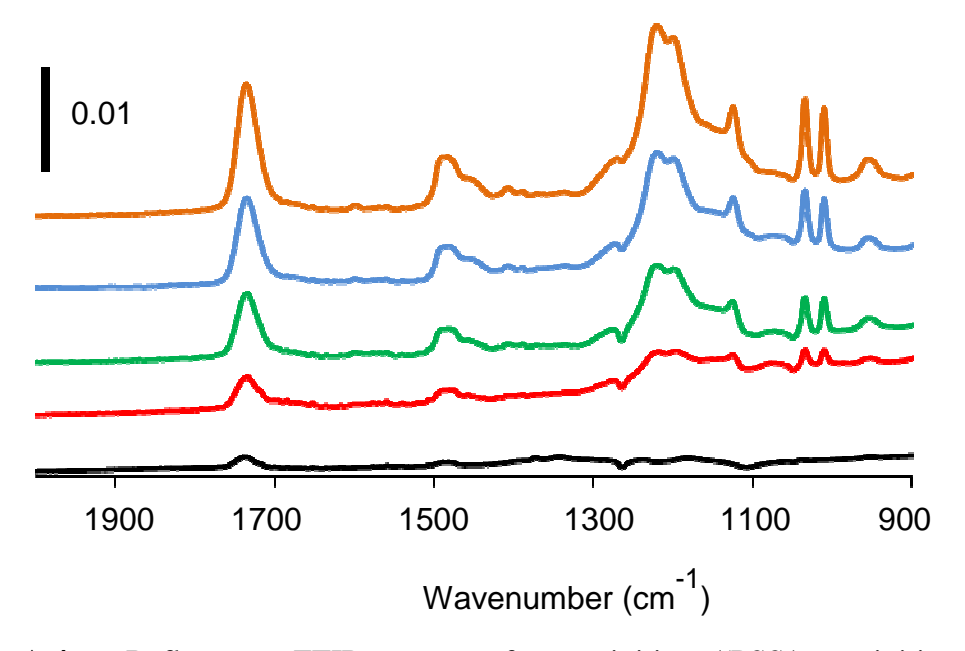


Figure A.4. Reflectance FTIR spectra of macroinitiator/(PSS/macroinitiator)_n films deposited on MPA-coated gold substrates (n = 0-4).

Reflectance FTIR spectra of these films show a reasonably linear increase in the absorbance at 1730 cm⁻¹, which corresponds to the ester carbonyl in the macroinitiator, as a function of number of deposited layers of the initiator. The absorbances due to CH₃ and CH₂ groups in the macroinitiator (~1490 cm⁻¹) and the vibrations at 1200, 1010 and 1040 cm⁻¹ due to PSS also show regular film growth and confirm controlled deposition. The ellipsometric thickness of the films increases by an average of 4.2 nm with each additional bilayer.

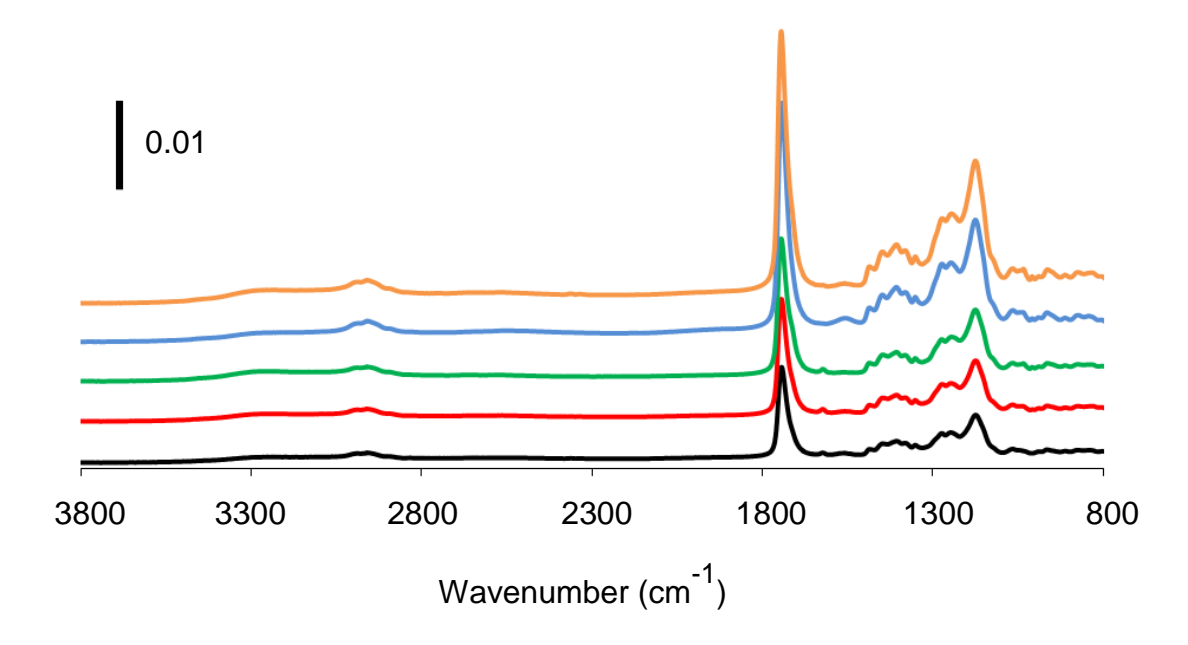


Figure A.5. Reflectance FTIR spectra of poly(MES) films grown from macro initiator/(PSS/macro initiator) \mathbf{n} films deposited on Au-MPA substrate ($\mathbf{n} = 0$ -4).

To investigate the ability of multilayers of macroinitiator to initiate polymerization, we grew poly(MES) brushes from the initiator-coated films using ATRP for 2 h. The appearance of the ester carbonyl peak at 1730 cm⁻¹ in the reflectance FTIR spectra of the films confirms the growth of the polymer from the initiator-modified surface (Figure A.5). Moreover, the absorbance at 1730 cm⁻¹ and the ellipsometric thickness increase monotonically with the number

of PSS/macroinitiator bilayers. These data suggest that initiation sites throughout the multilayer film initiate poly(MES) growth or that the multilayer film gives a higher surface coverage.

Although the poly(MES) thickness increases with the number of macroinitiator/PSS bilayers, the protein binding does not. In fact, lysozyme binding shows a slight drop when the number of bilayers are above 2. This is consistent with the previous observation that protein binding increases initially with poly(MES) thickness and then plateaus due to steric hindrance to binding. These studies suggest that a single layer of macroinitiator should be sufficient to provide high binding capacities.

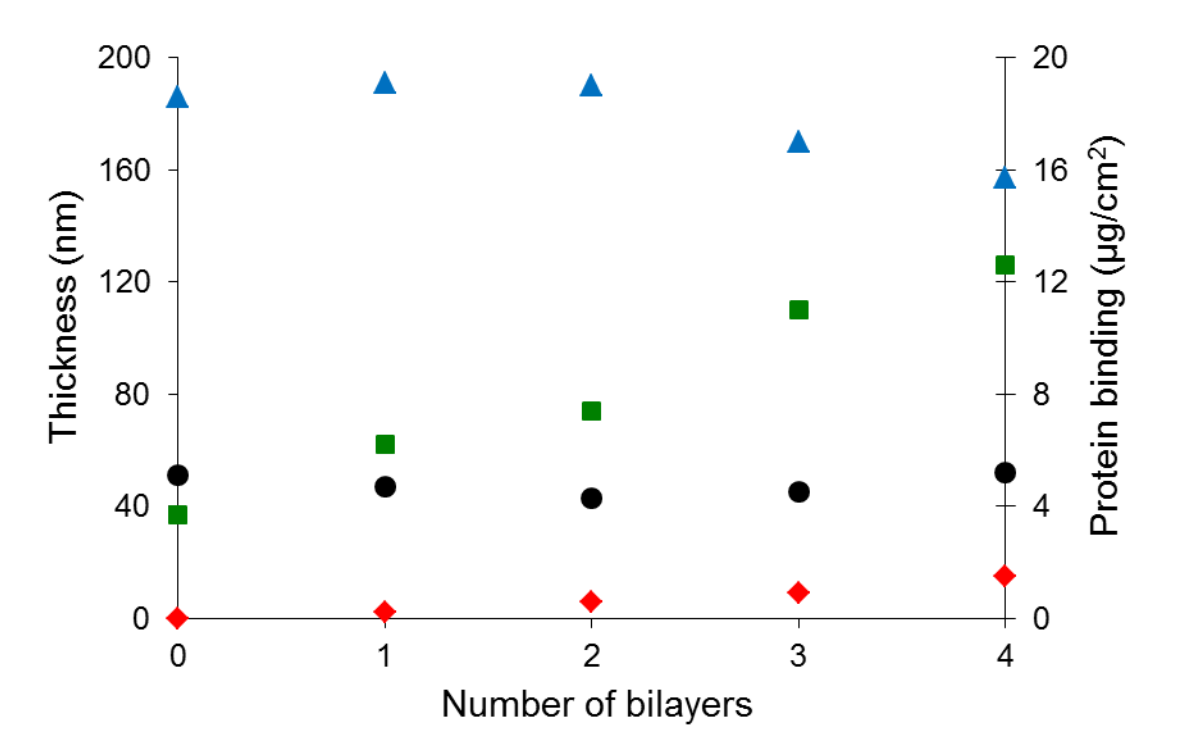


Figure A.6. Ellipsometric thicknesses of macroinitiator/(PSS/macro initiator)_n films (red diamonds) and of poly(MES) brushes grown on these films (green squares) (this thickness was obtained after subtracting the thickness of initiator/polyelectrolyte layer). The figure also shows the amounts of lysozyme (blue triangles) and BSA (black circles) binding to the poly(MES) grown from the macro initiator/(PSS/macro initiator)n films. In the case of BSA, the film was derivatized with NTA-Cu²⁺ prior to protein binding.

REFERENCES

A.3. References

- (1) Shah, R. R.; Merreceyes, D.; Husemann, M.; Rees, I.; Abbott, N. L.; Hawker, C. J.; Hedrick, J. L. *Macromolecules* **2000**, *33*, 597-605.
- (2) Jain, P.; Dai, J. H.; Baker, G. L.; Bruening, M. L. *Macromolecules* **2008**, *41*, 8413-8417.
- (3) Jain, P.; Vyas, M. K.; Geiger, J. H.; Baker, G. L.; Bruening, M. L. *Biomacromolecules* **2010**, *11*, 1019-1026.
- (4) Dai, J. H.; Bao, Z. Y.; Sun, L.; Hong, S. U.; Baker, G. L.; Bruening, M. L. *Langmuir* **2006**, 22, 4274-4281.
- (5) Jain, P.; Sun, L.; Dai, J. H.; Baker, G. L.; Bruening, M. L. *Biomacromolecules* **2007**, 8, 3102-3107.
- (6) Jain, P.; Dai, J.; Grajales, S.; Saha, S.; Baker, G. L.; Bruening, M. L. *Langmuir* **2007**, *23*, 11360-11365.